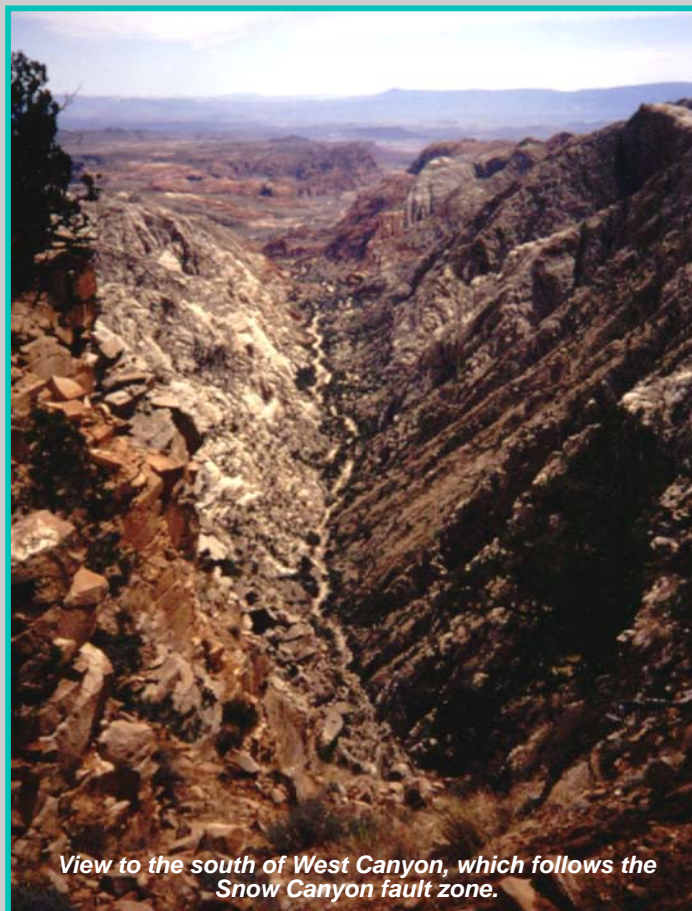


# THE GEOLOGY OF THE CENTRAL VIRGIN RIVER BASIN, SOUTHWESTERN UTAH, AND ITS RELATION TO GROUND-WATER CONDITIONS

by  
Hugh A. Hurlow

*Views of the Jurassic Navajo Sandstone in Snow Canyon State Park. The Navajo Sandstone is the principal aquifer in the study region.*



*View to the south of West Canyon, which follows the Snow Canyon fault zone.*



*Jointed Navajo Sandstone. Joints largely determine the permeability of the Navajo Sandstone aquifer.*



WATER-RESOURCES BULLETIN 26 1998  
UTAH GEOLOGICAL SURVEY  
a division of  
UTAH DEPARTMENT OF NATURAL RESOURCES

**STATE OF UTAH**  
*Michael O. Leavitt, Governor*

**DEPARTMENT OF NATURAL RESOURCES**  
*Kathleen Clarke, Executive Director*

**UTAH GEOLOGICAL SURVEY**  
*Kimm M. Harty, Acting Director*

**UGS Board**

<b>Member</b>	<b>Representing</b>
Craig Nelson (Chairman) .....	Civil Engineering
D. Cary Smith .....	Mineral Industry
C. William Berge .....	Mineral Industry
E.H. Deedee O'Brien .....	Public-at-Large
Robert Robison .....	Mineral Industry
Charles Semborski .....	Mineral Industry
Richard R. Kennedy .....	Economics-Business/Scientific
David Terry, Director, Trust Lands Administration .....	<i>Ex officio member</i>

**UTAH GEOLOGICAL SURVEY**

The **UTAH GEOLOGICAL SURVEY** is organized into five geologic programs with Administration, Editorial, and Computer Resources providing necessary support to the programs. The **ECONOMIC GEOLOGY PROGRAM** undertakes studies to identify coal, geothermal, uranium, hydrocarbon, and industrial and metallic resources; initiates detailed studies of these resources including mining district and field studies; develops computerized resource data bases, to answer state, federal, and industry requests for information; and encourages the prudent development of Utah's geologic resources. The **APPLIED GEOLOGY PROGRAM** responds to requests from local and state governmental entities for engineering-geologic investigations; and identifies, documents, and interprets Utah's geologic hazards. The **GEOLOGIC MAPPING PROGRAM** maps the bedrock and surficial geology of the state at a regional scale by county and at a more detailed scale by quadrangle. The **GEOLOGIC EXTENSION SERVICE** answers inquiries from the public and provides information about Utah's geology in a non-technical format. The **ENVIRONMENTAL SCIENCES PROGRAM** maintains and publishes records of Utah's fossil resources, provides paleontological and archeological recovery services to state and local governments, conducts studies of environmental change to aid resource management, and evaluates the quantity and quality of Utah's ground-water resources.

The UGS Library is open to the public and contains many reference works on Utah geology and many unpublished documents on aspects of Utah geology by UGS staff and others. The UGS has several computer data bases with information on mineral and energy resources, geologic hazards, stratigraphic sections, and bibliographic references. Most files may be viewed by using the UGS Library. The UGS also manages a sample library which contains core, cuttings, and soil samples from mineral and petroleum drill holes and engineering geology investigations. Samples may be viewed at the Sample Library or requested as a loan for outside study.

The UGS publishes the results of its investigations in the form of maps, reports, and compilations of data that are accessible to the public. For information on UGS publications, contact the Natural Resources Map/Bookstore, 1594 W. North Temple, Salt Lake City, Utah 84116, (801) 537-3320 or 1-888-UTAH MAP. E-mail: [nrugs.geostore@state.ut.us](mailto:nrugs.geostore@state.ut.us) and visit our web site at <http://www.ugs.state.ut.us>.

**UGS Editorial Staff**

J. Stringfellow .....	Editor
Vicky Clarke, Sharon Hamre .....	Graphic Artists
Patricia H. Speranza, James W. Parker, Lori Douglas .....	Cartographers

---

*The Utah Department of Natural Resources receives federal aid and prohibits discrimination on the basis of race, color, sex, age, national origin, or disability. For information or complaints regarding discrimination, contact Executive Director, Utah Department of Natural Resources, 1594 West North Temple #3710, Box 145610, Salt Lake City, UT 84116-5610 or Equal Employment Opportunity Commission, 1801 L Street, NW, Washington DC 20507.*

---



# CONTENTS

ABSTRACT . . . . .	1
INTRODUCTION . . . . .	2
Purpose and Scope of Project . . . . .	2
Physiography . . . . .	2
Previous Work . . . . .	4
GEOLOGIC AND HYDROGEOLOGIC FRAMEWORK . . . . .	4
Geologic Setting . . . . .	4
Hydrogeologic Setting . . . . .	7
GEOLOGY OF UNCONSOLIDATED DEPOSITS . . . . .	7
Introduction . . . . .	7
Stratigraphy . . . . .	8
Tertiary . . . . .	8
Tertiary alluvial-fan deposits (Taf) . . . . .	8
Quaternary-Tertiary . . . . .	8
Quaternary-Tertiary sediments (QTs) . . . . .	8
Quaternary-Tertiary alluvial-fan deposits (QTaf) . . . . .	8
Quaternary . . . . .	8
Quaternary sediments, undivided (Qs) . . . . .	8
Structure of New Harmony and Kanarraville Basins . . . . .	9
Overview . . . . .	9
Structure and Thickness . . . . .	10
New Harmony basin . . . . .	11
Kanarraville basin . . . . .	11
Structure of the St. George Basin . . . . .	11
STRUCTURAL GEOLOGY AND HYDROGEOLOGY OF THE NAVAJO SANDSTONE . . . . .	11
Lithology and Stratigraphy . . . . .	11
Regional Structure . . . . .	12
Introduction . . . . .	12
Compartment I: Red Hollow Area . . . . .	12
Compartment II: West of Gunlock Fault Zone . . . . .	12
Compartment III: Red Mountains . . . . .	13
Compartment IV: Between West and East Strands of the Snow Canyon Fault Zone . . . . .	13
Compartment V: Snow Canyon Fault to Upper Ash Creek Valley . . . . .	13
Compartment VI: Southeast Limb of Virgin Anticline . . . . .	13
Pine Valley Mountains and Bull Valley Mountains . . . . .	15
Fracture Systems . . . . .	15
Hydrogeologic Importance of Fractures . . . . .	15
Structural Characteristics of Fractures in the Navajo Sandstone . . . . .	16
Joints and joint zones . . . . .	16
Faults and fault zones . . . . .	16
Distribution of Fractures in the Navajo Sandstone . . . . .	20
Discussion . . . . .	22
Fracture Geometry and Permeability . . . . .	22
Relation Between Fracture Parameters and Hydraulic Conductivity . . . . .	24
Introduction . . . . .	24
Methods . . . . .	24
Results . . . . .	24
Discussion . . . . .	25
Hydrogeologic Significance of Structural Compartments . . . . .	26
Regional Hydrogeology . . . . .	26
Potential Target Areas for New Wells . . . . .	27
OTHER POTENTIAL AQUIFERS . . . . .	28

Introduction . . . . .	28
Cretaceous Sandstones . . . . .	28
Tertiary and Quaternary Igneous Rocks . . . . .	29
GEOLOGIC CONDITIONS BETWEEN ASH CREEK RESERVOIR AND TOQUERVILLE SPRINGS . . . . .	29
Introduction . . . . .	29
Previous Work . . . . .	29
Structural Geometry of Ash Creek Valley . . . . .	29
Discussion . . . . .	30
SUMMARY . . . . .	31
ACKNOWLEDGMENTS . . . . .	32
REFERENCES . . . . .	33

## TABLES

Table 1. Selected references on central Virgin River basin geology . . . . .	5
Table D.1. Well data constraining elevation of base of Navajo Sandstone . . . . .	45
Table D.2. Well data constraining elevation of top of Navajo Sandstone . . . . .	45
Table G.1 Aerial photograph fracture data . . . . .	50
Table G.2 Scanline data . . . . .	51
Table G.3 Fracture parameters and hydraulic conductivity . . . . .	52

## ILLUSTRATIONS

Figure 1a. Location map . . . . .	3
Figure 1b. Location map . . . . .	3
Figure 2. Geologic and geographic features of the central Virgin River basin . . . . .	4
Figure 3. Photograph of Beaver Dam Mountains . . . . .	6
Figure 4. Lithologic column . . . . .	6
Figure 5. Trough cross-bedding in Navajo Sandstone . . . . .	7
Figure 6. Unconsolidated deposits . . . . .	9
Figure 7. New Harmony and Kanarraville basins . . . . .	10
Figure 8a. View of Red Mountains . . . . .	14
Figure 8b. View of West Canyon . . . . .	14
Figure 8c. Photograph of Navajo Sandstone in Pine Valley Mountains . . . . .	15
Figures 9a and 9b. Photographs of joints in Navajo Sandstone . . . . .	17
Figures 9c and 9d. Photographs of joints in Navajo Sandstone . . . . .	18
Figure 9e. Photograph of joint zones reactivated as faults in Navajo Sandstone . . . . .	19
Figure 9f. Photograph of fault zone in Navajo Sandstone . . . . .	19
Figure 10. SEM image of fault gouge . . . . .	20
Figure 11. Plot of fracture density from aerial photographs versus scanlines . . . . .	21
Figure 12a. Plot of fracture density versus location, aerial photograph data . . . . .	22
Figure 12b. Plot of fracture density versus location, scanline data . . . . .	23
Figure 13. Relation between permeability tensor and fracture orientation . . . . .	24
Figure 14. Plot of hydraulic conductivity versus fracture parameters . . . . .	25
Figure 15. Photograph of Cretaceous Iron Springs Formation . . . . .	28
Figure 16. Photograph of Pine Valley monzonite . . . . .	29
Figure 17. Photograph of fractured basalt at Ash Creek Reservoir . . . . .	30
Figure C.1. Generalized geologic map of New Harmony and Kanarraville basins . . . . .	41
Figure C.2. Lithologic column for New Harmony and Kanarraville basins . . . . .	42



Figure F.1. Simplified geologic and fracture-trace map of Snow Canyon area . . . . .	48
Figure F.2. Rose diagrams . . . . .	49
Figure H.1. Cross section through Red Mountains . . . . .	52

**PLATES**

1. Interim geologic map of the St. George quadrangle . . . . .	in pocket
2. Cross sections and descriptions of map units . . . . .	in pocket
3. Schematic isopach map of unconsolidated deposits, New Hamony basin . . . . .	in pocket
4. Schematic isopach map of unconsolidated deposits, St. George basin . . . . .	in pocket
5A. Structure contour map, base of Navajo Sandstone . . . . .	in pocket
5B. Structure contour map, top of Navajo Sandstone . . . . .	in pocket
6. Structure compartments and fracture domains . . . . .	in pocket

**APPENDICES**

APPENDIX A Description of Geologic Units Shown on Plates 1 and 2 . . . . .	36
APPENDIX B Sources for Plate 1 . . . . .	40
APPENDIX C Late Tertiary-Quaternary Tectonic Evolution of New Harmony and Kanarraville Basins . . . . .	41
Introduction . . . . .	41
Geologic Setting . . . . .	42
Structural Geometry and Evolution . . . . .	43
Discussion . . . . .	43
APPENDIX D Control Points for Structure Contour Maps . . . . .	45
APPENDIX E Methods of Fracture Data Acquisition . . . . .	46
APPENDIX F Fracture Heterogeneity . . . . .	47
APPENDIX G Fracture Data Tables . . . . .	50
APPENDIX H Structure of the Red Mountains and Implications for Artificial-Recharge Projects . . . . .	53

# THE GEOLOGY OF THE CENTRAL VIRGIN RIVER BASIN, SOUTHWESTERN UTAH, AND ITS RELATION TO GROUND-WATER CONDITIONS

by  
*Hugh A. Hurlow*

## ABSTRACT

This report describes the geology of the central Virgin River basin in southwestern Utah, and characterizes the structure and lithology of the Jurassic Navajo Sandstone and the thickness and stratigraphy of Quaternary-late Tertiary unconsolidated deposits, the two main aquifers in the region. Southwestern Utah has experienced rapid population growth and increased demand on water supplies during the past 15 years, and the purpose of this report is to better define the ground-water resources of the area. Ground water provides approximately half of the public water supply in southwestern Utah, so future decisions regarding water use must be based on careful geologic characterization of the aquifers and their relation to the regional hydrologic system. The results of this study will be applied to ground-water modeling, evaluating regional and local hydrogeologic conditions, and assessing sites for development of ground water.

The central Virgin River basin is located in the transition zone between the Basin and Range and Colorado Plateau geologic provinces, and contains geologic characteristics of each. Most of the study area comprises gently dipping late Paleozoic to early Tertiary sedimentary rocks, and the northern part is dominated by Tertiary igneous rocks. Cretaceous folding and thrust faulting and mid-Tertiary to Quaternary normal faulting created structurally complex zones along Ash Creek valley, the Hurricane Cliffs, the northeastern part of the St. George basin, and in parts of the Beaver Dam and Bull Valley Mountains.

Unconsolidated deposits in the St. George basin are mainly Quaternary in age, are generally less than 125 feet (38 m) thick, and were deposited in fluvial, alluvial-fan, eolian, and mass-wasting environments. Quaternary sediments are locally up to 350 feet (107 m) thick adjacent to faults in the St. George basin and Ash Creek valley. Unconsolidated deposits in the New Harmony-Kanarrville area, 34 miles (55 km) northeast of St. George, are substantially thicker owing to a complicated Tertiary structural history that included folding followed by displacement

along the Hurricane and related normal faults. Quaternary and late Tertiary sediments together are 500 to 1,250 feet (150-380 m) thick below New Harmony and 2,000 to 2,500 feet (610-765 m) thick near the Hurricane fault, and were deposited in fluvial, alluvial-fan, eolian, and mass-wasting environments.

The Navajo Sandstone is a 2,000 to 2,800 foot-thick (610-850 m-), fine-grained eolian sandstone exposed over 234 square miles (606 km<sup>2</sup>) in the study area. The Navajo Sandstone comprises six fault-bounded structural compartments characterized by relatively simple and homogeneous internal structure. Compartment boundary zones are structurally complex.

Fracture permeability strongly influences ground-water conditions in the Navajo aquifer. Joints are the most prevalent fracture type, and their distribution is heterogeneous owing to development of discrete, linear zones of high joint density termed joint zones. Joint zones should be primary targets for future test wells, because their permeability is up to 35 times greater than adjacent rock with lower fracture density. The internal structure of fault zones in the Navajo Sandstone consists of a central core zone containing fault gouge, bounded on either side by damage zones, in which joint density is very high but gouge is absent. Damage zones greatly enhance permeability parallel to fault planes, but transverse permeability is minimal due to gouge in fault cores.

Data on joint orientations qualitatively indicate the orientation and degree of anisotropy of the two-dimensional permeability tensor for sample areas. Outcrop fracture data collected near water wells correlate with hydraulic conductivity calculated from single- and multiple-well aquifer tests according to the equation:

$$\log K = -0.590 \pm 0.217 + (0.801 \pm 0.107)[\log(fd \times aa \times 1000)]$$

where K is hydraulic conductivity in meters per day, fd is fracture density in meters per square meter, and aa is average aperture in millimeters. This relationship provides a tool for hydrogeologic modeling and for evaluating the relative merits of prospective well sites.

Cretaceous sandstones and Tertiary volcanic and intrusive rocks in the study area are potential aquifers where they are highly fractured and where stratigraphic and hydrologic conditions are favorable. Siting of test wells in these units should be based on careful geologic characterization of target areas.

The structural geology of Ash Creek Reservoir and Ash Creek valley constrains possible pathways for water lost from the reservoir by seepage. The natural abutments of the reservoir are highly fractured basalt that is up to 550 feet (168 m) thick. This basalt overlies up to 150 feet (46 m) of boulder-size gravel that was deposited on bedrock during Pleistocene time. Ground water likely resides in the lower part of the basalt and in the underlying gravel, and flows southwest. Much of this water may emerge at Toquerville Springs, as hypothesized by previous workers, but some may also be in gravel deposits and the Navajo Sandstone in a fault-bounded block west of Toquerville Springs.

## INTRODUCTION

### Purpose and Scope of Project

This report describes the geology of the central Virgin River basin in relation to the occurrence and movement of ground water. The central Virgin River basin (figures 1a and 1b) is characterized by an arid climate, rapid population growth, and reliance on bedrock aquifers for public ground-water supply. These factors make detailed knowledge of the geologic structure of the region critical to hydrogeologic studies. The objective of this report is to provide information that will be useful in implementing a new water-use management plan for the central Virgin River basin, including data essential for the construction of ground-water-flow models by the U.S. Geological Survey, Water Resources Division (work in progress), and identification of potential areas and geologic units for future development of ground-water resources.

The population of Washington County and adjacent parts of Iron County in southwestern Utah increased by 140 percent from 1980 to 1995, and this growth was accompanied by a 160-percent increase in public and industrial water use from surface and ground water (Utah Division of Water Rights, 1982, and unpublished data). Similar population-growth rates are projected for the foreseeable future. Most new development in the central Virgin River basin is in the municipalities of St. George, Santa Clara, Ivins, Washington, Hurricane, La Verkin, and Toquerville, and nearby rural areas such as New Harmony, Kanarraville, and alluvial valleys near St. George (figure 1a). This rapid growth has created the need for additional information about the ground-water resources to ensure their proper management and protection.

Successful water-use management plans rely in part on quantification of ground-water resources, which in turn

depends strongly on detailed geologic characterization of aquifers. Ground water extracted from wells provides 51 percent of the public water supply in the central Virgin River basin. Ground-water use has increased by about 320 percent since 1980 (Utah Division of Water Rights, 1982, and unpublished data).

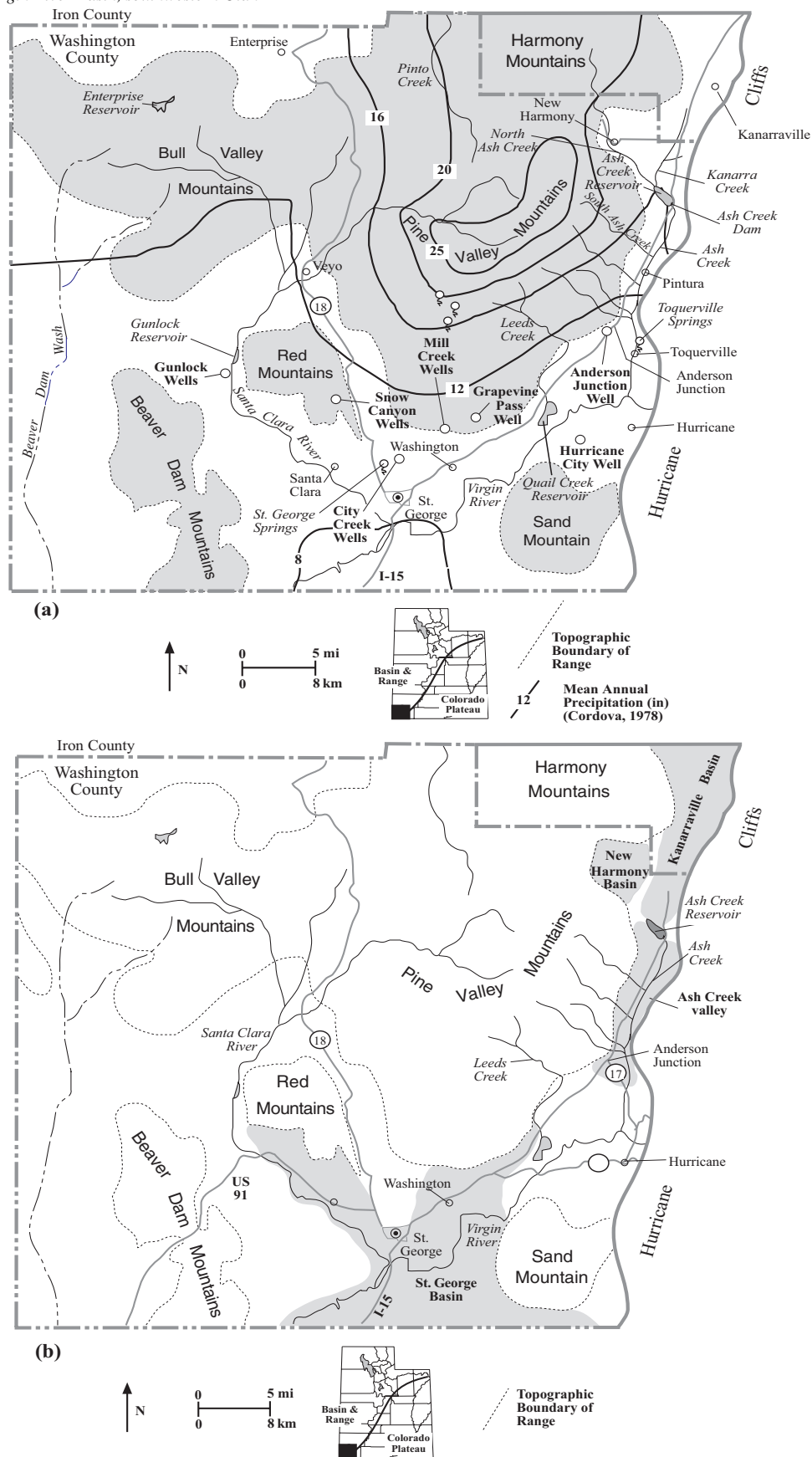
The Jurassic Navajo Sandstone and Quaternary to late Tertiary unconsolidated deposits are the primary focus of this report because they are the most important aquifers in the central Virgin River basin. Nearly all major public water-supply wells in Washington County are screened in the Navajo Sandstone, and most water wells in the New Harmony-Kanarraville area are in Quaternary-late Tertiary unconsolidated deposits. This report characterizes the thickness and stratigraphy of unconsolidated deposits, defines the structural geometry and lithology of the Navajo Sandstone, suggests areas and geologic units that may be suitable for future development of new public water-supply wells, and describes the geologic framework of Ash Creek Reservoir in the northeast part of the study area (figure 1a) to identify possible pathways for water lost by seepage from the reservoir.

### Physiography

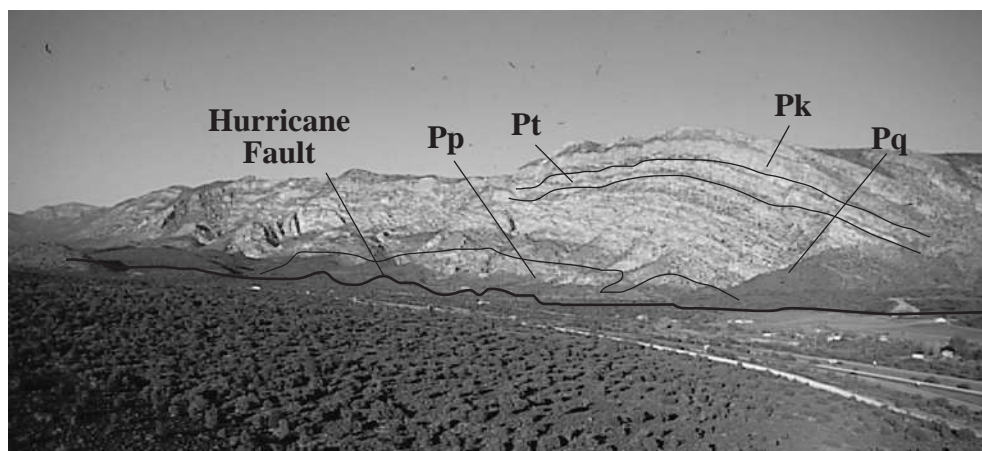
The study area contains broad, open basins in its south-central part, mountains of moderate to steep relief in its northern and southwestern parts, and is bounded on the east by the precipitous Hurricane Cliffs (figures 1a and 2a). The St. George basin south of St. George (figure 2b) includes parts of the Virgin and Santa Clara Rivers and is characterized by low topographic relief. Topographic relief is nearly 8,000 feet (2,440 m) between the Virgin River and Signal Peak, the highest point in the Pine Valley Mountains (figure 2b). The Bull Valley Mountains, characterized by moderate to steep topography, occupy the northeastern part of the study area. The Beaver Dam Mountains are a steep, north-trending range adjacent to a north-trending basin containing Beaver Dam Wash, which drains the Beaver Dam and southern Bull Valley Mountains.

Major streams include the Virgin River, which originates east of the study area; the Santa Clara River, which originates in the Pine Valley Mountains; tributaries of the Santa Clara River, which originate in the Bull Valley Mountains; and tributaries of the Virgin River, including Ash Creek, which emanate from the southeastern and eastern flanks of the Pine Valley Mountains. Many small reservoirs provide water for irrigation and domestic use.

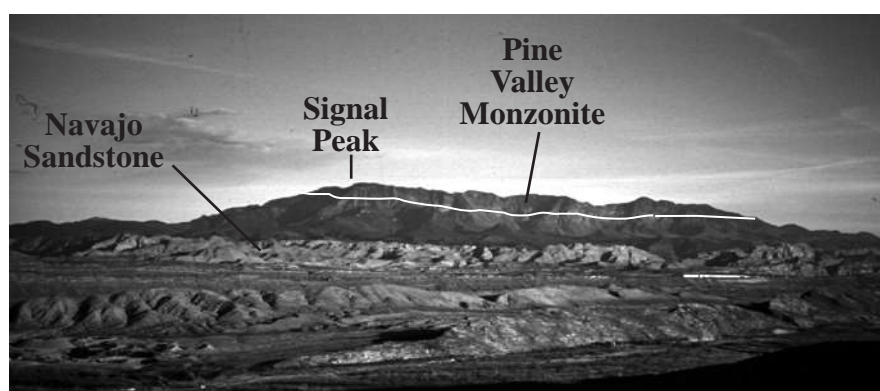
Precipitation is strongly controlled by elevation: average annual values range from over 25 inches (63 cm) above 8,000 feet (2,440 m) elevation in the Pine Valley Mountains to less than 8 inches (20 cm) in the southern St. George basin (figure 1a; Cordova, 1978). The Pine Valley Mountains accumulate the only appreciable snowpack in the study area, providing most of the runoff for the surface-water system and recharge to the ground-water system (Cordova, 1978).



**Figure 1.** Location maps of study area: (a) Geographic, hydrologic, and physiographic features; (b) Locations of St. George, New Harmony, and Kanarraville basins and Ash Creek valley.



(a)



(b)

**Figure 2.** Geologic and geographic features of the central Virgin River basin. (a) View to the northeast of Hurricane Cliffs between Pintura and Toquerville. Topographic relief is about 2,000 feet (610 m). Pk is Kaibab Limestone, Pt is Toroweap Formation, Pq is Queantoweap Formation, and Pp is Pakoon Formation (see figure 4 for lithologic column). (b) View to the north of Pine Valley Mountains. Central part of St. George basin is in foreground. Topographic relief between base of Navajo Sandstone cliffs and Signal Peak is about 7,090 feet (2,160 m).

## Previous Work

Cook (1960) established the modern geologic framework of the study area, including a 1:125,000-scale geologic map. Cook's (1960) work drew on previous regional-scale studies and detailed work related to development of mineral and petroleum resources (table 1). The mineral resources of the study area are summarized in Eppinger and others (1990). Detailed mapping in the Beaver Dam Mountains, St. George area, Pine Valley Mountains, and Hurricane Cliffs (table 1) have superseded parts of Cook's (1960) compilation map. The Hurricane fault, a major Quaternary to Recent(?) normal fault which forms the eastern boundary of the study area, has been studied by numerous workers (table 1).

The regional hydrogeology of the central Virgin River basin is summarized by Cordova and others (1972) and Cordova (1978), who present reconnaissance-level data on water levels, potentiometric surfaces, aquifer tests, and water chemistry.

## GEOLOGIC AND HYDROGEOLOGIC FRAMEWORK

### Geologic Setting

The geologic map (plate 1 and appendices A and B) and cross sections (plate 2) accompanying this report summa-

**Table 1.** Selected references on central Virgin River basin geology.

Region	References
Beaver Dam Mountains	Anderson and Hintze (1993b), Hintze and others (1994), Hintze and Hammond (1994)
Bull Valley Mountains	Blank (1959, 1993), Adair (1986)
Harmony Mountains	Mackin (1947, 1960), Doelling and Graham (1972), Averitt (1969)
Pine Valley Mountains	Cook (1957), Grant (1995)
St. George Basin	Dobbin (1939), K. Hamblin in Budding and Sommer (1986), Proctor and Brimhall (1986), Higgins and Willis (1995), Willis and Higgins (1995, 1996)
Hurricane fault	Gardner (1952), Kurie (1966), Hamblin (1966, 1984), Schramm (1994), Stewart and Taylor (1996), Stewart and others (1997)
Virgin oil field	Reeside (1922)
Zion National Park	Gregory (1950), Hamilton (1978), Grant (1987)

alize the geology of the central Virgin River basin. The study area lies in the transition zone between the Basin and Range and Colorado Plateau geologic provinces (Cook, 1960; Anderson and Mehnert, 1979). The Basin and Range province is characterized by long, straight, north-south-trending mountain ranges and adjacent, internally drained basins. Normal faulting and volcanism were the dominant geologic processes during Miocene to Recent time (15 million years ago to present). Examples of Basin and Range geology and physiography in the study area include the Beaver Dam Mountains and Beaver Dam Wash (figure 3), extensive Tertiary volcanism and plutonism, and the Gunlock, Washington, and Hurricane normal faults. The Colorado Plateau province is characterized by Paleozoic (570-240 million years ago) and Mesozoic (240-66 million years ago) sedimentary rocks that are mostly gently dipping but are locally disrupted by folds and faults of late Mesozoic and Tertiary (66-1.6 million years ago) age. Zion National Park and the lithologic character and gentle dips of Paleozoic and Mesozoic strata in the St. George basin and much of the Pine Valley Mountains are examples of Colorado Plateau geology.

Stratigraphic units of the central Virgin River basin range from Precambrian through Quaternary in age (figure 4 and appendix A; also see Cook, 1960, and Hintze, 1986). The following paragraphs provide an overview of the stratigraphic and geologic evolution of the study area, and later sections provide more detailed descriptions of unconsolidated deposits and the Navajo Sandstone.

Crystalline rocks of Precambrian age (570 million years ago and older) are exposed in the Beaver Dam Mountains and underlie the entire study area. The Precambrian rocks are overlain by Paleozoic through late Mesozoic (570-100 million years ago) limestone and sandstone units that were deposited in marine and near-marine settings on a slowly subsiding continental platform. A notable exception occurred during Early Jurassic time (about 200-187 million years ago) when the Utah-eastern Nevada region was covered by thick sand dunes. These dunes were buried by a shallow ocean, then lithified to form the Navajo Sandstone, the principal aquifer in the study area (figure 5). During Late Cretaceous to Early Eocene time (100-55 million years ago), thrust faults and folds formed through-

out the western U.S., manifested in the study area by the Square Top thrust fault, Virgin anticline, and deposition of 3,000 to 4,000 feet (914-1,220 m) of sandstone and conglomerate derived from highlands to the northwest (Hintze, 1986; Goldstrand, 1994).

Volcanic deposits derived locally and from southeastern Nevada covered much of the study area during Oligocene to Miocene time (38-5 million years ago) (Rowley and others, 1979; McKee and others, 1997). The Pine Valley Mountains are composed of the 21 Ma Pine Valley laccolith (figure 2b), a tabular intrusive body, and overlying cogenetic volcanic rocks, above early Tertiary and Mesozoic sedimentary rocks (Cook, 1960; McKee and others, 1997). The Bull Valley and Harmony Mountains are dominantly Miocene and Oligocene volcanic rocks. Volcanism accompanied and was outlasted by extensional and strike-slip faulting. Major crustal extension occurred during Miocene time along the western front of the Beaver Dam Mountains and in regions to the west (Anderson and Barnhard, 1993a, 1993b).

The elevation of the Colorado Plateau began to increase about 5.5 million years ago (Lucchitta, 1989), driving erosion and downcutting by streams which carved the canyon topography of southern Utah and northern Arizona. This erosion has removed the entire early Tertiary and Cretaceous and much of the Jurassic stratigraphic section, a total thickness of about 5,500 to 8,500 feet (1,676-2,590 m), from above the St. George basin. The Pine Valley laccolith was more resistant to erosion than subjacent sedimentary rocks, resulting in the great topographic relief between the Pine Valley Mountains and the St. George basin. The relatively high precipitation in the Pine Valley Mountains which enables continued population growth and development in the central Virgin River basin is, therefore, directly related to the geologic evolution of the area.

A second period of normal faulting, local folding, and basaltic volcanism occurred during Pliocene to Pleistocene time (1.6 million years ago to 10,000 years ago), when the Hurricane, Washington, and Gunlock faults formed (Anderson and Mehnert, 1979; Schramm, 1994). The Hurricane fault (figure 2a), a major north-south-striking structure in northern Arizona and southern Utah, uplifted





**Figure 3.** View to the south of western front of Beaver Dam Mountains and Beaver Dam Wash. Topographic relief between wash and range crest is about 2,625 feet (800 m).

Age	Geologic Unit		Thickness ft (m)	Lithology
Quaternary	Undifferentiated sediments		0-1200 (0-366)	
	Basalt		0-550 (0-168)	
	Boulder gravel		0-350 (0-107)	
Tertiary	Volcaniclastic conglomerate, sandstone, siltstone; boulder gravel	Upper mbr.	700 (213)	
		Middle mbr.	450 (137)	
		Lower mbr.	350 (107)	
	Intrusive Rocks			
	Miocene volcanic rocks		0-2500 (0-762)	
	Pine Valley igneous suite		0-3000 (0-914)	
	Miocene-Oligocene volcanic rocks		0-1800 (0-549)	
	Claron Formation		600-700 (183-213)	
Cret.	Iron Springs Fm (W of Hurricane Flt) Undiff. Cretaceous (E of Hurr. Flt)		3800-4000 (1158-1219)	
Jurassic	Entrada and Curtis Formations (E of Hurricane Fault)		450 (137)	
	Carmel and Temple Cap Formations		700 (213)	
	Navajo Sandstone		2000-2800 (610-853)	
	Kayenta Formation		500-700 (152-213)	
	Moenave Formation	Springdale Ss. Mbr.	150 (46)	
Dinosaur Cyn. & Whitmore Point Mbrs.		300 (91)		
Triassic	Chinle Formation	Petrified Forest Mbr.	400 (122)	
		Shinarump Mbr.	80-150 (24-46)	

Age	Geologic Unit		Thickness ft (m)	Lithology
Triassic	Moenkopi Formation	Upper Red Mbr.	360-500 (110-152)	
		Shnabkaib Mbr.	500-1000 (152-305)	
		Middle Red Mbr.	375-400 (114-122)	
		Virgin Limestone Mbr.	25-225 (8-69)	
		Lower Red Mbr.	25-650 (8-198)	
		Timpoweap Mbr.	3-61 (10-200)	
		Rock Canyon Mbr.	0-35 (0-11)	
Permian	Kaibab Limestone		800-1000 (244-305)	
	Toroweap Formation		295 (90)	
	Queantoweap Formation		1500 (457)	
	Pakoon Formation		750 (229)	
Dev.-Penn.	Callville Limestone		1550 (472)	
Miss.	Redwall Limestone		1100 (335)	
Dev.-Camb.	Dolomite, siltstone, limestone		550-2100 (168-640)	
Cambrian	Pioche Shale		210 (64)	
	Prospect Mountain Quartzite		530 (162)	
Pre-cambrian	Schist, gneiss, granitoid		>6560 (>2000)	

**Figure 4.** Lithologic column for study area, compiled principally from Cook (1960) and Hintze and others (1994).



**Figure 5.** Trough cross-bedding in Navajo Sandstone, Snow Canyon State Park. Relief on exposure is approximately 100 feet (30 m).

the Hurricane Cliffs during Quaternary time and is the most likely source of the magnitude 5.8 St. George earthquake of 1992 (Pechmann and others, 1994).

### Hydrogeologic Setting

Recharge of the Navajo Sandstone aquifer takes place by several mechanisms, including: (1) infiltration through overlying geologic units; (2) infiltration from streams flowing over Navajo Sandstone outcrop; (3) infiltration of precipitation onto the outcrop; and (4) lateral flow of ground water from other geologic units (Cordova and others, 1972; Cordova, 1978). A major goal of the hydrologic study in progress by the U.S. Geological Survey, Division of Water Resources, is to better quantify the relative contributions from these possible sources. Later sections discuss the implications of the cross sections, structure contour maps, and fracture characterization for evaluating the regional hydrogeology and the relative importance of different recharge mechanisms for the Navajo aquifer.

Cordova (1978) presented a generalized, large-scale map of the potentiometric surface in the Navajo Sandstone. Northwest of Interstate 15, the potentiometric surface generally slopes away from the Pine Valley Mountains, Red Mountains, and Beaver Dam Mountains and toward the Virgin and Santa Clara Rivers. In the Sand Mountain area southeast of Interstate 15, the potentiometric surface generally slopes away from the Hurricane Cliffs. Cordova (1978) noted that the Navajo Sandstone is unsaturated

where its base crops out along the southern margins of the Red Mountains, Pine Valley Mountains, and Sand Mountain.

Municipal and county water-supply wells in the Navajo Sandstone (figure 1a) supply over 12,274 acre-feet ( $4 \times 10^9$  gal;  $1.5 \times 10^{10}$  L) of water per year (Utah Division of Water Rights, unpublished data). Reservoirs and springs each supply about half as much water as wells (Utah Division of Water Rights, unpublished data). Water derived from the Navajo Sandstone generally meets minimum drinking-water quality standards, except for several wells located near faults and/or volcanic centers north of St. George and southwest of Hurricane (Cordova, 1978).

The hydrogeology of unconsolidated aquifers in the study area is less well understood than that of the Navajo Sandstone. This report provides important new information on the thickness and geometry of unconsolidated deposits in the St. George, New Harmony, and Kanarrville basins.

## GEOLOGY OF UNCONSOLIDATED DEPOSITS

### Introduction

Unconsolidated sediments in the central Virgin River basin were deposited by fluvial, alluvial-fan, mass-wasting, and eolian processes, range in age from late Tertiary to Recent, and have limited extent and thickness in most

places (plates 3 and 4). The thickest deposits are in Beaver Dam Wash, the New Harmony and Kanarraville basins, Ash Creek valley, and along the Virgin and Santa Clara Rivers in the St. George basin. Deposits in Beaver Dam Wash are the topic of a hydrogeologic investigation in progress by the U.S. Geological Survey. Rapidly growing residential developments in the New Harmony and Kanarraville basins utilize unconsolidated aquifers. Wells in unconsolidated deposits of the St. George basin are used primarily for irrigation and single-family use (Cordova, 1978).

## Stratigraphy

### Tertiary

**Tertiary alluvial-fan deposits (Taf):** A Miocene to Pliocene sequence of volcanoclastic debris flows and alluvial deposits crops out on the flanks of the Harmony Mountains, the northern and western margins of the New Harmony basin, and along the western margin of the Kanarraville basin. This unit dips away from the mountains, and underlies Quaternary deposits in the basins. Unit Taf consists of three informal members (figure 4; appendix A) described below. The geologic evolution and significance of unit Taf is discussed in appendix C and by Anderson and Mehnert (1979).

The middle (Tafm) and lower (Taf<sub>l</sub>) members are consolidated to semiconsolidated volcanoclastic breccia, conglomerate, sandstone, and siltstone with a combined thickness of 800 feet (244 m) (figure 4; appendix A). The lower two members are not potential aquifers based on their poor sorting, fine grain size, and strong cementation.

The upper member (Taf<sub>u</sub>) is poorly sorted, unconsolidated boulder gravel with pebble- to boulder-size (0.1-10 in [2->256 mm] diameter) clasts (figure 6a). Clasts include Paleozoic limestone, Mesozoic sandstone and limestone, Cenozoic limestone, and Cenozoic volcanic rocks. The upper member is 700 feet (213 m) thick along the eastern flank of the Harmony Mountains and may be thinner below the New Harmony basin. These sediments were deposited as debris flows, based on their poorly defined to absent layering, poor sorting, and the presence of clasts several feet in diameter as far as tens of miles from the source area (Anderson and Mehnert, 1979).

Unit Taf<sub>u</sub> is a good potential aquifer based on the coarse grain size of its matrix. Several private wells on the southern and eastern flanks of the Harmony Mountains are completed in this member (plate 3), but it is probably too deep to be an attractive aquifer where it underlies Quaternary sediments in the central New Harmony and Kanarraville basins.

### Quaternary-Tertiary

**Quaternary-Tertiary sediments (QTs):** This unit includes fluvial sediments adjacent to modern stream beds but now stranded above the level of active deposition due

to stream incision. They are mostly semi-consolidated to unconsolidated gravel and sand with cobble- to pebble-size clasts (>10 to 0.08 inches [256-2 mm] diameter) and well-bedded siltstone. Excellent examples of this unit are found along Utah Route 17 north and south of the La Verkin Creek bridge. The age of sediments in unit QTs is not precisely known and may vary with location; most are probably Pleistocene to Pliocene in age based on their position below Quaternary basalt. These Quaternary-Tertiary deposits have the appropriate lithologic characteristics to be aquifers but are above the water table and are locally semilithified.

### Quaternary-Tertiary alluvial-fan deposits (QTaf):

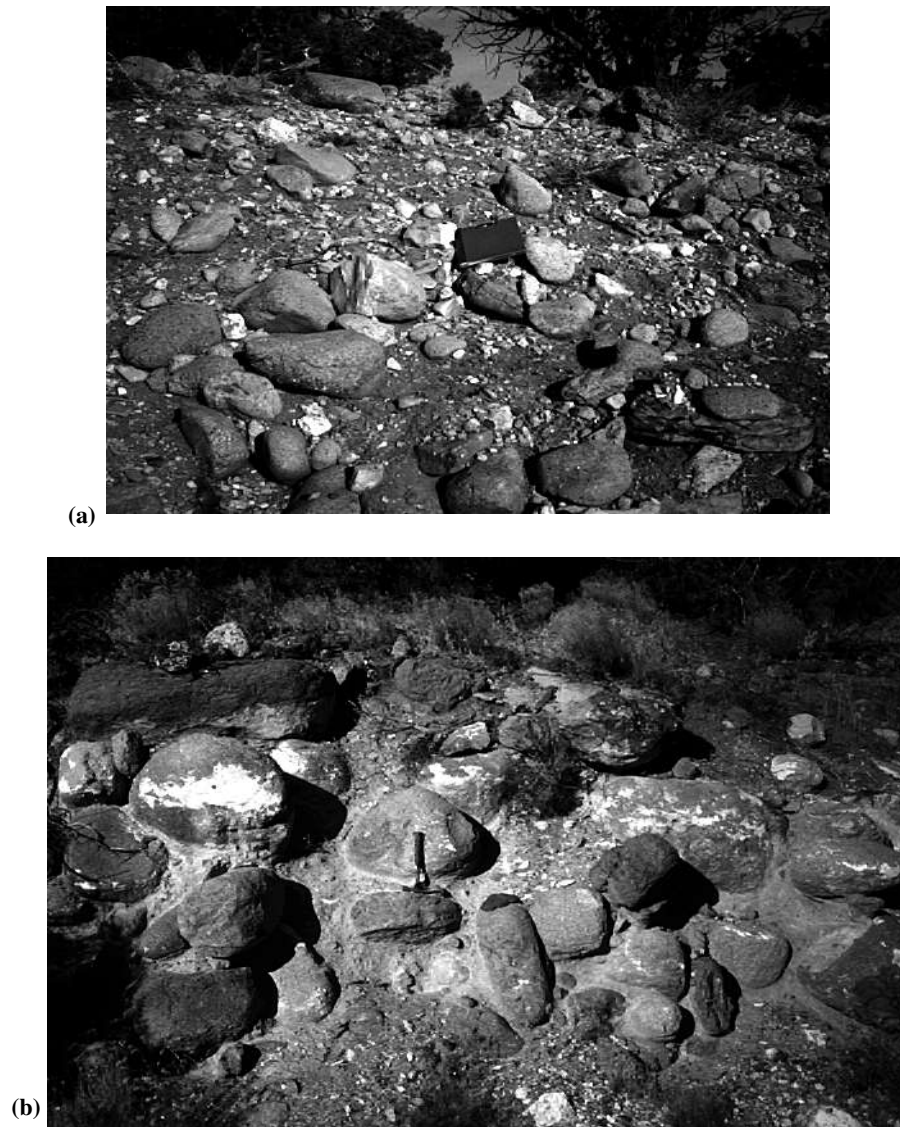
Unit QTaf consists of debris flows that emanated from the steep southern and southeastern slopes of the Pine Valley Mountains and were deposited in the foothills of the Pine Valley Mountains and in Ash Creek valley. The deposits are poorly sorted, matrix-supported boulder conglomerate with boulder- to pebble-size clasts (figure 6b). Both clasts and matrix are derived predominantly from the Pine Valley monzonite. The matrix is poorly sorted, coarse to medium sand-size, and may represent grus (coarse granitic sand derived from in-place weathering) of the Pine Valley monzonite that was mobilized with the debris flows. Exposures of this unit are found in a road cut on the frontage road east of Interstate 15 about 0.5 mile (0.8 km) south of Anderson Junction.

The debris flows and the alluvial surface on which they were deposited are incised by modern streams on the southern flanks of the Pine Valley Mountains. The deposits flowed around previously existing erosional topography northwest of Anderson Junction, and are interbedded with Quaternary-Tertiary basalt in Ash Creek valley and along the southern margin of the New Harmony basin. Unit QTaf is most likely Pleistocene in age, but it has not been directly dated and some deposits may be as old as Late Pliocene (3.4-1.6 million years ago).

Despite poor sorting, these alluvial-fan deposits are potential aquifers based on the coarse grain size of the matrix. Although unit QTaf is mostly found on alluvial-fan surfaces above the level of modern drainages, it also forms locally thick deposits interbedded with Quaternary-Tertiary basalt in Ash Creek valley (cross sections F-F', G-G', H-H', and I-I', plate 2).

### Quaternary

**Quaternary sediments, undivided (Qs):** This unit consists of fluvial, alluvial-fan, eolian, and mass-movement deposits. The latter are primarily along the base and slopes of the Hurricane Cliffs and consist of poorly sorted, massive boulder gravel, gravel, sand, and silt. The most common source units for clasts in the mass-movement deposits are Quaternary-Tertiary basalt, the Tertiary Pine Valley monzonite, the Jurassic Navajo Sandstone, the Triassic Moenkopi Formation, and the Permian Kaibab Limestone and Queantoweap Formation. Fluvial deposits are near and in modern streams and are well- to poorly bedded



**Figure 6.** Unconsolidated deposits. (a) Unit Tafu in eastern foothills of Harmony Mountains, showing unconsolidated nature of matrix and size of clasts. Boulders are Pine Valley monzonite, Tertiary volcanic rocks, and Cretaceous and Jurassic sedimentary rocks. Notebook is 9 inches (23 cm) wide. (b) Unit QTaf, along road cut southeast of Pintura. Boulders of Pine Valley monzonite supported by matrix derived from same unit. Deposit is interpreted as debris-flow material derived from Pine Valley Mountains. Hammer is 11 inches (28 cm) long.

gravel, sand, and silt. The presence of large boulders (>6 feet [2 m] diameter) in some stream beds indicates reworking of mass-wasting deposits in stream channels. Eolian deposits are derived primarily from the Navajo Sandstone, are composed of well-sorted, orange to white, medium to fine quartz sand, and are found chiefly in and adjacent to areas where that unit crops out.

Quaternary sediments vary from 0 to about 500 feet (0-152 m) in thickness. Alluvial deposits are the best prospective aquifers based on their high degree of sorting and on the presence of gravel and sand bars. Eolian deposits are typically above the water table, but may absorb precipitation and receive infiltration during high stream flow, providing recharge to the underlying Navajo Sandstone. The hydrologic properties of alluvial-fan de-

posits depend on their degree of sorting, and are worth investigating as potential aquifers where they are near recharge sources such as streams. The utility of mass-wasting deposits as aquifers may be limited by poor sorting and local extent.

## Structure of New Harmony and Kanarraville Basins

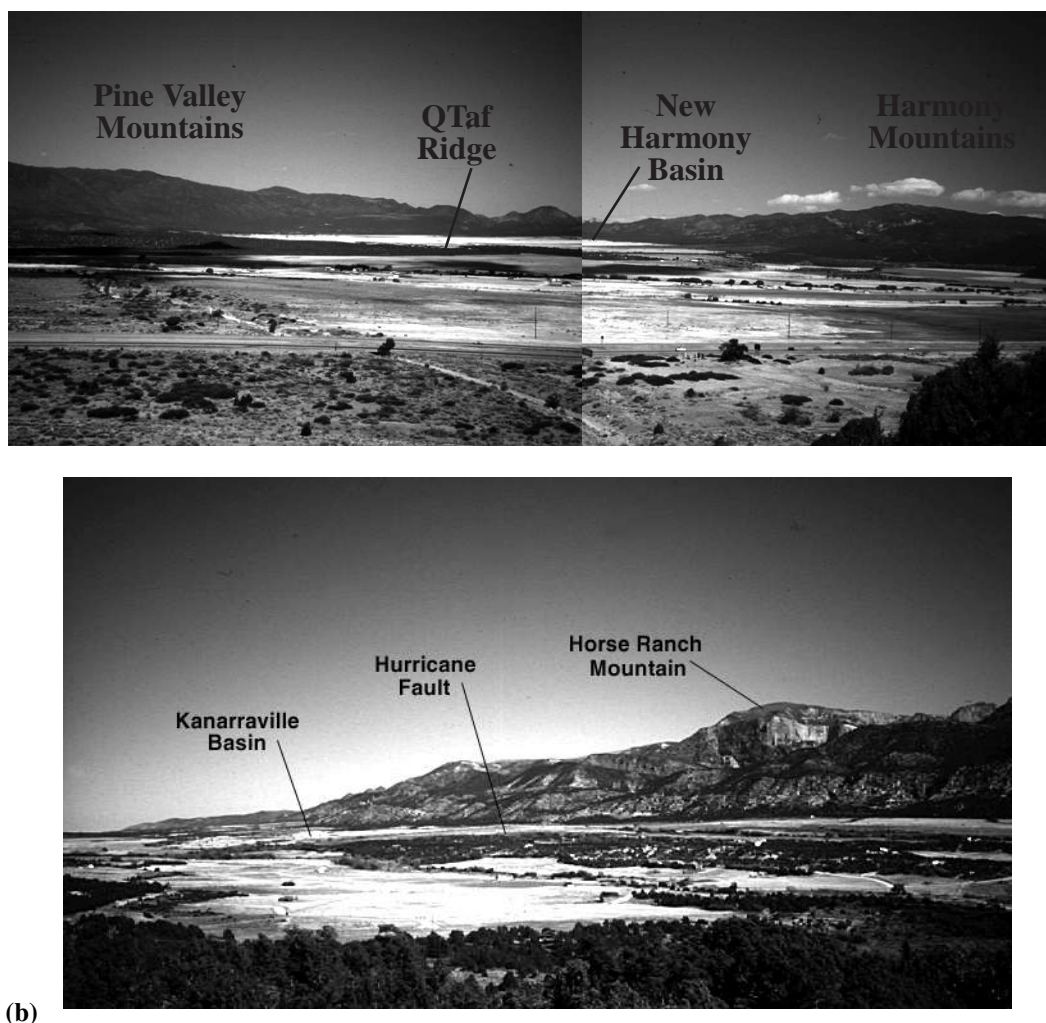
### Overview

The New Harmony and Kanarraville basins contain the most extensive and thickest unconsolidated deposits in the study area, apart from Beaver Dam Wash (figure 1b and plate 1). The basin surfaces are covered by alluvial and alluvial-fan sediments of Quaternary age that are about 10

to 500 feet (3-152 m) thick. Older unconsolidated alluvial-fan sediments (map units QTaf and Taf) underlie the Quaternary sediments and are exposed along the basin margins. The New Harmony basin trends west-northwest and is approximately 4.4 miles (7 km) long and 3.1 miles (5 km) wide (figure 7a). The basin is bounded on the north by the southern Harmony Mountains, on the west and south by the Pine Valley Mountains, and on the east by a north-south-trending ridge, composed of unit QTaf, that separates it from the Kanarraville basin. The Kanarraville basin (figures 7a and 7b) lies east of the New Harmony basin, trends northeast, is parallel and adjacent to the Hurricane Cliffs, and is approximately 11 miles (18 km) long and 1.6 miles (2.5 km) wide.

### Structure and Thickness

Cross sections A-A', B-B', C-C', and D-D' (plate 2) and the isopach map of unconsolidated sediments (plate 3) illustrate the structure of the New Harmony and Kanarraville basins. The basins evolved during late Tertiary to Pleistocene (5.3 million years ago to 10,000 years ago) regional deformation in the Colorado Plateau-Basin and Range transition zone, which included east-west crustal extension manifested by normal faults and coeval north-south shortening of the crust reflected by east-west-trending folds (Anderson and Barnhard, 1993a, 1993b; Hurlow, 1996). Appendix C describes a new model for the tectonic evolution of the New Harmony and Kanarraville basins (Hurlow, 1996).



**Figure 7.** New Harmony and Kanarraville basins. (a) View to the west of Kanarraville basin (foreground) and New Harmony basin (behind "QTaf Ridge"). (b) View to the northeast of southern part of Kanarraville basin and Hurricane Cliffs. Wooded ridge in foreground is QTaf ridge. Topographic relief from basin to Horse Ranch Mountain is about 3,000 feet (914 m).



**New Harmony basin:** Cross sections B-B', C-C', and D-D' (plate 2) show that the New Harmony basin is underlain by an asymmetric, east-southeast-trending syncline, herein named the New Harmony syncline. The northern limb of the syncline is steeper and is locally overturned (cross section D-D', plate 2). The fold deforms unit Taf but not QTaf or Qs, which filled the depression created by the fold. The syncline plunges to the east, demonstrated by the presence of the southeast-dipping lower member of Taf in the foothills of the northeastern Pine Valley Mountains (plate 1; cross section B-B', plate 2). Unconsolidated sediments are up to 1,250 feet (380 m) thick in the center of the New Harmony basin (plate 3). A normal fault may project from the Harmony Mountains south into the basin to create this local thickness maximum (plate 3). Units Qs and QTs, the best potential aquifers, are together no greater than about 250 feet (76 m) thick in the New Harmony basin and thin toward the basin margins. The irregular isopach pattern (plate 3) along the southern basin margin reflects deposition of units QTaf and Qs around previously existing erosional topography in the Pine Valley monzonite.

**Kanarraville basin:** The Kanarraville basin is wedge-shaped in cross section, thickening toward the Hurricane fault, which forms its eastern boundary (cross sections A-A' and B-B', plate 2; plate 3). Unit Qs achieves a maximum thickness of about 1,100 feet (335 m) near the Hurricane fault, but unit Taf maintains an approximately constant thickness of 1,500 feet (457 m). These relations are based on work by Anderson and Mehnert (1979) which shows that unit Taf was deposited prior to development of the Hurricane fault. Slip on the Hurricane fault occurred primarily after 1 million years ago, and unit Qs filled a subsiding depression adjacent and parallel to the fault. The resulting basin structure is an asymmetric, linear trough west of and parallel to the Hurricane Cliffs (plate 3). Qs thins westward toward the Harmony Mountains and the north-south-trending ridge on the eastern margin of the Kanarraville basin.

### Structure of the St. George Basin

As mentioned in the Geologic Summary above, the Colorado Plateau region, including the St. George basin, is undergoing regional uplift, causing streams to incise into their beds and transport their sediment load toward the ocean. Unconsolidated sediments in this type of geologic setting accumulate only in areas of local subsidence, such as adjacent to fault zones. The isopach map of unconsolidated sediments in the St. George basin (plate 4) reflects these geologic conditions.

Most unconsolidated sediments in the St. George basin were deposited by alluvial and alluvial-fan processes. Fluvial sediments accumulate adjacent to modern streams and in their present or former floodplains, and are typically less than 100 feet (30 m) thick and are, therefore, of limited use as aquifers for public water supply. The thickest accumulations of unconsolidated sediments in the St. George basin are found adjacent to the Washington fault southeast of St.

George and adjacent to a splay of the Hurricane fault, south of Pintura (plate 4; cross section I-I', plates 1 and 2). Deposits adjacent to the Washington fault likely contain abundant fine-grained sediment because they are chiefly shed from fine sandstone and gypsiferous shale of the Triassic Moenkopi Formation, which forms the hills east of the fault. These deposits may be substantially thicker south of the study area, because offset on the Washington fault increases southward (Cook, 1960). The small basin south of Pintura is at least 360 feet (110 m) thick and probably contains unit QTaf interbedded with fluvial sediments of Ash Creek. This basin is a prospective aquifer although it is relatively small and its recharge sources are limited.

## STRUCTURAL GEOLOGY AND HYDROGEOLOGY OF THE NAVAJO SANDSTONE

### Lithology and Stratigraphy

The Navajo Sandstone is a fine- to medium-grained, well-sorted quartzose sandstone colored red-brown, orange-brown, and pale gray. Accessory constituents total less than 17 percent and include chert, clay, rock fragments, feldspar, and heavy minerals (Cordova, 1978). Cement is generally calcite except in the upper 30 feet (9 m) of the formation, which is silica cemented. Trough cross-bedding, reflecting an eolian depositional environment, is a pervasive and distinctive feature of the Navajo Sandstone (figure 4). Roughly planar beds of reddish-brown fine sand to shale are present sporadically in the lower third of the unit and probably represent flooding surfaces.

Cordova (1978) divided the Navajo Sandstone into three informal "units": a lower unit of red-brown, planar-bedded sandstone, siltstone, and mudstone, with thin beds of trough cross-bedded sandstone; a middle unit of light orange-brown, trough cross-bedded sandstone; and an upper unit of pale gray, weakly cemented, trough cross-bedded sandstone. Cordova's (1978) lower unit corresponds to the transition zone between the Kayenta Formation and the Navajo Sandstone, described below. The upper unit corresponds to parts of the Navajo Sandstone, mostly in the upper half of the formation, that have been bleached by hydrothermal fluids and/or ground water. The downward limit of bleaching has an irregular shape and does not correspond to a lithologic boundary in the Navajo Sandstone, and therefore should not be designated as an informal stratigraphic unit. The presence of the bleached zone is hydrogeologically important, however, because partial dissolution of the cement in the Navajo Sandstone during bleaching resulted in softening of the rock and most likely an increase in secondary porosity.

The Navajo Sandstone is about 2,800 feet (853 m) thick west of the Gunlock fault zone (Hintze and others, 1994) and about 2,000 feet (610 m) thick at Sandstone Mountain west of Hurricane and in Zion National Park (Gregory,



1950). The thickness of the Navajo Sandstone could not be measured elsewhere in the study area due to lack of internal paleohorizontal markers and variable dips of upper and lower bounding units. Fossils have not been recovered from the Navajo Sandstone, but its age is constrained as Early Jurassic by fossils in the underlying Kayenta Formation and overlying Carmel Formation (Hintze and others, 1994).

The lower 100 to 150 feet (30-46 m) of the Navajo Sandstone is transitional with the underlying Kayenta Formation. In this transition zone, reddish-brown, fine-grained sandstone and thin shale beds typical of the Kayenta Formation are interbedded with trough-cross-bedded eolian sandstone typical of the Navajo Sandstone, and with <200 foot-thick (6m) tabular sand beds with poorly developed, fine, wavy bedding. Sansom (1992) interpreted the latter beds as representing sabkha (intertidal clastic and evaporite) deposits and the transition zone as representing a change in depositional environment from shallow marine to eolian. In this study the Navajo-Kayenta contact is placed at the top of the last shale bed greater than 1 foot (0.3 m) thick, following Cook (1960) and Willis and Higgins (1996). The interpretation that the transition zone contains evaporite deposits is important for the hydrogeology of the Navajo Sandstone, because it suggests that ground water in the transition zone may have high salinity and/or total dissolved-solid content and that the rocks may have lower porosity than the overlying eolian deposits. Hintze and others (1994) and Hintze and Hammond (1994) included the transition zone in their upper member of the Kayenta Formation. The Navajo Sandstone is overlain by shale, gypsiferous shale, and sandstone of the Jurassic Temple Cap Formation and by marine limestone of the Jurassic Carmel Formation, which are undivided in figure 4 and plates 1 and 2.

Cordova (1978) reported an average effective porosity of 17 percent for the Navajo aquifer based on laboratory measurements of unfractured samples, and an average total porosity of 32 percent based on resistivity and neutron logs of wells. The higher value for the total porosity likely reflects the presence of fractures. Hood and Danielson (1979) reported effective porosity measurements of 20 to 25 percent for the Navajo Sandstone in southeastern Utah. The U. S. Geological Survey recently completed three aquifer tests of the Navajo aquifer in the study area which yielded hydraulic conductivity values of 0.18 to 31.7 feet per day (0.05-9.7 m/d) (V. Heilweil, USGS, Anderson Junction, Hurricane Bench, and Grapevine Pass aquifer tests, written communication, 1997).

## Regional Structure

### Introduction

The geologic map (plate 1), cross sections (plate 2), structure-contour maps (plates 5A and 5B), and fracture-domain map (plate 6) illustrate the structure of the Navajo Sandstone in the central Virgin River basin. The structure-

contour maps (plates 5A and 5B) were constructed primarily from surficial structural data; few wells penetrate the base of the Navajo Sandstone or reach its top where it is buried (appendix D), and geophysical data are lacking. The stratigraphic thickness of the Navajo Sandstone was assumed to vary linearly between the Gunlock fault zone and Sandstone Mountain, the only places where it could be measured directly. Evaluating the structure of the Navajo Sandstone is further complicated by the lack of internal paleohorizontal surfaces, so dips in areas far from its upper and lower contacts are based on geologically reasonable estimates that incorporate outcrop width and stratigraphic thickness.

The structure-contour maps can be used to estimate the drilling depth to the base or top of the Navajo Sandstone, by subtracting the elevation of the base or top, respectively, from the ground-surface elevation at the point of interest. Elevations at points between contour lines can be estimated by linear interpolation. More precise estimates of drilling depth should be obtained using smaller scale maps, detailed structural data, and well data, if available.

The Navajo Sandstone aquifer is subdivided into six structural compartments (plates 5A, 5B, and 6), defined as discrete fault-bounded masses with internally consistent structure. The structure and bounding faults of each structural compartment are described below. Structural compartments include the exposed areas indicated on plate 6, plus subsurface regions approximately 1,000 to 2,000 feet (300-500 m) below and, where the top of the Navajo Sandstone dips below the ground surface, laterally away from outcrops. Physical boundaries of structural compartments may be erosional, where the bottom of the Navajo Sandstone is exposed, or may be faults.

### Compartment I: Red Hollow Area

Several faults completely sever the Navajo Sandstone between compartments I and II, and Compartment I is highly faulted and jointed. Bedding in both the Kayenta and Carmel Formations dips 30 degrees northeast, indicating a stratigraphic thickness of 2,800 feet (853 m) for the Navajo Sandstone.

### Compartment II: West of Gunlock Fault Zone

The structure of compartment II is characterized by northeast dips of 20 to 25 degrees in its northwestern part and by the Shivwits syncline in its southeastern part (plates 1 and 5A). The hinge of the Shivwits syncline trends north to northeast and plunges gently north, and the fold dies out northward near the Gunlock fault zone.

The Gunlock fault zone (figure 8a), which forms the eastern boundary of compartment II, has components of down-to-the-west normal slip and left-lateral strike-slip (Hintze and Hammond, 1994). Stratigraphic separation across the Gunlock fault zone decreases from the north, where Cretaceous rocks are juxtaposed against the Navajo Sandstone, to the south, where it is zero. This complicated

geometry results from the combined effects of southward-decreasing throw (Hintze and Hammond, 1994) and a pre-existing northward dip of stratigraphic units. As a result, the Navajo Sandstone is completely disconnected across the Gunlock fault zone (figure 8a; cross section K-K', plate 2) except along a 1.6 mile (1 km) stretch south of Gunlock Reservoir, where the vertical overlap is less than about 330 feet (100 m).

### **Compartment III: Red Mountains**

The Navajo Sandstone strikes approximately east-west and dips 6° to 10° north between the Gunlock and Snow Canyon fault zones (plate 5A; figure 8a), but its dip must decrease northward based on its width of exposure and stratigraphic thickness, which decreases gradually to the east.

### **Compartment IV: Between West and East Strands of the Snow Canyon Fault Zone**

The relatively small, triangular area between strands of the Snow Canyon fault zone is provisionally designated as a separate structural compartment. The main strand of the Snow Canyon fault zone strikes northwest and defines West Canyon in Snow Canyon State Park (figure 8b), and a north-northwest-striking fault splay defines East Canyon. Exposures of these faults reveal 3 foot-thick (1 m) gouge zones between 3 to 6 foot-thick (1-2 m) zones of highly jointed rock. Neither the sense nor the amount of slip on these fault strands are known due to lack of stratigraphic markers and diagnostic structures in the fault zones.

### **Compartment V: Snow Canyon Fault to Upper Ash Creek Valley**

The Navajo Sandstone is structurally continuous between the Snow Canyon fault zone and the northeasternmost extent of outcrops east of upper Ash Creek valley. Several northeast-striking normal faults disrupt the physical continuity of the Navajo Sandstone in and west of Ash Creek valley (cross sections H-H' and I-I', plate 2), forming the southeastern boundary of compartment V.

The Navajo Sandstone curves gradually from a northeast dip direction south of Snow Canyon, to a north dip direction near St. George and Washington, to a northwest dip direction northeast of Washington, defining the St. George syncline (plates 1 and 5A; Cordova, 1978). The dip in the Navajo-Kayenta transition zone increases gradually from about 5 degrees near Washington, to about 18 degrees at Leeds Creek (plate 5A), due to folding in the Virgin anticline. The top of the Navajo Sandstone dips about 5 degrees to 10 degrees northward in the foothills of the Pine Valley Mountains (figure 8c), and projects into the subsurface below the crest of the range. The surface elevation also increases steadily to the north, so that the top of the Navajo Sandstone is about 8,200 feet (2,500 m) deep below Signal Peak (cross section K-K', plate 2).

The Navajo Sandstone is cut by three major north- to northwest-striking faults between St. George and Leeds Creek: the St. George, Washington, and Washington Hollow faults (plates 1, 5A, and 5B). The St. George fault has about 400 feet (122 m) of down-to-the-west normal throw near St. George, and its trace disappears northward (Willis and Higgins, 1995). The Washington Hollow fault has about 500 feet (152 m) of down-to-the-west normal throw where it cuts the Navajo-Carmel Formation contact (Willis and Higgins, 1995). The Washington fault has about 700 feet (213 m) of down-to-the-west normal throw near Washington (Willis and Higgins, 1995), and slip on this fault increases to the south where it continues to the Grand Canyon (Cook, 1960). The trace of the Washington fault becomes indistinct within the Navajo Sandstone, but Cordova (1978) connected it with the Washington Hollow fault to the north. In this report, the two faults are not considered to be connected based on field and photo-geologic interpretations.

The structure of the Navajo Sandstone northeast of Leeds Creek reflects the complex tectonic evolution of Ash Creek valley and vicinity (cross sections E-E', F-F', G-G', H-H', I-I', and K-K', plate 2). The Navajo Sandstone was folded in the Virgin anticline during Late Cretaceous time (about 100-80 million years ago). The Virgin anticline plunges out near Anderson Junction. Northeast of Anderson Junction is a northeast-striking anticline-syncline-anticline set with axes along the Hurricane Cliffs, Ash Creek Valley (syncline now buried), and low foothills of the Pine Valley Mountains (Cary, 1963), respectively. Erosion during Late Cretaceous to Early Eocene time (about 80-50 million years ago) breached the crest of the anticline in the foothills of the Pine Valley Mountains so that Paleocene to Middle Eocene conglomerates and the Eocene-Oligocene Clarion Formation were deposited directly on the Navajo Sandstone there (Cook, 1960; Goldstrand, 1994). These folds were then cut by at least two generations of normal faults, including the Hurricane fault, that were localized along the fold axes (Kurie, 1966; Anderson and Mehnert, 1979). This tectonic history resulted in a complex structural geometry characterized by steeply- to moderately-dipping fault blocks (cross sections E-E', F-F', G-G', H-H', and I-I', plate 2). The Navajo Sandstone in this region is highly jointed and is cut by numerous north- to northeast-striking faults. Northwest of this complexly deformed area, the Navajo Sandstone is less faulted and dips 15 degrees to 25 degrees northwest.

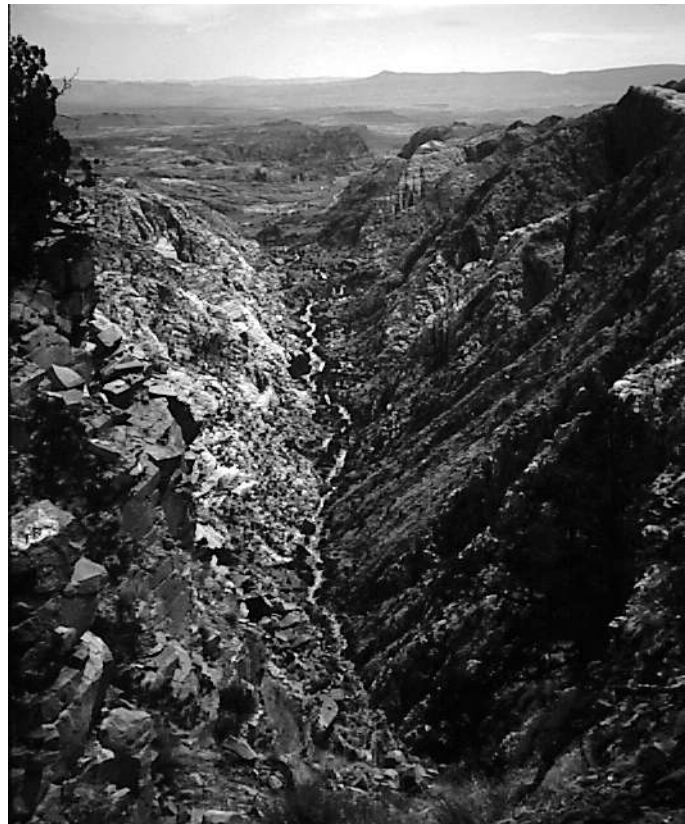
The Navajo Sandstone is in the hinge zone of the Virgin anticline north of Anderson Junction (plate 1), where its structural continuity is disrupted by northeast-striking normal faults (cross section I-I', plate 2).

### **Compartment VI: Southeast Limb of Virgin Anticline**

Two distinct outcrop areas on the southeast limb of the Virgin anticline, the Sandstone Mountain and Sand Mountain areas, comprise structural compartment VI. These areas are separated by a Quaternary-late Tertiary basaltic



(a)



(b)

**Figure 8.** Regional structure of the Navajo Sandstone. (a) View to the east of western Red Mountains, showing juxtaposition of Navajo Sandstone (Jn) in the hanging wall of the Gunlock fault zone against Kayenta Formation (Jk) and lower Jn in the footwall, virtually disconnecting the Navajo across the fault. Qb is Quaternary basalt cut by the Gunlock fault zone. Santa Clara River valley is in foreground. Maximum relief of cliffs is about 1,600 feet (488 m). (b) View to the south of West Canyon, Snow Canyon State Park, underlain by the Snow Canyon fault zone which cuts the Navajo Sandstone. Topographic relief is about 1,400 feet (427 m).



**Figure 8(c).** View to the north of Navajo Sandstone dipping 10 degrees northwest in foothills of Pine Valley Mountains. Photo taken from top of Navajo Sandstone southwest of Quail Creek. Light-colored unit above Navajo is Jurassic Carmel Formation. Topographic relief on cliff face is about 1,312 feet (400 m).

volcanic field near the town of Hurricane, and the structural continuity of the Navajo Sandstone is likely disrupted by feeder dikes below the cinder cones. In the Sandstone Mountain area, the Kayenta Formation dips 20 degrees to 35 degrees east in the southeastern limb of the Virgin anticline (plate 5A) and Navajo Sandstone is highly jointed and faulted. The Navajo Sandstone dips up to 15 degrees southeast along the northwest margin of Sand Mountain, but its dip must decrease eastward to 5 degrees or less. The dip direction of the Navajo Sandstone changes gradually along the southern margin of Sand Mountain, defining the broad, open, Sand Mountain syncline (plates 1 and 5A; Cordova, 1978).

### Pine Valley Mountains and Bull Valley Mountains

The Navajo Sandstone in the northern part of the study area is buried beneath up to 5,000 feet (1,524 m) of younger sedimentary and volcanic rocks, and its structural continuity may be disrupted by intrusions, including the Pine Valley laccolith and intrusions in the Bull Valley Mountains, and by numerous faults (plate 1). Consequently, the position of the Navajo Sandstone below the Pine Valley and Bull Valley Mountains cannot be inferred with confidence. North of the study area, a deep bore hole and seismic-reflection data near The Three Peaks, 5 miles (8 km) northwest of Cedar City, place the Navajo Sandstone at about 6,300 feet (1,920 m) below the surface and show that it lies in the footwall of the Cretaceous Iron Springs thrust (van Kooten, 1988). However, this information is of limited use to this study because the regional structure between The Three Peaks and the St. George area is poorly known. The Carmel Formation is exposed adjacent to intrusions in the Bull Valley Mountains and Iron Mountain

district (plate 1), so the Navajo Sandstone is near the surface in those areas but its structure is likely complex.

The 21 million-year-old Pine Valley monzonite intruded the upper part of the Claron Formation as a tabular sheet parallel to bedding (figure 2b; cross sections J-J' and K-K', plate 2B; Cook, 1960), but the structure below the central part of the intrusion is uncertain. Cook (1960) illustrated the Pine Valley laccolith as a stratigraphic layer concordant with the underlying Claron Formation, but dikes that fed the intrusion must be present beneath it. Field work for this study revealed an exposed intrusive neck in the western Pine Valley Mountains, and D. Hacker (Kent State University, verbal communication, 1995) hypothesizes that intrusive centers are also present in the central and northeastern parts of the range. Based on these observations, cross sections J-J' and K-K' (plate 2) illustrate a system of dikes inferred to have fed the Pine Valley laccolith and related volcanic eruptions, though the geometry and location of this system are speculative. These dikes would disrupt the structural continuity of the Navajo Sandstone beneath the Pine Valley Mountains, so that it does not project below and north of the laccolith in a simple manner.

## Fracture Systems

### Hydrogeologic Importance of Fractures

The following sections use the term *permeability* to describe interconnected void space in rocks, and the term *hydraulic conductivity* to describe movement of ground water through an aquifer as measured by aquifer tests or other hydrogeologic data. Both terms are prevalent in the hydrogeologic literature and usage varies, so that the terms

are virtually interchangeable. Because hydrogeologic data from the study area are presently sparse, much of the discussion below addresses the theoretical effects of fractures on ground-water flow.

Fractures increase the hydraulic conductivity of bedrock aquifers by providing high-permeability flow pathways and increasing bulk porosity, and preferred orientation in a fracture population results in anisotropic permeability and hydraulic conductivity. For example, laboratory measurements on unfractured sample cores of Navajo Sandstone from the study area yielded an average hydraulic conductivity of 2.1 feet per day (0.6 m/d), whereas well tests yielded hydraulic conductivities of 3.4 to 6.1 feet per day (1-1.9 m/d) (Cordova, 1978). The higher hydraulic conductivity values recorded by the field data are due primarily to joints (Cordova, 1978). Thus, characterization of the fracture systems of a bedrock aquifer is essential to understanding its hydrogeology. This section describes the character, geometry, and distribution of fractures in the Navajo Sandstone, and presents quantitative data on their density and orientations. Joints, joint zones, faults, and fault zones deform the Navajo Sandstone in the study area. Joints are by far the most abundant type of fracture, but are probably matched in hydrogeologic importance by joint zones and fault zones.

The density and orientations of fractures in the Navajo Sandstone are quantified at both outcrop scale and with 1:20,000-scale aerial photographs. Outcrop-scale data collection utilized the scanline technique (La Pointe and Hudson, 1985), in which fracture properties are recorded along two perpendicular sampling traverses. Aerial-photograph data were based on graphic analysis of fracture-trace maps derived from the photographs. Appendix E describes these methods in more detail.

## Structural Characteristics of Fractures in the Navajo Sandstone

**Joints and joint zones:** Joints are planar fractures that form when opposite sides of rock move apart perpendicular to the direction of fracture propagation (Twiss and Moores, 1994). Joint zones are discrete zones of tightly spaced, subparallel joints (figures 9a and 9b) (Antonellini and Aydin, 1994). Because there is no relative movement parallel to the fracture plane during their formation, joints lack material products of faulting, such as gouge and breccia, that affect permeability. Ground water travels both parallel and perpendicular to joint surfaces in rocks having primary porosity such as the Navajo Sandstone, but permeability is about an order of magnitude greater within the joint plane (Antonellini and Aydin, 1994).

Joints form parallel to the local direction of maximum compressive stress and perpendicular to the direction of least compressive stress, so joint populations commonly have preferred orientations. Consolidated rock aquifers containing joints with a preferred orientation have anisotropic hydraulic conductivity, with the major axis of the effective permeability tensor parallel to the mean strike of

the preferred orientation (Ritzi and Andolsek, 1992). Joint populations in the Navajo Sandstone typically contain one strongly defined preferred orientation and one preferred orientation of lesser magnitude. This report designates the statistically most prominent preferred orientation as the principal joint set, and less prominent preferred orientations as secondary joint sets. Joints of the principal set typically have greater lateral and vertical trace lengths than those of the secondary sets.

Individual joints in the Navajo Sandstone are planar to gently curved and typically lack surface structures and infilling minerals. Many joint surfaces are oxidized to a red-orange to brown color, reflecting circulation of ground water when the rocks were more deeply buried. Apertures measured at the surface vary from <0.04 to 20 inches (1 mm-50 cm), but most joints are probably "tight" (aperture of less than 0.04 inches [1 mm]) below the weathering zone, approximately 50 feet (15 m) below the surface (Nelson and Handin, 1977). Neither cementation nor aperture vary systematically with joint orientation in the study area, but pronounced variations in frequency and average length with orientation are common, reflecting the presence of primary and secondary joint sets.

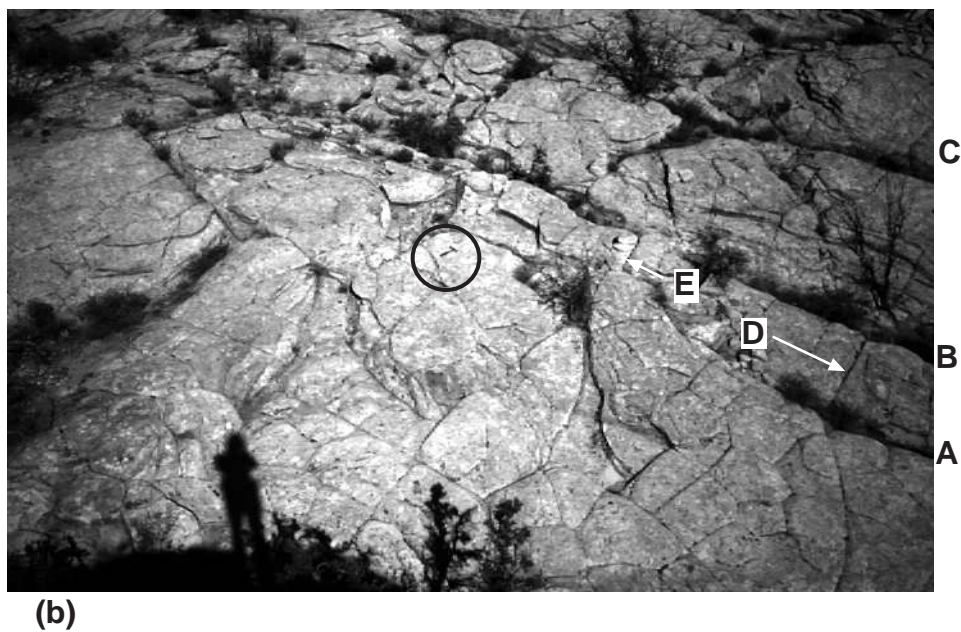
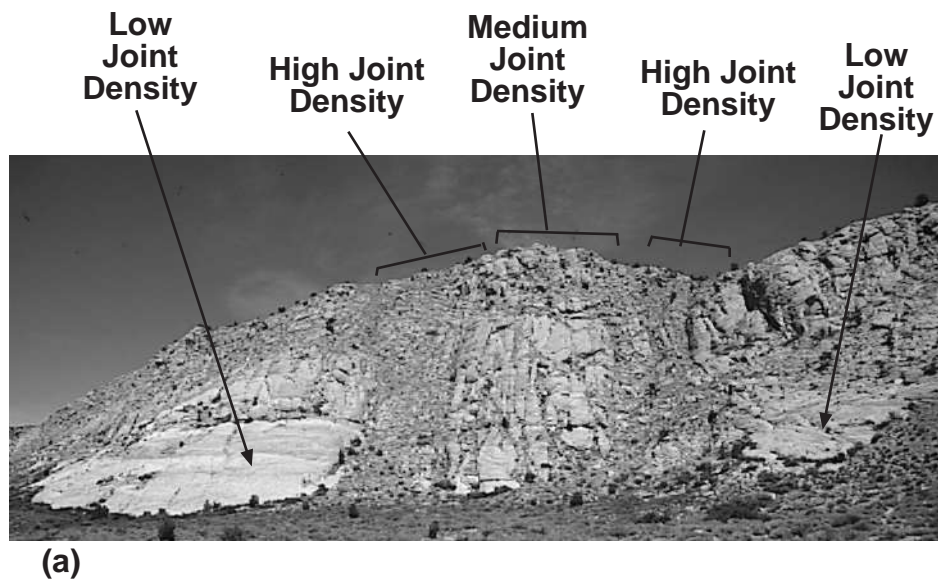
Most joints in the study area dip greater than 70 degrees, and have average lengths of 0.5 to 600 feet (0.15-200 m). Individual joints of the principal set may terminate in undeformed rock, in sets of closely spaced joints that intersect an adjacent principal joint (figure 9c), or they may curve toward and intersect adjacent principal joints (figure 9b). Joints of the secondary set typically are perpendicular to and bounded by joints of the principal set, so they are shorter and spaced more widely than joints of the principal set (figure 9b). The secondary joints link individual members of the principal set throughout the rock mass and near their terminations (figure 9b). Principal joints are thereby physically connected over length scales of hundreds to thousands of feet (33-1,500 m), and likely provide important transport pathways for ground water.

Joints that form along cross-bedding planes dip about 40 degrees or less, are less than 6 feet (2 m) long, and are spaced 0.4 inches to 33 feet (1 cm-10 m) apart. These bedding-plane joints are probably closed below the weathering zone due to the weight of overlying rock, and their main hydrologic importance in the study area may be to capture surface runoff during rainfall and flooding.

Joints within joint zones define the local principal set and are spaced approximately 0.2-4 inches (5 mm-10 cm) apart (figure 9d), an order of magnitude closer than in adjoining areas. Joint zones are commonly 150 to 3,000 feet (46-914 m) long and likely penetrate the entire thickness of the Navajo Sandstone. Joint zones result in heterogeneous distribution of joint density (figures 9a and 9b), posing problems for characterizing fracture density and determining ground-water conditions. Appendix F provides a more detailed account of the heterogeneous distribution of joints.

**Faults and fault zones:** Faults are fractures that accommodate the relative movement of rocks on either side,





**Figure 9.** Joints and faults in the Navajo Sandstone. (a) View to the northeast of Navajo Sandstone from State Route 18, 8 miles (13 km) north of St. George. Joint density is heterogeneous and is classified into high-, medium-, and low-density zones. Topographic relief on cliff is about 600 feet (183 m). (b) Low-density jointing, sample site f-1-bh. Persistent joints in upper-right corner, labeled A, B, and C, define the principal set and strike north-south. Joint A terminates by curving toward joint B. Joints D and E of the secondary set link joints A and B. Hammer (circled) is 11 inches (28 cm) long.



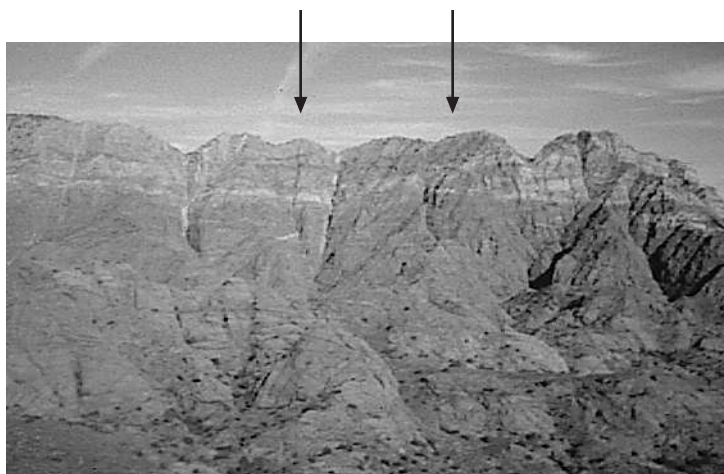


(c)

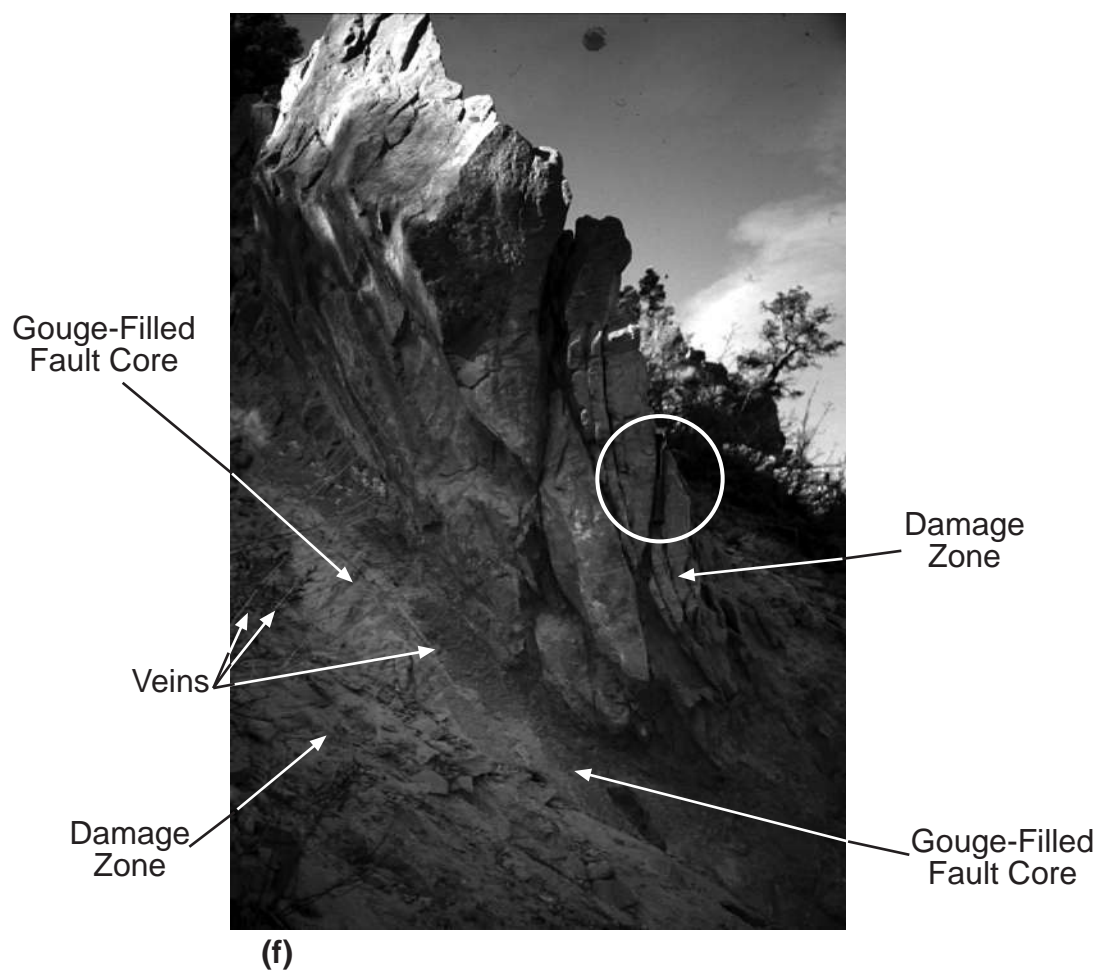


(d)

**Figure 9.** (c) View to the northeast of southeast-dipping, short joints (near hammer) linking longer, northeast-striking joints A and B. Sample site f-5-gpw. Hammer (circled) is 11 inches (28 cm) long. (d) Detail of north-striking, high-density joint zone, sample f-7-scw-ab, Snow Canyon State Park, just south of where East and West canyons merge. Hammer is 11 inches (28 cm) long.



(e)

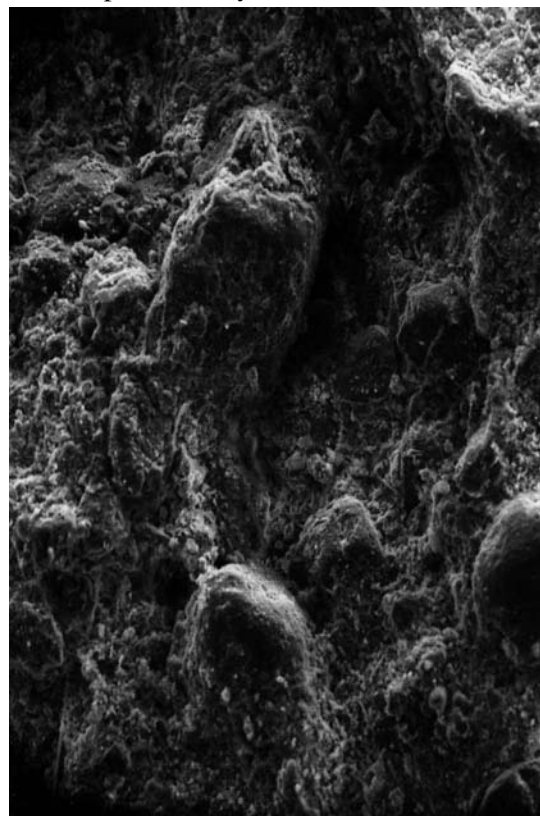


(f)

**Figure 9.** (e) View to the northeast of joint zones that have been reactivated as faults (indicated by arrows), northeast wall of Washington Hollow. Note northwest-side-down separation of horizontal, light-colored layer by southeastern fault (on right). Topographic relief of cliffs is about 1,000 feet (335 m). (f) Fault zone in Navajo Sandstone, along South Ash Creek, about 2 miles (3.2 km) northeast of Interstate 15, displaying fault core-damage zone structure. Hammer (circled) is 11 inches (28 cm) long.

and fault zones are composed of numerous, subparallel faults and associated joints. The processes and structures associated with faulting are different from those associated with joints and, consequently, the two types of fractures have different hydrologic properties. Most faults have high permeability parallel to their planes and low transverse permeability, but the relative magnitudes of these permeabilities vary with rock type and displacement (Antonellini and Aydin, 1994; Caine and others, 1996).

Displacement on a fault results in fracturing and grain-size reduction of rock in and adjacent to the slip surface, producing breccia, cataclasite, and gouge (listed in order of decreasing average grain size, from 10 to 0.002 inches [250 mm-0.05 mm]). Fault-zone material is commonly less permeable than unfaulted rock due to its finer grain size and the angular shape of fractured grains (figure 10). Fractured grains and clay minerals in gouge and cataclasite commonly define a geometric fabric with the long axes of the particles oriented parallel to the fault plane. This fabric reduces permeability perpendicular to the fault plane (Antonellini and Aydin, 1994). Fault breccia may be highly permeable if it is uncemented, but circulation of hydrothermal fluids commonly results in cementation which drastically reduces permeability.



5 μm (0.00031 in)

**Figure 10.** Scanning electron microscope (SEM) image of fault gouge in the Navajo Sandstone, from fault zone shown in figure 9f. Larger grains are quartz; finer particles are fine-grained quartz, clay minerals, oxides, and sulfates interstitial to and coating the quartz grains. Weak foliation in fault gouge is vertical in this view. Hand specimen of gouge is white, very fine grained, and flaky.

Fault-zone materials are located in the central part or core of the fault zone, and are bounded on either side by deformed regions called damage zones (figure 9f) (Caine and others, 1996). The characteristics and thickness of gouge and damage zones vary with rock type and displacement. Damage zones contain dense arrays of joints and minor faults but lack fault-zone material, and consequently may be highly permeable (Caine and others, 1996). Because damage zones are parallel to fault planes, they enhance fault-parallel permeability.

Faults may juxtapose geologic units with different permeabilities, possibly resulting in hydrologic compartmentalization of aquifers (Ashland and others, 1996). Conversely, some faults may provide a hydraulic connection between aquifers (Stone, 1967). Faults within a single aquifer but with thick, gouge-filled core zones may also restrict or alter ground-water flow paths.

Major structures that cut the Navajo Sandstone include the Gunlock, Washington, Washington Hollow, and Hurricane faults (plate 1). Numerous faults that cut the Navajo Sandstone but do not offset its contacts are omitted from plate 1 but may be hydrologically important, as discussed below. Many joint zones have been reactivated as fault zones, particularly in the region between Snow Canyon and Washington Hollow (figure 9e), and on Sandstone Mountain.

The internal structure of fault zones and reactivated joint zones in the Navajo Sandstone is characterized by a core zone containing gouge bounded on either side by damage zones with high joint density (figure 9f). The gouge is white to red, clay-rich, and about 2 inches to 3.5 feet (1 cm-1 m) thick. A subtle planar fabric, defined by elongate clay minerals and mineral fragments, is oriented parallel to the fault plane. Examination of fault gouge with a scanning electron microscope at 400x magnification (figure 10) reveals angular to rounded quartz grains mantled by very fine, platy clay, oxide, and sulfate minerals. This very fine-grained material likely results in low permeability within the gouge zone (Antonellini and Aydin, 1994). Hard, fine-grained calcite veins locally cut the gouge, further reducing permeability (figure 9f). The damage zones are 3 to 6 feet (1-2 m) thick and are characterized by joints and minor faults spaced approximately 0.4 to 3 inches (10 mm-10 cm) apart. Joints in the damage zone typically have variable orientations, form a complex, well-connected network, and lack cement (figure 9f). Based on these characteristics, fault zones in the Navajo Sandstone likely act as barriers perpendicular to the fault plane but as excellent conduits parallel to the fault plane.

### Distribution of Fractures in the Navajo Sandstone

Plate 6 and tables G.1 and G.2 show the orientation and density of fractures in the Navajo Sandstone, derived from scanline analyses, aerial photographs, and field work. Structural compartments are subdivided into fracture domains, defined as regions with distinct fracture populations as distinguished by orientation. Plate 6 depicts the fracture data as rose diagrams, which are geographically oriented,



polar-coordinate histograms showing the relative frequency of fracture orientations grouped into 15-degree sectors. The scanline data omit bedding-plane joints to emphasize the steeply dipping joints, which are hydrologically more important. Rose-diagram plots derived from aerial photographs show the orientations of joint zones and very long joints. The rose diagrams indicate the orientations and relative importance of the principal and secondary joint sets (also see tables G.1 and G.2). The rose-diagram plots derived from scanline data depict relative joint frequency, while those derived from aerial-photograph data depict joint frequency weighted according to length (see appendix E for more details).

Fracture densities (plate 6 and tables G.1 and G.2) are useful in evaluating the relative degree of fracturing between different sample sites. However, fracture densities for outcrop and aerial photograph data should not be compared directly because they reflect different scales of features and methods of data acquisition. Figure 11 shows that there is no correlation between fracture densities derived from the two techniques.

Fracture population characteristics of each structural compartment and fracture domain are summarized below.

I. Fractures visible on aerial photographs are abundant and have relatively long traces. Most fractures are oriented north-northeast, but several anomalously long, northwest-striking fault or joint zones that are not well expressed on the rose plot are also present.

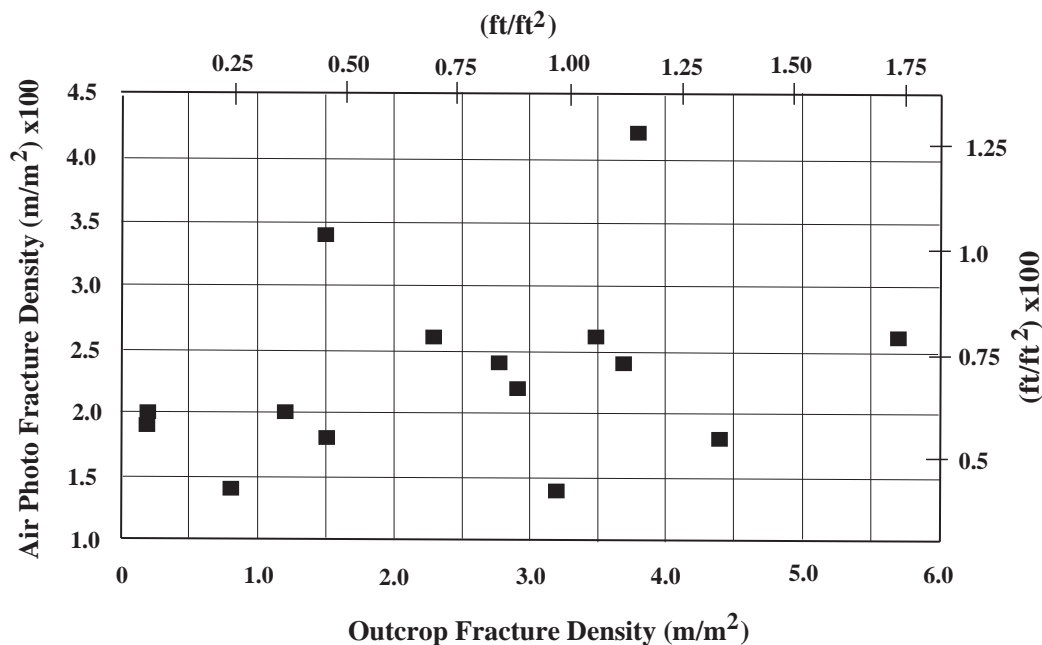
II. Most fractures in domain IIa are oriented north-

northeast to northeast, although a few northwest-striking fault or joint zones with long outcrop traces are present. Domain IIb is characterized by high fracture density, and the strikes of primary fracture sets vary with location.

III. Vertical displacement on the Snow Canyon fault zone is not large, and the sense of motion on the fault is not known, but its western and eastern strands are designated as compartment boundaries because their cores contain 3 foot-thick (1 m) gouge zones. Compartment III consists of one fracture domain characterized by variable orientations and numbers of primary sets. Most sample sites contain one primary fracture set oriented north-northwest to northeast, but several sites have two subequal principal sets oriented north to northeast and west to northwest.

IV. No fracture data were collected from this compartment due to poor exposure and its remote location.

V. Fracture domain Va is characterized by one north-northeast-striking principal joint set. One exception is aerial photograph sample bh1, which also contains widely spaced, northwest-striking joint zones that do not show prominently on the rose diagram. Field work indicates that these northwest-striking joints are younger than the north-northeast-striking principal set, and utilize minor fault zones that predated all jointing. Domain Vb contains two principal sets, representing northeast- and northwest-striking joints and joint zones, with the northeast set more prominent at most locations. Some members of both principal sets have been reactivated as faults (figure 9e) and contain a core of fine, white to red, clay-rich gouge. Joints



**Figure 11.** Comparison of fracture densities measured by scanline and aerial photograph techniques where sample areas for the two methods coincide. No correlation exists ( $R^2 = 0.1$ ).

and joint zones in fracture domain Vc are organized into a dominant primary set that strikes north-northeast to north-east. Domain Vd is distinguished by high fracture density and numerous northeast-striking fault zones.

VI. Domain VIa is characterized by high fracture density, variably oriented principal sets, and reactivation of joint zones as faults, reflecting a complex tectonic history. Domain VIb contains one principal set comprising north-east- to north-northeast-striking joints and joint zones, and has low fracture density. Joints and joint zones in domain VIc comprise one primary set oriented north-northwest.

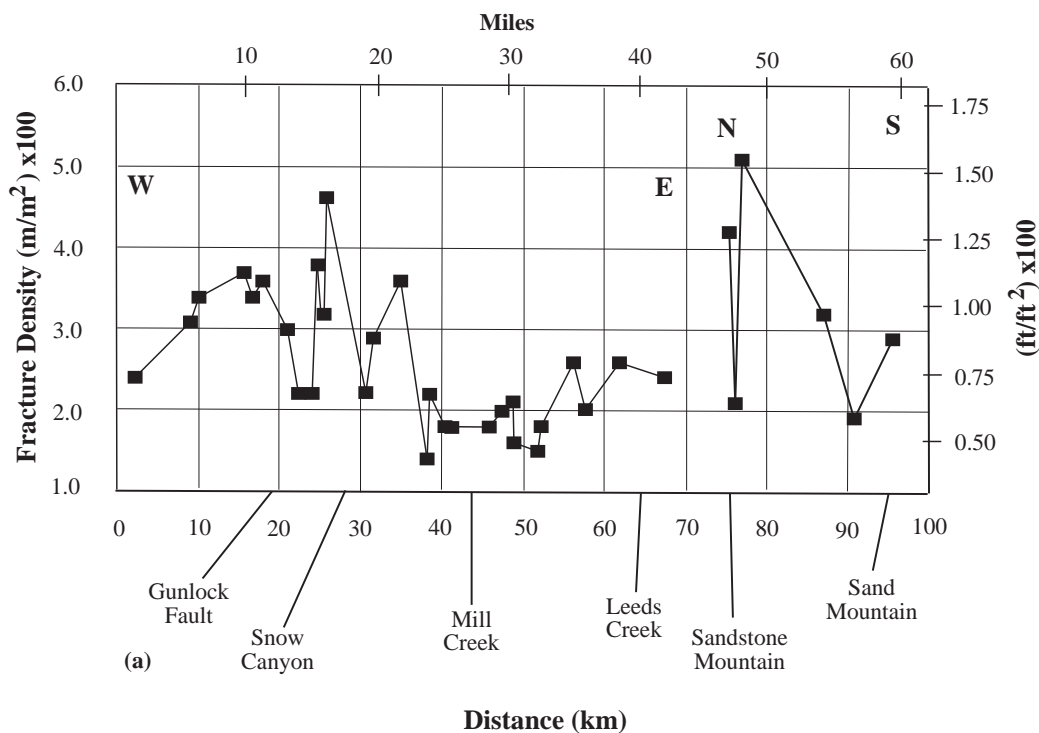
Figures 12a and 12b show regional variations in fracture density. Both outcrop and aerial photograph data show heterogeneous distribution of fracture density, although some large-scale systematic trends are apparent. Fracture density based on aerial photograph data (figure 12a) is relatively high near the Gunlock and Snow Canyon fault zones, near Anderson Junction, and at Sandstone Mountain, and is relatively low in the vicinity of Mill Creek and Sand Mountain. Variation in outcrop-scale fracture density (figure 12b) is less systematic but also shows high values near the Snow Canyon fault zone, Anderson Junction, and Sandstone Mountain, and low values on Sand Mountain. Some of the variation in outcrop-scale fracture density reflects sampling of an inhomogeneous population (appendix F), but a basic regional trend is apparent.

The high fracture densities near the Gunlock and Snow Canyon fault zones likely reflect the effects of protracted slip and large displacements, in effect representing large-scale damage zones. Outcrop samples f-11-ds1 and f-12-ds2, located northwest of Anderson Junction (plate 6), illustrate this relation. Sample f-11-ds1 is adjacent to a major normal fault and has a relatively high fracture density of 1.1 feet per square foot ( $3.7 \text{ m/m}^2$ ), while sample f-12-ds2 is far from any observed fault and has a lower fracture density of 0.84 feet per square foot ( $2.8 \text{ m/m}^2$ ). Dense fracturing with variable orientations in the Anderson Junction and Sandstone Mountain areas reflects their positions in and near the hinge zone of the Virgin anticline and their proximity to the Hurricane and related normal faults. Fracture density on Sand Mountain is relatively low, consistent with its gently dipping structure.

## Discussion

### Fracture Geometry and Permeability

The hydraulic conductivity of bedrock aquifers is a function of several parameters, including density and orientation of fractures, primary porosity of the unfractured rock mass, stratigraphy, and structural geometry. This



**Figure 12.** Variation in fracture density with location in the Navajo Sandstone. Data are projected to a median line through the middle of the Navajo outcrop area. West-to-east section is along the main outcrop area, from the northwesternmost outcrop point near Square Top Mountain, through the Red Mountains, the City Creek-Mill Creek area, to the northeasternmost outcrop point west of Ash Creek Reservoir. North to south section is along outcrop area southeast of Interstate 15, from Anderson Junction to the southern end of Sand Mountain. (a) Data from 1:20,000 scale, black and white aerial photographs.

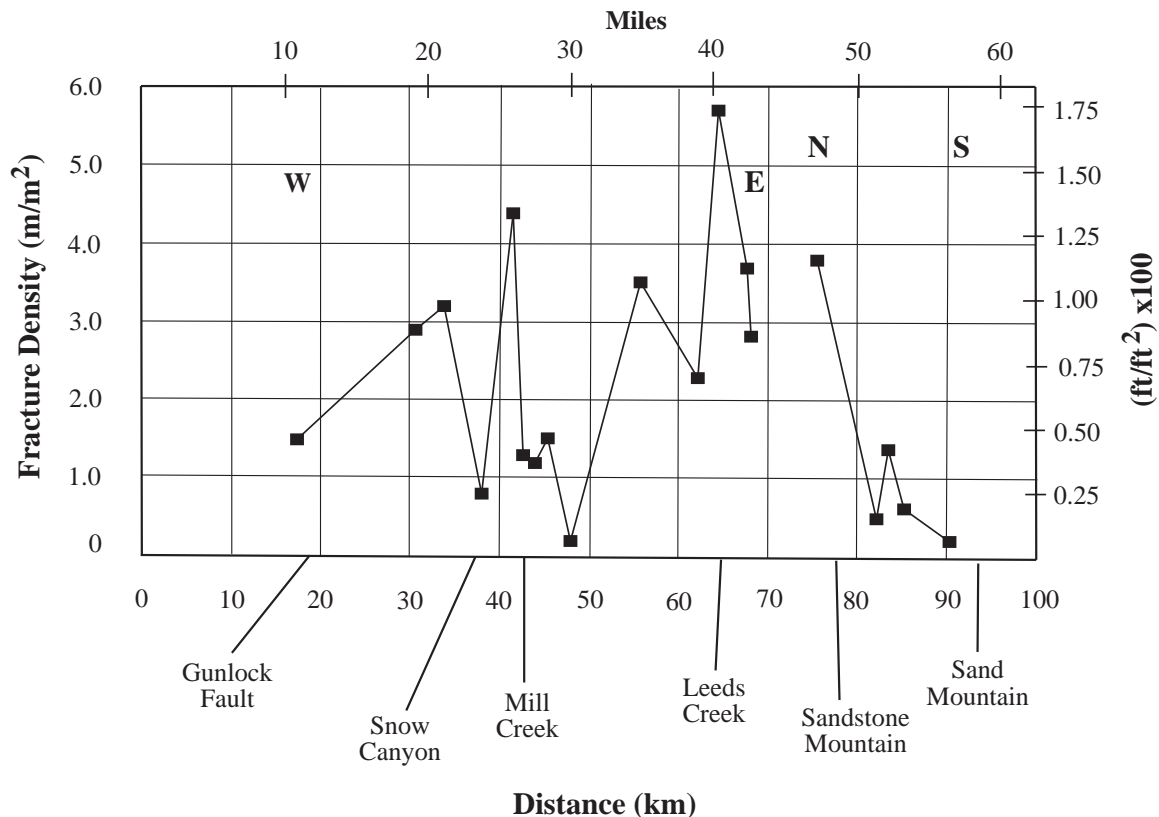


Figure 12. (b) Outcrop data.

section discusses the relationship between fracture parameters and permeability to aid interpretation of the fracture data (plate 6 and appendix G).

Zhang and others (1996) presented a method to calculate the two-dimensional permeability tensor of natural rock outcrops whose joint systems have been mapped (figures 13a and 13b). A rose plot of the outcrop fracture map used by Zhang and others (1996) shows that the principal joint set is parallel to the major axis of the model two-dimensional permeability tensor (figure 13c). The aspect ratio of the rose petals representing the principal and secondary joint sets is 1.2:1, similar to the aspect ratio of the major and minor axes of the model permeability tensor, 1.4:1. These relations indicate that the rose diagrams on plate 6 qualitatively show the orientation and degree of anisotropy of the two-dimensional permeability tensor for near-surface, two-dimensional flow in the sample area.

Drill-hole packer tests and mathematical modeling indicate that connectivity determines the ability of a joint system to transport fluids (Long and Witherspoon, 1985; Neuman, 1987). The principal joint set in the Navajo Sandstone in the study area typically has the greatest average trace length, and individual joints of the principal set are well-connected, as described above (Hurlow, 1997). These observations reinforce the interpretation that the principal joint set is parallel to the greatest principal per-

meability direction in the Navajo aquifer. This relation does not necessarily apply to other regions or aquifers.

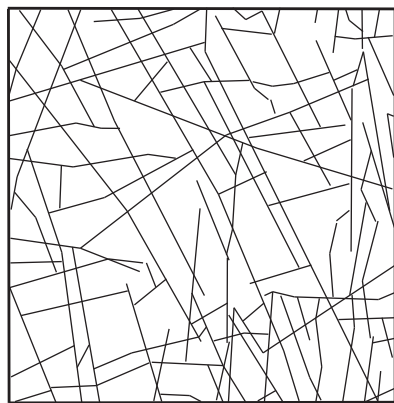
The relation between fracture population characteristics and permeability described above represents the bulk permeability of the entire sample volume and is valid only when the sample area is large compared to the length of most joints. Individual fractures within the sample volume may be more or less permeable than the bulk value, and flow is highly anisotropic within a single fracture. Aquifer tests may or may not corroborate the bulk permeability tensors derived from fracture data, depending on the heterogeneity of fracture distribution within the sample volume and the possibility of the well intersecting fractures with anomalously high hydraulic conductivity.

The anisotropy of the bulk permeability tensor can also be estimated from scanline data by the geometric anisotropy factor of Zhang and Sanderson (1995), which compares fracture density along the two perpendicular sampling traverses. Anisotropy factors for scanline data are included in table G.2. The equation for anisotropy factor is

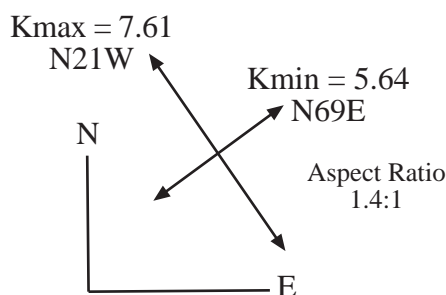
$$A_f = (\Sigma \gamma_i / L_x) / (\Sigma \gamma_j / L_y) \quad (1)$$

where  $A_f$  is the anisotropy factor,  $L_x$  is the length of sampling traverse  $x$ ,  $\gamma_i$  is the angle between the  $i$ th fracture and sampling traverse  $x$ ,  $L_y$  is the length of sampling tra-

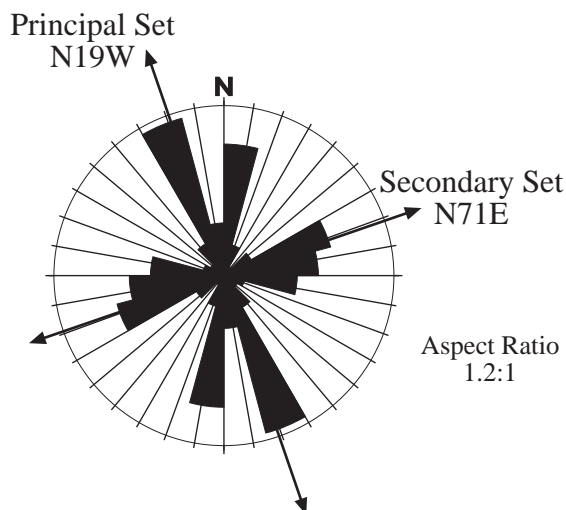




(a)



(b)



(c)

**Figure 13.** Relation between 2-D permeability tensor and fracture orientation. (a) Fracture-trace map of 6.5 foot x 6.5 foot (2 m x 2 m) outcrop used as input to model (Zhang and others, 1996, p. 23). (b) Model 2-D permeability tensor derived from figure 13a (Zhang and others, 1996, p. 23). Rose diagram derived from figure 13a. Directions of principal and secondary joint sets based on average petal directions weighted according to length. Principal axes and aspect ratios of rose diagram closely correspond to the model permeability tensor in (b).

verse  $y$ , and  $\gamma_j$  is the angle between the  $j$ th fracture and sampling traverse  $y$  (Zhang and Sanderson, 1995). Table G.2 includes aspect ratios of rose diagram petals for comparison with aerial photograph data.

Model hydraulic conductivity tensors can be calculated from fracture geometries and densities (Zhang and others, 1996), but doing so requires simplifying assumptions regarding the geometry and hydrologic properties of individual fractures which may misrepresent their natural properties (Neuman, 1987). An additional complication for defining hydraulic conductivity values is that fracture intersections have greater permeability than fracture planes (Neuman, 1987) so that, where two steeply dipping fracture sets are present, vertical permeability is important.

### Relation Between Fracture Parameters and Hydraulic Conductivity

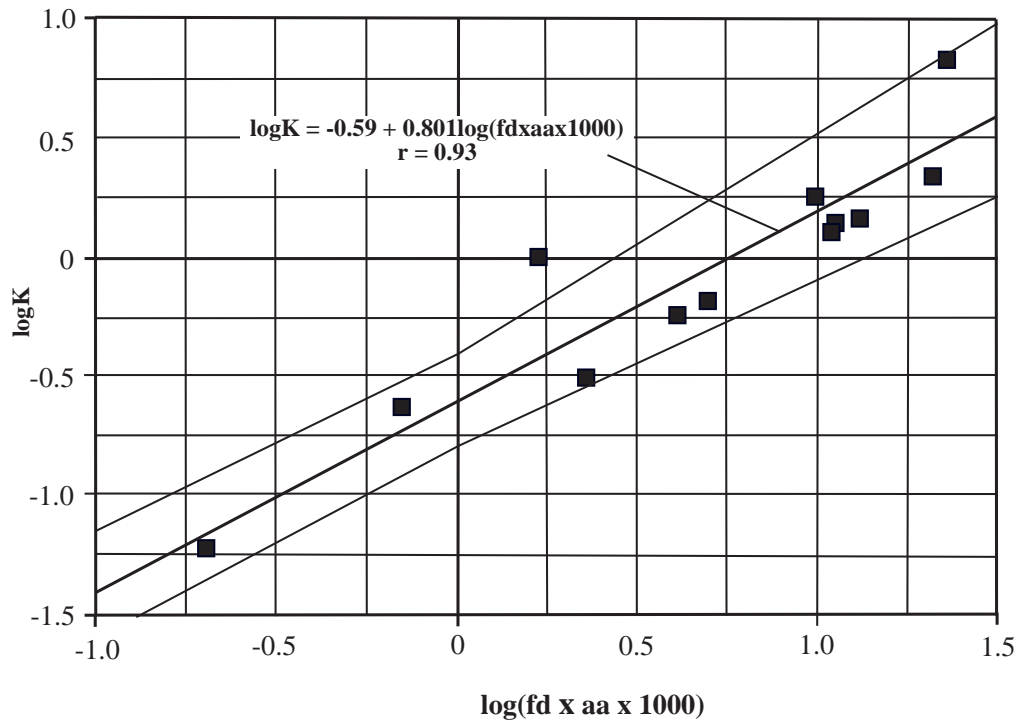
**Introduction:** This section further explores the hydrologic significance of fractures in the Navajo aquifer by examining the quantitative relation between fracture parameters and hydraulic conductivity. This relation is a useful tool in determining aquifer properties and evaluating prospective well sites. Constitutive relations between hydraulic conductivity and fracture parameters are very complex and are incompletely understood, so a quantitative relation must be derived empirically (see Gates, 1997, for a similar approach).

**Methods:** Scanline data were obtained from outcrops near wells for which single-well or multiple-well aquifer-test data are available (table G.3). The scanline data provide quantitative estimates of the fracture parameters for the portion of the Navajo aquifer affected by the wells. The hydraulic conductivity of the Navajo aquifer in the vicinity of each well was estimated using the computer program "Tguess" (Bradbury and Rothschild, 1985) and specific capacity data from single-well aquifer tests. Aquifer thicknesses were obtained from plate 5A or from detailed cross sections. The U.S. Geological Survey provided hydraulic conductivity values derived from aquifer tests for three wells. Linear regression reveals the relation between hydraulic conductivity and various combinations of fracture parameters, including log values to account for possible exponential relations.

**Results:** A log-log linear regression of hydraulic conductivity versus the product of fracture density and average aperture provides the best correlation (figure 14). The derived equation is

$$\log K = -0.590 \pm 0.217 + (0.801 \pm 0.107)[\log(\text{fd} \times \text{aa} \times 1000)] \quad (2)$$

where  $K$  is hydraulic conductivity in meters per day,  $\text{fd}$  is fracture density in meters per square meter, and  $\text{aa}$  is average aperture in millimeters. The correlation coefficient for the equation is 0.93, and the cited uncertainties are one standard error. The 95% confidence interval (figure 14) indicates that the uncertainty of any particular prediction of  $K$  from equation (2) is about 4.3 to 9.5 feet



**Figure 14.** Log-log plot of hydraulic conductivity ( $K$ ) against the product of fracture density ( $fd$ ) times average aperture ( $aa$ ) times 1000. Regression line (thicker line) and 95% confidence interval (thinner lines) are shown. See table G.3 for data. Hydraulic conductivity is in meters per day, fracture density is in meters per square meter, and aperture is in millimeters.

per day (1.3-2.9 m/d) for values of  $K$  between 3.3 and 33 feet per day (1-10 m/d), respectively.

**Discussion:** Because the Navajo aquifer is a fractured porous medium, the hydraulic conductivity values derived from the aquifer-test data are the sum of primary and secondary (fracture-related) hydraulic conductivities, expressed as

$$K_T = K_p + K_f \quad (3)$$

where  $K_T$  is total hydraulic conductivity and  $K_p$  and  $K_f$  are primary and secondary (fracture-related) hydraulic conductivities, respectively. This equation has the form  $y = mx + b$ , in which  $b$  is the y-intercept and  $m$  is the slope. If primary permeability is considered constant and fracture density (secondary permeability) is variable, then  $K_p$  corresponds to  $b$  and  $K_f$  corresponds to  $mx$ . The x-coefficient of equation (2), therefore, describes the exponential relation between fracture-related hydraulic conductivity and the fracture parameters, which can also be expressed as

$$K_f = (fd \times aa \times 1000)^{0.801 \pm 0.107} \quad (4)$$

The y-intercept of equation (2) provides an estimate for  $K_p$ , the hydraulic conductivity related to primary porosity, of 0.84 feet per day ( $0.590 \pm 217$  m/d).

The values of  $K_T$  (table G.3) and  $K_p$  derived in this study are consistent with hydraulic conductivity values reported by the U.S. Geological Survey (Cordova, 1978; V. Heilweil, USGS, Anderson Junction, Hurricane Bench, and Grapevine Pass aquifer tests, written communication, 1997) for the Navajo aquifer from the study area: 0.18 to 31.7 feet per day (0.05-9.7 m/d) from aquifer tests and 0.36 to 5.0 feet per day (0.1-1.5 m/d) for unfractured core samples. Huntley and others (1992) present an empirical relation between transmissivity and specific capacity for fractured granitic bedrock aquifers in the Peninsular Ranges of southwestern California, but their equation does not reproduce the values of transmissivity derived from aquifer tests of the Navajo Sandstone conducted by the U.S. Geological Survey in the study area, probably because their data are from fractured granite aquifers with little or no interfracture permeability.

Regression of the log of hydraulic conductivity against the log of the product of fracture density and average aperture provides a better correlation than against fracture density alone. Fracture apertures are likely uniformly less than 1 mm below the weathering zone, which extends to about 50 feet (15 m) depth, so apertures measured at the surface have little or no relation to those below the weathering zone. Fracture aperture near the surface may correlate positively with specific capacity because wider apertures

allow greater infiltration from surface streams and direct precipitation, resulting in more water flowing to the wells.

The uncertainties cited in equation (2) reflect the precision of the regression, but estimates of hydraulic conductivity from fracture parameters likely carry greater uncertainty that is difficult to quantify. Important potential sources of inaccuracy in the data include: (1) heterogeneity in fracture density, such that the well may sample rock masses with higher or lower fracture density than the average value derived from the scanline data; and (2) inaccuracy of the single-well aquifer-test data used to derive the hydraulic conductivity estimates, due to problems such as well-bore storage or variable pumping rates. In light of these problems, estimates of hydraulic conductivity using equation (2) should carry conservative uncertainties of about 33%.

There are some important limitations to the approach of deriving hydraulic conductivity from single-well aquifer-test data. Single-well data are one-dimensional, so do not provide information on anisotropy of hydraulic conductivity, which is important in the Navajo aquifer, as revealed by the results of an aquifer test conducted at Anderson Junction by the U.S. Geological Survey (V. Heilweil, USGS, written communication, 1997). The hydraulic conductivity values in table G.3, therefore, represent the average of several different flow directions having different hydraulic conductivity values due to aquifer anisotropy. Single-well aquifer-test data are generally considered less accurate than aquifer tests that employ multiple monitoring wells. Equation (2) may be modified as more data become available, though its correlation coefficient may either improve or worsen with the additional data, and it should only be applied to the Navajo aquifer in the study area.

Despite the limitations and potential inaccuracies discussed above, equation (2) is a useful relationship. The fracture data are relatively inexpensive to obtain, and can provide greater regional coverage than aquifer tests. Single-well aquifer tests are cheaper and logistically easier to perform than aquifer tests utilizing multiple observation wells. Hydrologic data for the Navajo aquifer are limited in number and geographic extent, so equation (2) provides a method of estimating hydraulic conductivity in areas lacking wells. Such estimates provide important information for hydrogeologic modeling and, because of the heterogeneity of fracture density in the study area, are better than the alternative of making educated guesses based on extrapolation of hydrologic data.

Equation (2) is also a useful tool for evaluating prospective well sites in coordination with other geologic and hydrologic studies. Transmissivity at specific sites can be estimated from hydraulic conductivity values derived from equation (2) using the relation  $T = Kb$ , where  $T$  is transmissivity in square meters per day and  $b$  is saturated thickness. Saturated thickness in unconfined aquifers is the difference between the local ground-water level, which can be determined from wells and/or springs, and the formation thickness which, for the Navajo Sandstone, can

be derived from plate 5A or preferably from smaller scale cross sections based on local field data. Despite the uncertainties in the predicted value of hydraulic conductivity, equation (2) provides a valid basis for comparing the relative hydraulic conductivity values likely to be found at different well sites.

### Hydrogeologic Significance of Structural Compartments

The following discussion is based on the general principles of the relation between faults and ground water because hydrologic data appropriate to test the existence of hydrologic boundaries in the study area are not available.

Little or no hydrologic connection likely exists within the Navajo aquifer between compartments I and II, II and III across the Gunlock fault zone, or between compartments V and VI across Anderson Junction, because faults at these locations almost entirely sever the Navajo Sandstone (cross sections K-K' and I-I', respectively, plate 2B). Structural blocks of Navajo Sandstone in these two areas are connected across only small parts of the total stratigraphic thickness of the unit and are bounded by faults which most likely have low transverse permeability. The upper Kayenta Formation is saturated in some areas, as indicated by the presence of springs in the upper 100 feet (30 m) of this formation in much of the study area. The upper Kayenta aquifer and the Navajo aquifer may be hydraulically connected where they are juxtaposed by faults, but hydrologic communication is likely limited by low permeability perpendicular to these faults as described above.

The hydrologic significance of the two major splays of the Snow Canyon fault zone is less clear, because these faults have gouge-rich cores which probably have low transverse permeability, but their vertical displacement is minor so the Navajo Sandstone is in structural contact over most of its stratigraphic thickness across the faults. Based on the observed structural relations, comparison with other examples of fault-bounded hydrologic compartments (Ashland and others, 1996) and the permeability structure of fault zones (Caine and others, 1996), strands of the Snow Canyon fault zone likely act as leaky barriers across their planes but as excellent conduits parallel to their fault planes.

### Regional Hydrogeology

Cordova (1978) noted that the primary recharge mechanisms for the Navajo aquifer are infiltration through overlying geologic units, infiltration from streams flowing over its outcrop area, and infiltration of precipitation; but he did not estimate their relative importance. Cordova (1978) also noted that the Navajo Sandstone is highly jointed and that the joints probably influence ground-water movement, but provided no details. Quantifying the contributions of different recharge sources, as well as the influences of fractures on ground-water movement, is critical to understanding the hydrogeology of the Navajo aquifer and is a

major goal of current work by the U.S. Geological Survey, Water Resources Division. This section describes geologic relations which influence calculations of recharge to the Navajo aquifer and discusses the probable effects of fracture systems on regional flow patterns.

Because most precipitation in the study area falls on the high country of the Pine Valley Mountains, it is important to consider how much recharge the Navajo aquifer may receive from infiltration from that area through overlying rocks. The rate of such infiltration is a function of how far and through what geologic units ground water must travel to reach the Navajo aquifer. Cross sections J-J' and K-K' (plate 2) and plate 5B show that the Navajo Sandstone is about 8,200 feet (2,500 m) below the land surface that receives the maximum precipitation. The upper third of the Cretaceous section in the Pine Valley Mountains probably has low permeability because it is dominantly clayey mudstone with interbedded sandstone. This interpretation is consistent with the great number of springs localized near the contact between the Tertiary Claron and Cretaceous Iron Springs formations in the Pine Valley Mountains. The Jurassic Carmel Formation also contains a substantial thickness of calcareous siltstone which may have low permeability, although this facies is highly fractured and may have secondary permeability. The great thickness and low permeability of overlying units indicates that recharge to the Navajo aquifer by infiltration from the high terrain of the Pine Valley Mountains must occur over a long time scale, although the volume may be great.

Most principal fracture sets in domains III, IV, and Va are oriented north-south, parallel to the maximum gradient of the regional potentiometric surface illustrated by Cordova (1978), suggesting that regional ground-water movement is highly anisotropic and is directed from north to south in these areas. Joint zones are 5 to 35 times more permeable than rock masses with low fracture density (see appendix F), suggesting that ground water may be channelized. North-striking faults such as the Gunlock and Snow Canyon fault zones and the St. George and Washington faults probably add to the anisotropy of the Navajo aquifer. Local variations in fracture orientation and topography and the presence of faults may alter these relations in detail.

Northeast of domain Va (plate 6), fracture populations are characterized by either one northeast-striking principal set or two principal sets oriented northeast and northwest, and many joint zones have been reactivated as faults. The northeast-striking fracture set is typically dominant and is oriented perpendicular to the maximum gradient of the regional potentiometric surface as illustrated by Cordova (1978). At the scale of an aerial photograph sample area (860,670 square feet [80,000 m<sup>2</sup>]), the major axis of the horizontal permeability tensor is oriented northeast in areas with one northeast-striking principal fracture set, and north to north-northeast in areas with two principal sets. Ground-water flow in the latter areas is parallel to the "most significant pathway of fracture intersection" (Ritzi and Andolsek, 1992), which approximately bisects the

acute angle between the two principal sets. At smaller scales, however, ground-water movement is likely complex (appendix F), with an important vertical component of flow where joint zones intersect.

Dense fracturing of variable orientation in domain VIa suggests that permeability is high and ground-water pathways are complex. Hydrologic connection between domains VIa and VIb in the Navajo Sandstone may be disrupted by feeder dikes to the numerous volcanic cinder cones west of Hurricane. Most joints and joint zones in domain VIb are oriented northeast, perpendicular to the maximum gradient of the potentiometric surface for Sand Mountain (Cordova, 1978). Fracture density is generally low in domain VIb, implying low permeability.

### Potential Target Areas for New Wells

As emphasized in the introduction to this report, water managers in the study area are faced with rapidly increasing demands in a region of limited precipitation, so it is important to identify new potential sources for public water supply. The Navajo aquifer is an attractive target for new wells because its suitability as an aquifer is proven, but it is already extensively developed near population centers. The results from this project indicate that the low foothills of the Pine Valley Mountains north of Anderson Junction and northwest of Interstate 15 have good potential for future ground-water development in the Navajo aquifer. The following discussion is based solely on geologic data because considering the economic, legal, and environmental aspects of such development is beyond the scope of this project.

The fracture characteristics, structure, and hydrologic setting of the Navajo aquifer northwest of Anderson Junction suggest that it may contain useable amounts of ground water. As discussed above, the Navajo Sandstone in this area is densely fractured and is cut by numerous northeast-striking faults, implying relatively high permeability. The faults cut the Navajo Sandstone into several structural blocks, probably enhancing northeast-southwest permeability but limiting the physical and hydrologic connectivity in the northwest-southeast direction. In the foothills north of Anderson Junction and west to southwest of Pintura, fault-bounded blocks of Navajo Sandstone are present below about 10 to 150 feet (3-50 m) of Quaternary boulder gravel and up to 330 feet (100 m) of Claron Formation (cross sections G-G', H-H', and I-I', plate 2). This area is traversed by several perennial streams emanating from the Pine Valley Mountains and receives 14 to 16 inches (36-41 cm) of precipitation annually, which is greater than the outcrop areas to the southwest which host major public-supply well fields and which receive 9 to 12 inches (23-30 cm) annually (figure 1a; Cordova, 1978). The unconsolidated sediments may receive infiltration during precipitation and from stream loss, and some of this water may infiltrate the underlying Navajo aquifer. Siting of wells should be based on careful construction of local cross sections, perhaps aided by test wells, to locate the



depth to the top of the Navajo aquifer where it is buried or the depth to its base where it is exposed, and by detailed fracture surveys utilizing aerial photographs and field work to locate joint zones and faults.

## OTHER POTENTIAL AQUIFERS

### Introduction

Cretaceous sandstones and some Tertiary igneous rocks in the study area are potential aquifers where factors affecting permeability, recharge, and storage are favorable. The suitability of these rock units as aquifers depends in large part on their lithologic character, stratigraphic relations, and structure, which are briefly summarized in this section. The lithologic descriptions and suggestions for possible well locations presented below are based on reconnaissance work and are preliminary. Siting of test wells should be based on careful geologic characterization of target areas.

### Cretaceous Sandstones

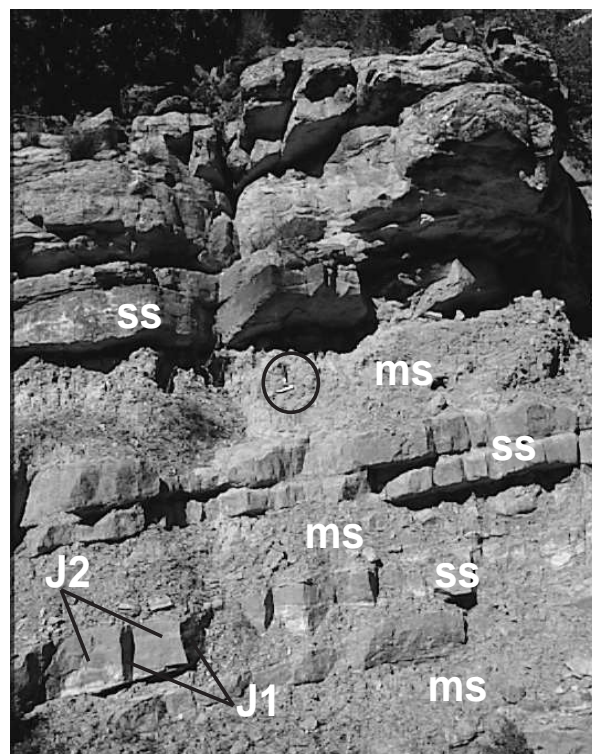
Cretaceous units in the study area are chiefly interbedded sandstone, mudstone, and conglomerate of the 3,500 to 4,000 foot-thick (1,067-1,219 m) Iron Springs Formation (figure 15; Goldstrand, 1994; Hintze and others, 1994). Most of the Cretaceous stratigraphic section is fine- to medium-grained, quartz-rich sandstone in beds approximately 2 to 50 feet (0.6-15 m) thick. The sandstone is strongly to moderately cemented and may retain little primary permeability, although estimates of porosity and permeability have not been made for this study. Two sets of steeply dipping joints with average spacing of 1 to 3 feet (0.3-1 m) are pervasive in the sandstone, thus secondary permeability may locally be important. The sandstone beds are separated by 1 to 10 foot-thick (0.3-3 m) mudstone layers. The mudstone is soft, clay-rich, and lacks discrete fractures. Conglomerate layers are 2 to 30 feet (0.6-9 m) thick, contain well-rounded quartzite and limestone clasts in variable proportions, and are most common at the bottom and top of the Cretaceous section (Goldstrand, 1994; Hintze and others, 1994). Joint characteristics in conglomerate layers are similar to those in the sandstone.

Regional stratigraphic variations affect the potential suitability of Cretaceous rocks as aquifers. The average grain size and relative abundance of both sandstone and conglomerate decrease eastward (Goldstrand, 1994). Near Gunlock, Cretaceous sandstones are relatively coarse, moderately to weakly cemented, and are overlain by a 1,970 foot-thick (600 m) section of conglomerate (Hintze and others, 1994) that is weakly to moderately jointed. Cretaceous shale and bentonite layers below the Iron Springs Formation near Gunlock and in the western Pine Valley Mountains (Cook, 1960; Hintze and others, 1994) may increase storage of ground water in the lower Iron

Springs Formation by acting as a confining or leaky confining layer. In contrast to the Gunlock area, the upper third of the Cretaceous section is predominantly mudstone in the central and eastern foothills of the Pine Valley Mountains.

Cretaceous rocks have relatively simple structure west of the Gunlock fault zone and in the Pine Valley Mountains, but are faulted and tilted southeast of Enterprise and near Stoddard Mountain. West of the Gunlock fault, the Cretaceous rocks dip about 10 to 20 degrees northeast in a relatively unfaulted homoclinal section (Hintze and others, 1994). Structural complexity and internal deformation increase markedly to the northwest near the Square Top thrust, which truncates the Cretaceous units in its footwall. Dips are typically 3 to 5 degrees northwest to northeast in the foothills of the Pine Valley Mountains. Cretaceous sandstones southeast of Enterprise are highly faulted and are thinner than in the Pine Valley Mountains (Blank, 1993). Emplacement of the Miocene Stoddard Mountain intrusion caused structural thinning, tilting to steep dips, faulting, and hydrothermal alteration, but these effects decrease rapidly away from the intrusions (Mackin, 1960).

The geologic characteristics summarized above indicate that Cretaceous sandstones may serve as low-yield aquifers in areas where joint density and the proportion of sandstone to mudstone are high, and where the unit forms a large, structurally continuous body in contact with a



**Figure 15.** Interbedded sandstone (ss) and mudstone (ms) of the Cretaceous Iron Springs Formation, along road to Oak Grove Park about 4.5 miles (1.4 km) from Interstate 15. Sandstone is cut by two joint sets (J1 and J2) that are approximately perpendicular and parallel, respectively, to the photograph. Hammer (circled) is 11 inches (28 cm) long.

source of recharge. Areas that may meet these criteria include: (1) the subsurface projections of outcrops along the Santa Clara River near Gunlock, although the river may be the principal recharge source for this area; (2) the lower third of the section in the western and central foothills of the Pine Valley Mountains; and (3) the subsurface projection of outcrops dipping away from the Stoddard Mountain intrusion, although hydrothermal alteration may adversely affect water chemistry.

### Tertiary and Quaternary Igneous Rocks

Igneous rocks are characterized by heterogeneous permeability that depends strongly on primary lithology as well as development of secondary permeability. Yields from igneous bedrock aquifers vary considerably, from 10 to >100 gal/min (2.6-260 L), and water chemistry is typically good (Fetter, 1994). Selection of well sites carries relatively high risk and should be based on careful geologic characterization of target areas.

Basalt may have primary permeability due to cooling joints, discontinuities between different flows, and lava tubes, and may develop secondary permeability along tectonic joints and faults. Quaternary basalt in the study area is typically above the local water table, except below Pine Valley, the southern New Harmony basin, and Ash Creek valley. Several domestic wells are completed in basalt in Ash Creek valley, but their yields were not determined for this study.

The Pine Valley monzonite is highly jointed (figure 16), is locally cut by faults, and crops out high in the Pine Valley Mountains, the region of greatest precipitation in the study area. Well location in the Pine Valley monzonite should be based in part on geologic interpretation of aerial photographs and field characterization of fracture density, because well yield likely depends strongly on heterogeneous fracture characteristics. Faults and especially intersections of two or more faults should be primary targets for siting wells in fractured intrusive rock.



**Figure 16.** View to the northwest of highly jointed Pine Valley monzonite, southwest of Saddle Mountain, western Pine Valley Mountains. Topographic relief of cliff is about 600 feet (183 m).

The Bull Valley Mountains expose mostly Tertiary silicic volcanic rock (plate 1). The lithology, thickness, and areal distribution of silicic volcanic rocks are heterogeneous due to the nature of associated eruptive processes. Volcanic facies with the greatest potential for relatively high permeability are highly jointed flows, shallow intrusions, indurated ash-flow tuffs, and volcanoclastic breccia. Identification of aquifers in Tertiary volcanic rocks in the study area would, therefore, require detailed geologic mapping in addition to collection and analysis of hydrologic data. The Miocene Quichapa Group is a potential aquifer because: (1) the ash-flow tuffs that make up this unit are highly indurated and densely jointed; and (2) the Group is composed of three distinct eruptive units of regional extent that can be treated as stratigraphic units (Mackin, 1960), aiding in structural analysis and prediction of their subsurface location and thickness.

## GEOLOGIC CONDITIONS BETWEEN ASH CREEK RESERVOIR AND TOQUERVILLE SPRINGS

### Introduction

Ash Creek Dam (figure 1a) was completed in 1960 in conjunction with the construction of Interstate 15. The bedrock foundation for the dam is densely jointed (figure 17); consequently, the dam abutment and reservoir basin are highly permeable and the reservoir loses water through seepage. The fate of water lost from the reservoir is uncertain but has important implications for water rights and dam stability. This section describes new geologic observations which describe the most likely pathways for water lost from Ash Creek Reservoir.

### Previous Work

Cordova and others (1972) and Mower (1982) inferred that water lost by seepage from Ash Creek Reservoir influences flow rates at Toquerville Springs, about 10 miles (16 km) downstream from the reservoir, via a pressure-wave effect, but were unable to quantify this relation in terms of water volume or time lag. Dye studies conducted between 1972 and 1980 to test the connection between Ash Creek Reservoir and Toquerville Springs yielded inconclusive results due to lack of detection downstream.

### Structural Geometry of Ash Creek Valley

The Hurricane normal fault, which was active during late Tertiary and Quaternary time (Anderson and Mehnert, 1979; Stewart and Taylor, 1996), determines the first-order





**Figure 17.** View to the northeast of fractured Quaternary basalt that forms natural abutment for Ash Creek Dam. Cliff is about 50 feet (15 m) high.

geologic structure of Ash Creek valley between Ash Creek Reservoir and Toquerville Springs (cross sections E-E' through I-I', plate 2). The trace of the Hurricane fault lies along the base of the Hurricane Cliffs (figure 2a), which comprise the uplifted footwall block. Ash Creek valley lies in the hanging wall of the Hurricane fault and is underlain by Quaternary basalt and sediments above Tertiary and Mesozoic sedimentary rocks. Pre-Quaternary rocks were faulted and tilted about 30 degrees eastward during late Tertiary time, then all units were cut by the Hurricane and related faults during Quaternary time.

Quaternary basalt that forms the abutments of Ash Creek Dam (figure 17) is up to 550 feet (167 m) thick and is underlain by approximately 50 to 120 feet (15-37 m) of boulder conglomerate. This relation is demonstrated by outcrops which overlie unit QTaf along North Ash Creek in the southern New Harmony basin and west of Pintura, and by water well (C-40-13)1cca which encountered unconsolidated sediment between 0 and 100 feet (0-30 m), "lava", interpreted here as Quaternary basalt, from 100 to 140 feet (30-43 m), unconsolidated gravel and clay between 140 and 200 feet (43-61 m), lava between 200 and 230 feet (61-70 m), and unconsolidated gravel, interpreted here as unit QTaf, from 230 to 350 feet (70-107 m). Both units are cut by Quaternary normal faults, including the Hurricane fault, and are folded by an open, northeast-trending anticline defined by progressively increasing eastward dips toward the Hurricane fault, a structural style known as reverse drag (Hamblin, 1966). The Quaternary basalt is physically discontinuous between Ash Creek Reservoir and Toquerville Springs due to erosion and/or depositional thinning.

The structural geometry of Ash Creek valley and the Hurricane fault changes from northeast to southwest. Between Ash Creek Reservoir and Pintura, the Hurricane fault is a single strand and no major Quaternary faults are present in its hanging wall. South of Pintura, the structure of the hanging wall becomes more complex. About 1 mile (1.6 km) southeast of Pintura, a subsidiary normal fault uplifts Quaternary basalt just west of the Hurricane Cliffs. A topographically higher area, underlain by monzonite of the Pine Valley laccolith near Interstate 15 and by Quaternary basalt near the Hurricane Cliffs, is about 3 miles (4 km) south of Pintura (Cook, 1960; plate 1; cross section H-H', plate 2). The Pine Valley monzonite is present in Ash Creek valley because it was dropped down 3,400 to 4,000 feet (1,036-1,219 m) from the main body of the Pine Valley laccolith by an east-side-down normal fault (cross section H-H', plate 2) during late Tertiary time. Units QTaf and Qb were then deposited, followed by west-side-down slip on the

Hurricane fault which was accompanied by a reverse-drag fold in the Quaternary basalt.

The Hurricane fault splits into eastern and western splays about 3.5 miles (5.8 km) south of Pintura (plate 1; cross section I-I', plate 2). Ash Creek and Toquerville Springs are along the eastern fault splay. The western fault splay juxtaposes a hanging wall of units QTaf and Claron Formation overlying Navajo Sandstone with a footwall composed of Quaternary basalt overlying QTaf and Navajo Sandstone (plate 1 and cross section I-I', plate 2).

## Discussion

Water lost by seepage from Ash Creek Reservoir likely percolates through joints in Quaternary basalt and travels southwest in the lower part of the basalt and in unit QTaf. Southwest flow of ground water is probably restricted to the narrow topographic floor of Ash Creek valley, because steep surface slopes on either side of the valley likely result in potentiometric surfaces that slope toward the valley axis (Cordova, 1978). Recharge to Ash Creek valley south of Ash Creek Reservoir may come from the Navajo aquifer to the west, by seepage from east-flowing streams emanating from the Pine Valley Mountains, and possibly from ground-water inflow across the Hurricane fault.

Inflow from the Hurricane Cliffs into Ash Creek valley is likely influenced by the internal structure of the Hurricane fault and the lithology of rock units in its footwall. The Permian Queantoweap and Pakoon formations are

highly indurated and very densely fractured in the footwall of the Hurricane fault. Fault-zone materials in these units are thin and poor in clays, so the Hurricane fault may have transverse permeability adjacent to these units (Caine and others, 1996). Conversely, sediments of the Triassic Moenkopi Formation are primarily gypsiferous shale and fine-grained sandstone, which tend to form broad "smear zones" of complex deformation and clay-rich fault gouge adjacent to the Hurricane fault, features which reduce fault-normal permeability (Caine and others, 1996). Therefore, hydrologic connection between the Hurricane Cliffs and Ash Creek valley may exist only where the Permian units are present in the footwall.

The structure of Ash Creek valley south of Pintura may cause ground water to bifurcate into two distinct subsurface pathways. The topographic high south of Pintura creates two narrow subsurface channels underlain by unit QTaf, one along Ash Creek at the base of the Hurricane Cliffs and one beneath Interstate 15 (cross section H-H', plate 2). These pathways of preferred ground-water movement may continue south along the western and eastern splays of the Hurricane fault (cross section I-I', plate 2). Along the western fault splay, ground water may percolate through unit QTaf and enter the highly fractured Navajo Sandstone.

Based on the structural relations described above, some of the water lost from Ash Creek Reservoir may emerge at Toquerville Springs, but some of it is also likely dispersed in unit QTaf and the Navajo Sandstone near Anderson Junction. Mixing of ground water derived from Ash Creek Reservoir with ground-water inflow from the Navajo aquifer and the tortuous pathway that the ground water must follow through fractured basalt and boulder conglomerate probably caused the inconclusive results of the dye tests described above, by creating very long travel time for southward flow and by dilution.

The ground-water pathways suggested above are based solely on the structural geometry and topography of Ash Creek valley as illustrated in the cross sections and geologic map, and should be regarded as working hypotheses that can be tested with hydrogeologic data and geochemical tracer tests. The results of previous hydrologic work (Cordova and others, 1972; Mower, 1982) imply that no direct connection exists between Ash Creek Reservoir and Toquerville Springs, but instead that the flow of Toquerville Springs is influenced primarily by regional climatic conditions. Seepage from Ash Creek Reservoir adds a minor amount of recharge to ground water below Ash Creek valley, which is the principal source of Toquerville Springs, but other recharge sources below Ash Creek Reservoir are likely more important. Future dye tests are likely to produce inconclusive results unless large amounts of dye with very long residence time and a very long sampling program are utilized. If another dye test is performed, wells near Anderson Junction and below Ash Creek Reservoir should be monitored in addition to the outflow of Toquerville Springs.

Analysis of nonradiogenic isotopes may help clarify the

fate of ground water that seeps from Ash Creek Reservoir if the isotopic composition of water in the reservoir is different from water entering the Ash Creek valley aquifer from the Pine Valley Mountains and Hurricane Cliffs. The advantage of an isotopic study is that its success is independent of the travel time for water from Ash Creek Reservoir to Toquerville Springs and Anderson Junction, because the ground-water system has been operating over geologic time and is presumably in geochemical equilibrium. Geologic units that recharge perennial streams feeding Ash Creek Reservoir but which are not present south of the reservoir include volcanic rocks of the Miocene Quichapa Group (map unit Tv<sub>1</sub>, plate 1) and the Miocene Stoddard Mountain intrusion (map unit Ti, northwest of New Harmony). Isotopic data have not been published for these units in the study area. Reconnaissance sampling of these units and of water in North Ash Creek, Kanarra Creek, Ash Creek Reservoir, and in drainages emanating from the Pine Valley Mountains south of the reservoir would determine the feasibility of such a study.

## SUMMARY

1. The geologic evolution and resulting structural architecture of the central Virgin River basin strongly influence its hydrology. The Jurassic Navajo Sandstone is the principal aquifer in the region, due to its combination of fracture permeability created during Mesozoic and Cenozoic tectonic deformation and retention of some primary porosity. Precipitation that falls on the Pine Valley Mountains is the most important source of waters recharging the Navajo aquifer. The Pine Valley Mountains stand 7,000 to 8,000 feet (2,100-2,400 m) above the St. George basin and receive the greatest annual precipitation in the study area due to the orographic effect. These mountains have withstood regional erosion related to downcutting of the Colorado River basin because they are capped by the Miocene Pine Valley monzonite, a 2,000 to 2,500 foot-thick (610-762 m), tabular intrusive mass that is more resistant to erosion than subjacent rocks.

2. Regional erosion has prevented the accumulation of thick Quaternary deposits in the St. George basin, limiting the size of unconsolidated aquifers. Unconsolidated sediments in the St. George basin are dominantly fluvial deposits in and adjacent to modern drainages, eolian deposits on and near outcrops of Navajo Sandstone, and alluvial-fan deposits adjacent to fault-line scarps. In contrast, the New Harmony and Kanarraville basins northeast of St. George have not undergone extensive erosion and locally contain up to 2,500 feet (760 m) of unconsolidated deposits that accumulated in the hanging wall of the Quaternary Hurricane normal fault and in a depression in the New Harmony area caused by late Tertiary folding. Quaternary deposits in the New Harmony and Kanarraville basins are chiefly fluvial and alluvial-fan sediments, and unconformably overlie Pleistocene and late Tertiary alluvial-fan boulder gravels.

3. The Navajo Sandstone is structurally separated into six large, gently dipping, fault-bounded structural compartments. Compartment-boundary faults mostly or entirely disconnect the Navajo aquifer and have low transverse permeability, severely limiting or eliminating hydrologic connection between adjacent structural compartments. Fault gouge is common and probably restricts transverse permeability of faults in the Navajo aquifer, but high-density fracturing adjacent to the gouge zones likely results in high permeability parallel to fault planes.

4. Fractures in the Navajo Sandstone are dominantly joints and joint zones (the latter defined as discrete zones of high joint density); faults are locally important. Principal joint and joint-zone sets strike north-northwest to north-northeast west of the latitude of St. George, and strike northeast and/or northwest east of St. George. Joint density is markedly heterogeneous, with high-density joint zones spaced 30 to 3,300 ft (10-1000 m) apart, separated by regions of lower joint density.

5. Joint populations with preferred orientations influence ground-water flow by creating anisotropic hydraulic conductivity, with the greatest principal permeability direction commonly parallel to the principal joint set. Permeability in joint zones is up to 35 times greater than in adjacent, less densely jointed rock masses. Where two prominent joint sets exist, the direction of maximum principal permeability approximately bisects the acute angle between the two sets.

6. Detailed surveys of fracture parameters at outcrops adjacent to water wells provide quantitative information about the relationship between nearby surface fracturing and hydraulic conductivity within the Navajo aquifer. The best correlation is between the log of hydraulic conductivity and the log of the product of fracture density (fd) and average aperture (aa):

$$\log K = -0.590 \pm 0.217 + (0.801 \pm 0.107)[\log(fd \times aa \times 1000)] \quad (r = 0.93)$$

This equation can be used to predict the relative suitability of potential well sites located near exposed Navajo Sandstone outcrops, and its use should be limited to the Navajo Sandstone within the study area.

7. Percolation from the area of highest precipitation in the Pine Valley Mountains down to the Navajo aquifer is likely retarded due to the probable confining layers in intervening rock units. The upper third of the Cretaceous sequence contains abundant clayey mudstone. Sandstone in the lower two-thirds of the Cretaceous is interbedded

with mudstone, and calcareous siltstone and gypsum are common in the Jurassic Carmel Formation.

8. Cretaceous sandstones and Tertiary silicic volcanic rocks in the Pine Valley Mountains and Bull Valley Mountains are potential aquifers in the study area. Thick beds of fractured sandstone in the lower third of the Cretaceous sequence and highly fractured ash-flow tuffs and shallow intrusive rocks provide the best possibilities. Siting of test wells in these units should be based on careful geologic characterization of target areas because facies distributions and fracture density are heterogeneous.

9. The Ash Creek Reservoir in the northeast part of the study area loses water through fractures in its natural basalt abutments. The reservoir is situated at the north end of a basaltic volcanic deposit that is up to 550 feet (168 m) thick and overlies 50 to 120 feet (15-37 m) of Pleistocene boulder gravel. Water from the reservoir likely percolates down to the lower part of the basalt sequence and into the underlying gravel layer, and moves southward. Some of this water may emerge 10 miles (16 km) downstream at Toquerville Springs as hypothesized by previous workers. However, the structural geology of Ash Creek valley suggests that some ground water may divert to the west around a fault-bounded block to reside in thick Pleistocene boulder gravel and underlying Navajo Sandstone north of Anderson Junction.

## ACKNOWLEDGMENTS

This study was largely funded by the Utah Division of Water Rights. I thank Jerry Olds, Allyson Traficonte, and Margie Wilkins, Utah Division of Water Rights, for providing plots of well and spring locations and other logistical support. I thank Victor Heilweil, Geoffrey Freethey, and Dale Wilberg, U.S. Geological Survey, Water Resources Division, for their help in understanding the hydrogeology of the area, sharing unpublished data, and providing locations of water wells in the New Harmony-Kanarraville area. Janae Wallace (Utah Geological Survey) drafted the cross sections in plate 2 and provided SEM analyses, and Jim Parker (Utah Geological Survey) drafted all other plates. Dr. Lehi Hintze (Brigham Young University), Victor Heilweil, Geoffrey Freethey, Jerry Olds, Allyson Traficonte, and Dr. William Woessner (University of Montana) provided reviews which improved the manuscript.

## REFERENCES

- Adair, D. H., 1986, Structural setting of the Goldstrike District, Washington County, Utah, *in* Griffen, D. T., and Phillips, W. R., editors, Thrusting and extensional structures and mineralization in the Beaver Dam Mountains, Southwestern Utah: Utah Geological Association Publication 15, p. 129-135.
- Anderson, R. E., and Barnhard, T. P., 1993a, Aspects of three-dimensional strain at the margin of the extensional orogen, Virgin River depression area, Nevada, Utah, and Arizona: Geological Society of America Bulletin, v. 105, p. 1019-1052.
- 1993b, Heterogeneous Neogene strain and its bearing on horizontal extension and vertical contraction at the margin of the extensional orogen, Mormon Mountains area, Nevada and Utah: U. S. Geological Survey Bulletin 2111, 43 p., 6 plates, scale 1:24,000.
- Anderson, R. E., and Christenson, G. E., 1989, Quaternary faults, folds, and selected volcanic features in the Cedar City 1° x 2° quadrangle, Utah: Utah Geological and Mineralogical Survey Miscellaneous Publication 89-6, 29 p., 2 plates, scale 1:250,000.
- Anderson, R. E., and Hintze, L. F., 1993, Geologic map of the Dodge Spring quadrangle, Washington County, Utah, and Lincoln County, Nevada: U.S. Geological Survey Geologic Quadrangle Map GQ-1721, 1 plate, scale 1:24,000.
- Anderson, R. E., and Mehnert, H. H., 1979, Reinterpretation of the history of the Hurricane fault in Utah, *in* Newman, G. W., and Goode, H. D., editors, 1979 Basin and Range Symposium: Rocky Mountain Association of Geologists, p. 145-165.
- Antonellini, Marco, and Aydin, Atila, 1994, Effect of faulting on fluid flow in porous sandstones -- Petrophysical properties: American Association of Petroleum Geologists Bulletin, v. 78, p. 355-377.
- Ashland, F. X., Bishop, C. E., Lowe, Mike, and Mayes, B. H., 1996, The geology of the Snyderville basin and its relation to ground-water conditions: Utah Geological Survey Open-File Report 337, 124 p., 15 pl.
- Averitt, Paul, 1962, Geology and coal resources of the Cedar Mountain quadrangle, Iron County, Utah: U.S. Geological Survey Professional Paper 389, 71 p., 3 plates, scale 1:24,000.
- 1969, Geology of the Kanarrville quadrangle, Iron County, Utah: U.S. Geological Survey Map GQ-694, 1 plate, scale 1:24,000.
- Blank, H. R., 1959, Geology of the Bull Valley district, Washington County, Utah: Seattle, University of Washington, Ph.D. thesis, 177 p.
- 1993, Preliminary geologic map of the Enterprise quadrangle, Washington and Iron Counties, Utah: U.S. Geological Survey Open-File Report 93-203, 1 plate, scale 1:24,000.
- Bradbury, K., and Rothschild, E., 1985, TGUSS -- A program to estimate aquifer transmissivity and hydraulic conductivity from specific capacity tests: Ground Water, v. 23, p. 240-246.
- Budding, K. E., and Sommer, S. N., 1986, Low-temperature geothermal assessment of the Santa Clara and Virgin River valleys, Washington County, Utah: Utah Geological and Mineralogical Survey Special Study 67, 34 p., 1 plate, scale 1:100,000.
- Caine, J. S., Evans, J. P., and Forster, C. B., 1996, Fault zone architecture and permeability structure: Geology, v. 24, p. 1025-1028.
- Cary, R. S., 1963, Pintura anticline, Washington County, Utah, *in* Heylum, E. B., editor, Guidebook to the geology of southwestern Utah: Intermountain Association of Petroleum Geologists, 12th Annual Field Conference, Salt Lake City, Utah, p. 172-179.
- Cook, E. F., 1957, Geology of the Pine Valley Mountains, Utah: Utah Geological and Mineralogical Survey Bulletin 58, 111 p.
- 1960, Geologic atlas of Utah, Washington County: Utah Geological and Mineralogical Survey Bulletin 70, 119 p.
- Cordova, R. M., 1978, Ground-water conditions in the Navajo Sandstone in the central Virgin River basin, Utah: Utah Department of Natural Resources Technical Publication 61, 66 p.
- Cordova, R. M., Sandberg, G. W., and McConkie, W., 1972, Ground-water conditions in the central Virgin River Basin, Utah: Utah Department of Natural Resources Technical Publication 40, 64 p.
- Dobbin, C. E., 1939, Geologic structure of St. George District, Washington County, Utah: American Association of Petroleum Geologists Bulletin, v. 23, p. 121-144.
- Doelling, H. H., and Graham, R. L., 1972, Southwestern Utah coal fields -- Alton, Kaiparowits Plateau and Kolob-Harmony: Utah Geological and Mineralogical Survey Monograph No. 1, 333 p.
- Eppinger, R. G., Winkler, G. R., Cookro, T. M., Shubat, M. A., Blank, H. R., Crowley, J. K., Kucks, R. P., and Jones, J. L., 1990, Preliminary assessment of the mineral resources of the Cedar City 1° x 2° quadrangle, Utah: U. S. Geological Survey Open-File Report 90-34, 129 p., map scale 1:250,000.
- Fetter, C. W., 1994, Applied Hydrology: New York, Macmillan College Publishing Company, 691 p.
- Gardner, L. S., 1952, The Hurricane Fault, *in* Guidebook to the geology of Utah -- Cedar City, Utah to Las Vegas, Nevada: Intermountain Association of Petroleum Geologists, Salt Lake City, Utah, p. 15-22.
- Gates, W. C. B., 1997, The hydro-potential (HP) value -- A rock classification technique for evaluation of the ground-water potential in fractured bedrock: Environmental and Engineering Geoscience, v. 3, p. 251-267.
- Goldstrand, P. M., 1994, Tectonic development of upper Cretaceous to Eocene strata of southwestern Utah: Geological Society of America Bulletin, v. 106, p. 145-154.
- Grant, S. K., 1995, Geologic map of the New Harmony quadrangle, Washington County, Utah: Utah Geological Survey Miscellaneous Publication 95-2, 2 plates, scale 1:24,000.
- Grant, S. K., Fielding, L. W., and Noweir, M. A., 1994, Cenozoic fault patterns in southwestern Utah and their relationships to structures of the Sevier orogeny, *in* Blackett, R. E., and Moore, J. N., editors, Cenozoic geology and geothermal systems of southwestern Utah: Utah Geological Association Publication 23, p. 139-153.
- Gregory, H. E., 1950, Geology and geography of the Zion Park region, Utah and Arizona: U. S. Geological Survey Professional Paper 220, 200 p., 5 plates, scale 1:125,000.

- Hacker, D.B., 1995, Deformational structures related to the emplacement and growth of the Pine Valley laccolith, southern iron axis region, Washington County, Utah [abs.]: EOS, Transactions, American Geophysical Union, v. 76, no. 46, p. F625.
- Hamblin, W. K., 1966, Origin of "reverse drag" on the down-thrown side of normal faults: Geological Society of America Bulletin, v. 76, p. 1145-1164.
- 1984, Direction of absolute movement along the boundary faults of the Basin and Range-Colorado Plateau margin: Geology, v. 12, p. 116-119.
- Hamilton, W. L., 1978, Geologic map of Zion National Park, Utah: Zion Natural History Association, 1 plate, scale 1:31,680.
- Higgins, J. M., and Willis, G. C., 1995, Interim geologic map of the St. George quadrangle, Washington County, Utah: Utah Geological Survey Open-File Report 323, 2 plates, scale 1:24,000.
- Hintze, L. F., 1963, Geologic map of southwestern Utah, in Intermountain Association of Petroleum Geologists Guidebook, 12th Annual Field Conference: Utah Geological and Mineralogical Survey, 1 sheet, scale 1:250,000.
- 1986, Stratigraphy and structure of the Beaver Dam Mountains, southwestern Utah, in Griffen, D. T., and Phillips, W. R., editors, Thrusting and extensional structures and mineralization in the Beaver Dam Mountains, southwestern Utah: Utah Geological Association Publication 15, p. 1-36.
- Hintze, L. F., Anderson, R. E., and Embree, G. F., 1994, Geologic map of the Motoqua and Gunlock quadrangles, Washington County, Utah: U.S. Geological Survey Miscellaneous Investigations Series Map I-2427, 1 plate, scale 1:24,000.
- Hintze, L. F., and Hammond, B. J., 1994, Geologic map of the Shivwits quadrangle, Washington County, Utah: Utah Geological Survey Map 153, 2 plates, scale 1:24,000.
- Hood, J. W., and Danielson, T. W., 1979, Aquifer tests of the Navajo Sandstone near Caineville, Wayne County, Utah: Utah Department of Natural Resources Technical Publication 66, 69 p.
- Huntley, David, Nommensen, Roger, and Steffey, Duane, 1992, The use of specific capacity to assess transmissivity in fractured-rock aquifers: Ground Water, v. 30, p. 396-402.
- Hurlow, H. A., 1996, Contraction, extension, and strike-slip faulting in the Colorado Plateau-Basin and Range transition zone: Neogene-Quaternary tectonic evolution of the New Harmony and Kanarraville basins, southwest Utah [abs.]: Geological Society of America Abstracts With Programs, v. 28, no. 7, p. A-449.
- 1997, Heterogeneous joint and fault systems in the Navajo Sandstone, southwestern Utah, and their influence on permeability, in Close, J. C., and Casey, T. A., editors, Natural Fracture Systems in the Southern Rockies: Durango, CO, Four Corners Geological Society, p. 41-52.
- Kurie, A. E., 1966, Recurrent structural disturbance of Colorado Plateau margin near Zion National Park, Utah: Geological Society of America Bulletin, v. 77, p. 867-872.
- LaPointe, P. R., and Hudson, J. A., 1985, Characterization and interpretation of rock mass jointing patterns: Geological Society of America Special Paper 199, 25 p.
- Long, J. C. S., and Witherspoon, P. A., 1985, The relationship of the degree of interconnection to permeability in fracture networks: Journal of Geophysical Research, v. 90, p. 3087-3098.
- Lucchitta, Ivo, 1989, History of the Grand Canyon and of the Colorado River in Arizona, in Jenney, J. P., and Reynolds, S. J., editors, Geologic evolution of Arizona: Tuscon, Geological Society of Arizona Digest 17, p. 701-715.
- Mackin, J. H., 1947, Some structural features of the intrusion of the Iron Springs district, Utah: Utah Geological Society guidebook to the geology of Utah No. 2, 62 p.
- 1960, Structural significance of Tertiary volcanic rocks in southwestern Utah: American Journal of Science, v. 258, p. 81-131.
- McKee, E. H., Blank, H. R., and Rowley, P. D., 1997, Potassium-argon ages of Tertiary igneous rocks in the eastern Bull Valley Mountains and Pine Valley Mountains, southwestern Utah: U. S. Geological Survey Bulletin 2153, p. 241-252.
- Mower, R. W., 1982, Relationship between seepage from Ash Creek Reservoir and flow from Toquerville Springs: Salt Lake City, Unpublished Report to Utah Division of Water Resources, 24 p.
- Nelson, R.A., and Handin, J., 1977, Experimental study of fracture permeability in porous rock: The American Association of Petroleum Geologists Bulletin, v. 61, p. 227-236.
- Neuman, S. P., 1987, Stochastic continuum representation of fractured rock permeability as an alternative to the REV and fracture network concepts, in Farmer, I. W., Daemen, J. J. K., Desai, C. S., Glass, C. E., and Neuman, S. P., editors, Proceedings of the 28th U.S. symposium on rock mechanics: Boston, Balkema, p. 533-561.
- Pechmann, J. C., Arabasz, W. J., and Nava, S. J., 1994, Refined analysis of the 1992 M<sub>L</sub> 5.8 St. George, Utah, earthquake and its aftershocks [abs.]: Seismological Research Letters, v. 65, p. 32.
- Proctor, P. D., and Brimhall, W. H., 1986, Silver Reef mining district, revisited, Washington County, Utah, in Griffen, D. T., and Phillips, W. R., editors, Thrusting and extensional structures and mineralization in the Beaver Dam Mountains, Southwestern Utah: Utah Geological Association Publication 15, p. 129-135.
- Reeside, J. B., 1922, Oil prospects in Washington County, Utah: U. S. Geological Survey Bulletin 726, p. 87-107.
- Ritzi, R. W., Jr., and Andolsek, R. H., 1992, Relation between anisotropic transmissivity and azimuthal resistivity surveys in shallow, fractured, carbonate flow systems: Ground Water, v. 30, p. 774-780.
- Rowley, P. D., Steven, T. A., Anderson, J. J., and Cunningham, C. G., 1979, Cenozoic stratigraphic and structural framework of southwestern Utah: U.S. Geological Survey Professional Paper 1149, 22 p.
- Sansom, P. J., 1992, Sedimentology of the Navajo Sandstone, southern Utah, USA: London, England, Wolfson College, Ph.D. dissertation, 291 p.
- Schlische, R.W., 1995, Geometry and origin of fault-related folds in extensional settings: American Association of Petroleum Geologists Bulletin, v. 79, p. 1661-1678.
- Schramm, M. E., 1994, Structural analysis of the Hurricane fault in the transition zone between the Basin and Range Province and the Colorado Plateau, Washington County, Utah: Las Vegas, University of Nevada-Las Vegas, M.S. thesis, 90 p.
- Stewart, M. E., and Taylor, W. J., 1996, Structural analysis and

- fault segment boundary identification along the Hurricane fault in southwestern Utah -- *Journal of Structural Geology*, v. 18, p. 1017 - 1029.
- Stewart, M. E., Taylor, W. J., Pearthree, P. A., Solomon, B. J., and Hurlow, H. A., 1997, Neotectonics, fault segmentation and seismic hazards along the Hurricane fault in Utah and Arizona - An overview of environmental factors in an actively extending region, *in* Link, P.K., and Kowallis, B.J., editors, *Geological Society of America Field Trip Guidebook: Brigham Young University Geology Studies*, v. 42, part II, p. 235-254.
- Stone, D. S., 1967, Theory of Paleozoic oil and gas accumulation in Bighorn Basin, Wyoming: *American Association of Petroleum Geologists Bulletin*, v. 51, p. 2056 - 2114.
- Twiss, R. J., and Moores, E. M., 1994, *Structural Geology*: New York, W. H. Freeman and Company, 532 p.
- Utah Division of Water Rights, 1982, Water use data for public water suppliers and self-supported industry in Utah 1980: *Water Use Report No. 3*, 94 p.
- van Kooten, G. K., 1988, Structure and hydrocarbon potential beneath the Iron Springs laccolith, southwestern Utah: *Geological Society of America Bulletin*, v. 100, p. 1533-1540.
- Willis, G. C., and Higgins, J. M., 1995, Interim geologic map of the Washington quadrangle, Washington County, Utah: *Utah Geological Survey Open-File Report 324*, 2 plates, scale 1:24,000.
- 1996, Interim geologic map of the Santa Clara quadrangle, Washington County, Utah: *Utah Geological Survey Open-File Report 339*, 2 plates, scale 1:24,000.
- Zhang, Xing, and Sanderson, D. J., 1995, Anisotropic features of geometry and permeability in fractured rock masses: *Engineering Geology*, v. 40, p. 65-75.
- Zhang, Xing, Sanderson, D. J., Harkness, R. M., and Last, N. C., 1996, Evaluation of the 2-D permeability tensor of fractured rock masses: *International Journal of Rock Mechanics, Mining Science, and Geomechanical Abstracts*, v. 33, p. 17-37.



## APPENDIX A

### *Description of Geologic Units Shown on Plates 1 and 2*

Principal sources for the lithologic descriptions below are Cook (1960), Hintze and others (1994), Higgins and Willis (1995), and unpublished field work by the author.

#### Quaternary

Qs      **Quaternary sediments** -- Fluvial, alluvial-fan, colluvial, eolian, and mass-movement deposits. Thickness ranges from 0 to >1,000 feet (0-305 m).

#### Quaternary-Tertiary

QTb      **Basaltic flows and cinder cones** -- Flows are quartz-bearing basaltic trachyandesite with plagioclase phenocrysts, trachybasalt and alkaline basalt with olivine phenocrysts, and basalt with olivine and pyroxene phenocrysts. Thickness ranges from 0 to 900 feet (0-274 m). Most deposits are Quaternary; some flows near Hurricane (K. Hamblin *in* Budding and Sommer, 1986) and west of New Harmony (Grant, 1995) may be late Tertiary.

#### *disconformity*

QTaf      **Older alluvial-fan deposits** -- Matrix-supported boulder conglomerate with clasts derived predominantly from the Pine Valley igneous suite (unit Tvip below). Deposited on erosional surfaces and in drainages on the eastern and southern flanks of the Pine Valley Mountains. Deposited both above and below Quaternary basalt in Ash Creek valley. Thickness ranges from 0 to 150 feet (0-46 m).

QTs      **Older sediments** -- Alluvial gravel, sand, and silt. Thickness ranges from 0 to 30 feet (0-10 m) in most of map area, but may be >100 feet (>30 m) on eastern slope of Beaver Dam Mountains.

#### *unconformity*

#### Tertiary

Taf      **Alluvial-fan deposits** -- Undivided (Taf) on plate 1; informally divided into upper (Tafu), middle (Tafm), and lower (TafL) members on plate 2. Total thickness is about 1,500 feet (457 m).

Tafu      **Upper Member** -- Boulder gravel with clasts of Paleozoic quartzite, Paleozoic and/or Mesozoic limestone units, Navajo Sandstone, Iron Springs Formation, Claron Formation, and Tertiary volcanic rocks. Thickness about 700 feet (213 m).

Tafm      **Middle Member** -- Pale orange to orange-tan, thin-bedded tuffaceous siltstone interbedded with 1 to 3 foot-thick (0.3-1 m) lenses of matrix-supported pebble conglomerate, containing clasts of white crystal tuff. Thickness about 450 feet (137 m).

TafL      **Lower Member** -- Tan to grayish-tan, planar-bedded conglomerate with clasts of Tertiary volcanic rocks and Paleozoic(?) quartzite. Thickness about 350 feet (107 m).

#### *unconformity*

Tmc      **Muddy Creek Formation** -- Light tan to buff boulder conglomerate, gravel, and pebbly to silty sandstone with interbedded light gray to white tuff. A lower member of gray basalt not shown on this map yielded a K-Ar date of 8.8 ± 0.3 Ma (Hintze and others, 1994). Thickness ranges from 0 to 1,400 feet (0 to 427 m).

#### *unconformity*

Ti      **Tertiary plutonic rocks** -- Monzonite porphyry intrusions (Cook, 1960). About 50 percent plagioclase phenocrysts in a microgranular to cryptocrystalline groundmass, the former including orthoclase and quartz crystals. Magnetite, commonly weathered to limonite, is a major hydrothermal alteration product.

- Tv<sub>2</sub> Miocene volcanic rocks** -- Rhyolitic ash-flow and ash-fall tuff and related volcanoclastic rocks. Includes: Page Ranch Formation, Ox Valley Tuff (K-Ar date of 12.6 Ma on sanidine; Hintze and others, 1994), Cove Mountain Formation, and Flattop Mountain Suite of Cook (1960); and rhyolitic ash-flow tuff (K-Ar date of 14-15 Ma), Hiko Tuff (K-Ar date of 18.6 Ma), andesite flows and breccia, and Racer Canyon Tuff (K-Ar date of 19 Ma) of Anderson and Hintze (1993) and Hintze and others (1994). Thickness ranges from 0 to approximately 4,000 feet (1,219 m).

*unconformity*

- Tvp Pine Valley igneous suite** -- Subdivided into Tip (monzonite) and Tvp (latite) on cross sections E-E', F-F', and H-H', plate 2; undivided on plate 1 and other cross sections of plate 2. Grayish-brown, pale-gray, and greenish-gray latite and monzonite porphyry with plagioclase, pyroxene, and biotite phenocrysts and orthoclase megacrysts. Differentiation of volcanic and plutonic rocks is extremely difficult (Cook, 1957; Grant, 1995). Monzonite intruded as a laccolith in the middle part of the Claron Formation and latite erupted as ash-flow tuffs above the laccolith (Cook, 1957, 1960; Hacker, 1995). Monzonite yielded a K-Ar date of 21 Ma (McKee and others, 1997). Total thickness 2,000 to 2,500 feet (610-762 m).

*unconformity*

- Tv<sub>1</sub> Miocene-Oligocene volcanic rocks** -- Rhyolitic ash-flow tuff, andesite flows, quartz latite, volcanic breccia, ash-fall tuff, and lenticular volcanic sandstone and lacustrine deposits. Includes Rencher Formation (Cook, 1960), Quichapa Group (K-Ar and <sup>40</sup>Ar/<sup>39</sup>Ar dates of 22-23 Ma; Hintze and others 1994), Isom Formation (K-Ar date of 26 Ma; Anderson and Hintze, 1993), and Wah Wah Springs Tuff of Needles Range Group (K-Ar date of 29 Ma; Hintze and others, 1994). Thickness ranges from 0 to approximately 3,000 feet (0-914 m).
- Tv<sub>1,2</sub> Tertiary volcanic rocks** -- Rhyolitic to andesitic ash-flow tuff, volcanic breccia, and flows. Comprises undifferentiated Tv<sub>1</sub> and Tv<sub>2</sub>.

*disconformity*

- Tc Claron Formation** -- Sandstone, conglomerate, and fresh-water limestone. Sandstone is gray or stained bright red. Limestone is gray micrite, commonly stained lavender to yellow-red. Conglomerate clasts are predominantly limestone with variable amounts of quartzite. Thickness 700 to 1,500 feet (214-457 m).

*unconformity*

**Cretaceous**

- Ks Cretaceous sedimentary rocks** -- Sandstone, siltstone, mudstone, and conglomerate. Includes Grapevine Wash, Iron Springs, Kaiparowits, Wahweap, Straight Cliffs, Dakota, and Tropic Formations, rocks in the Pine Valley Mountains mapped as Entrada and Dakota Formations by Cook (1960), and Pine Hollow and Canaan Peak Formations of Goldstrand (1994). Cenomanian through Campanian; upper Grapevine Wash Formation may be early Tertiary (Hintze and others, 1994). Thickness 3,800 to 4,000 feet (1,158-1,219 m).
- Kis Iron Springs Formation** -- Shown on cross sections through the Pine Valley Mountains (plate 2). Tan to grayish-tan, fine-grained sandstone to mudstone, locally with basal layer of gray to tan conglomerate about 33 feet (10 m) thick. Thickness 3,800 to 4,000 feet (1,158-1,219 m). Includes rocks in the Pine Valley Mountains mapped by Cook (1960) as Entrada and Dakota Formations.

*unconformity*

**Jurassic**

- Jec Entrada Sandstone and Curtis Formation** -- Sandstone, limestone-clast conglomerate, and minor limestone. Thickness ranges from 250 to 500 feet (76-150 m).
- Jc Carmel and Temple Cap Formations** -- Pale gray to tan arenaceous to argillaceous limestone, locally fossiliferous. Temple Cap Formation is comprised of soft red sandstone, gypsiferous shale, and gypsum. About 660 feet (200 m) thick, ranging to 1,500 feet (457 m) in northeastern part of map area.

*disconformity*

- Jn Navajo Sandstone** -- Orange, red, and white eolian sandstone with prominent large-scale cross-bedding. Sandstone is fine grained, with calcite cement except in the upper 100 feet (30 m), which is mostly silica-cemented. Thickness ranges from 2,000 to 2,800 feet (610-853 m).
- Jk Kayenta Formation** -- Grayish-red to reddish-brown sandstone, siltstone, and silty mudstone. Thickness ranges from 380 to 920 feet (116-280 m).
- Jm Moenave Formation** -- Undivided (Jm) on plate 1 and cross sections C-C' through K-K', plate 2; divided into Springdale Sandstone (Jms) and Dinosaur Canyon (Jmd) members on cross sections A-A' and B-B'. Total thickness 345 to 650 feet (105-198 m).
- Jms Springdale Sandstone Member** -- Resistant, pale-orange to pinkish-orange, planar to crudely bedded sandstone, 115 feet (35 m) thick, ranging to 200 feet (61 m) in northeastern part of map area.
- Jmd Dinosaur Canyon and Whitmore Point Members** -- Reddish-brown to orange, thinly bedded siltstone and fine-grained sandstone, 230 feet (70 m) thick, ranging to 450 feet (137 m) in northeastern part of map area.

*unconformity***Triassic**

- Tc Chinle Formation** -- Divided into Petrified Forest (T<sub>cp</sub>) and Shinarump Conglomerate (T<sub>cs</sub>) members on plate 1 and cross sections A-A' through I-I', plate 2; undivided (T<sub>c</sub>) on cross sections J-J' and K-K', plate 2.
- T<sub>cp</sub> Petrified Forest Member** -- Variegated red, purple, yellow, and gray shale, claystone, and siltstone. A 10 to 20 foot-thick (3-6 m) bed of white cherty sandstone and chert-clast conglomerate is present in the middle part of the member. Total thickness about 385 to 700 feet (117-213 m).
- T<sub>cs</sub> Shinarump Conglomerate Member** -- White to pale-gray, medium- to coarse-grained sandstone and chert-pebble conglomerate. Thickness ranges from 75 to 185 feet (23-56 m).

*disconformity*

- Tm Moenkopi Formation** -- Undivided on plate 1 and cross sections E-E' through K-K', plate 2; divided into upper red (T<sub>mu</sub>), Shnabkaib (T<sub>ms</sub>), middle red (T<sub>mm</sub>), Virgin Limestone, (T<sub>mv</sub>), lower red (T<sub>ml</sub>), Timpoweap (T<sub>cp</sub>), and Rock Canyon (T<sub>cp</sub>) members on cross sections A-A' and B-B', plate 2. Total thickness ranges from 1,545 to 2,500 feet (471-762 m).
- T<sub>mu</sub> Upper red member** -- Red laminated siltstone, fine-grained sandstone, and mudstone. Thickness ranges from about 360 to 500 feet (110-152 m).
- T<sub>ms</sub> Shnabkaib Member** -- White, red, and pale-green gypsum and gypsiferous siltstone and mudstone. Thickness ranges from 500 to 1,000 feet (152 to 305 m).
- T<sub>mm</sub> Middle red member** -- Interlayered red to reddish-brown siltstone, mudstone, and gypsiferous mudstone and siltstone. Thickness 375 to 500 feet (114-152 m).
- T<sub>mv</sub> Virgin Limestone Member** -- Gray calcareous mudstone and tan-gray to medium gray, resistant micrite and calcarenite. Thickness ranges from about 25 to 225 feet (8-69 m).
- T<sub>ml</sub> Lower red member** -- Red to purplish-red mudstone and siltstone, locally gypsiferous. Thickness ranges from about 25 to 650 feet (8-200 m).
- T<sub>mt</sub> Timpoweap Member** -- Chocolate brown weathering, gray to tan calcareous shale and calcarenite. Thickness ranges from about 10 to 500 feet (3-152 m).

**Tmrc      Rock Canyon Member** -- Gray chert-clast conglomerate. Matrix is gray, medium- to coarse-grained sandstone. Clasts are rounded and matrix-supported, pebble-size, black, white, and butterscotch-colored chert. Thickness ranges from 0 to 35 feet (0-11 m).

*disconformity*

## Permian

**Pkt      Kaibab Limestone and Toroweap Formation** -- Undivided on plate 1 and cross sections A-A', B-B', E-E', F-F'; G-G' and H-H' (western part); and I-I' through K-K'. Subdivided into Kaibab Limestone (Pk) and Toroweap Formation (Pt) on cross sections F-F', G-G', and H-H' (eastern part). Combined thickness 880 to 1,300 feet (268-396 m).

**Pk      Kaibab Limestone** -- Gypsiferous gray to red silty shale, cherty micrite and calcarenite, and rare chert-clast conglomerate. Thickness about 984 feet (300 m).

**Pt      Toroweap Formation** -- Gray, massive to thickly bedded cherty limestone. Thickness approximately 295 feet (90 m).

**Pqp      Queantoweap and Pakoon Formations** -- Undivided on plate 1 and cross sections A-A' and E-E', and F-F' (western part), I-I', J-J', and K-K', plate 2. Subdivided into Queantoweap Formation (Pq) and Pakoon Formation (Pp) on cross sections F-F' (eastern part), G-G', and H-H', plate 2. Combined thickness 2,250 feet (686 m).

**Pq      Queantoweap Sandstone** -- White to grayish-white, massive to cross-bedded, highly indurated, fine-grained sandstone. Thickness about 1,500 feet (457 m).

**Pp      Pakoon Formation** -- Light gray, fine-grained dolomite that weathers light brownish-gray. Locally gypsum-bearing. Thickness about 750 feet (229 m).

*disconformity*

## Pennsylvanian

**IPc      Callville Limestone** -- Fine-grained gray limestone and dolomite with interbedded sandstone; basal cherty limestone. Thickness ranges from 1,496 to 1,620 feet (456-494 m).

## Mississippian

**Mr      Redwall Limestone** -- Gray limestone, dark-brown cherty limestone, and gray, hard, dense limestone. Approximately 1,120 feet (340 m) thick.

## Devonian-Cambrian

**€OD      Devonian through Cambrian formations** -- Interbedded dark- to light-gray limestone and dolomite. Up to 2,100 feet (640 m) thick. Includes the Devonian Temple Butte and Muddy Peak Limestones and the Cambrian Nopah and Bonanza Peak Formations and Muar Limestone.

## Cambrian

**€ppm      Pioche Shale and Prospect Mountain Quartzite** -- Pioche Shale is reddish-brown to green micaceous shale. Prospect Mountain Quartzite is red-brown, micaceous and feldspathic quartzite. Combined thickness 748 feet (228 m).

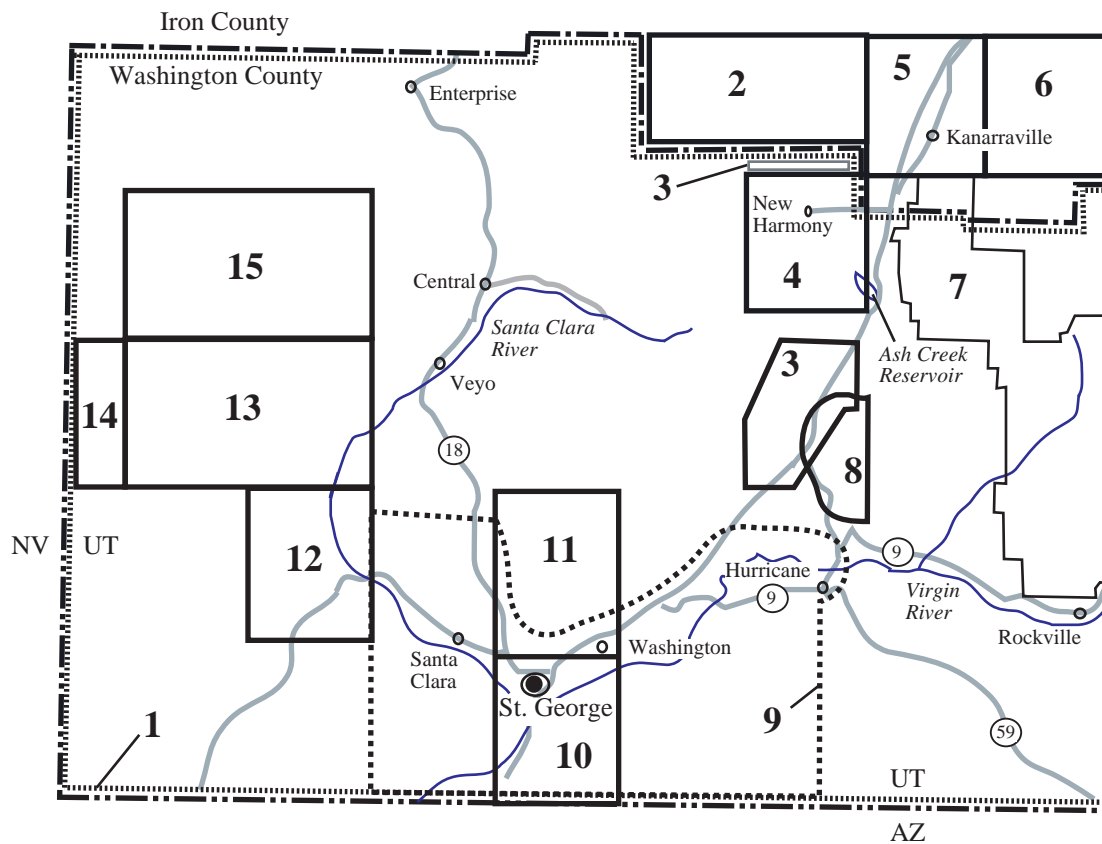
*nonconformity*

## Precambrian

**pC      Precambrian rocks** -- Granitoid gneiss, pegmatitic granite, amphibolite, and quartzofeldspathic schist and gneiss.

## APPENDIX B

### *Sources of Plate 1 Map Compilation*



1. Cook (1960).
2. Hintze (1963).
3. Hurlow, unpublished mapping, 1995-1996.
4. Grant (1995).
5. Averitt (1969).
6. Averitt (1962).
7. Hamilton (1978).
8. Schramm (1994).
9. Budding and Sommer (1986).
10. Higgins and Willis (1995).
11. Willis and Higgins (1995).
12. Hintze and Hammond (1994).
13. Hintze and others (1994).
14. Anderson and Hintze (1993).
15. E. A. Anderson, unpublished mapping, 1984.

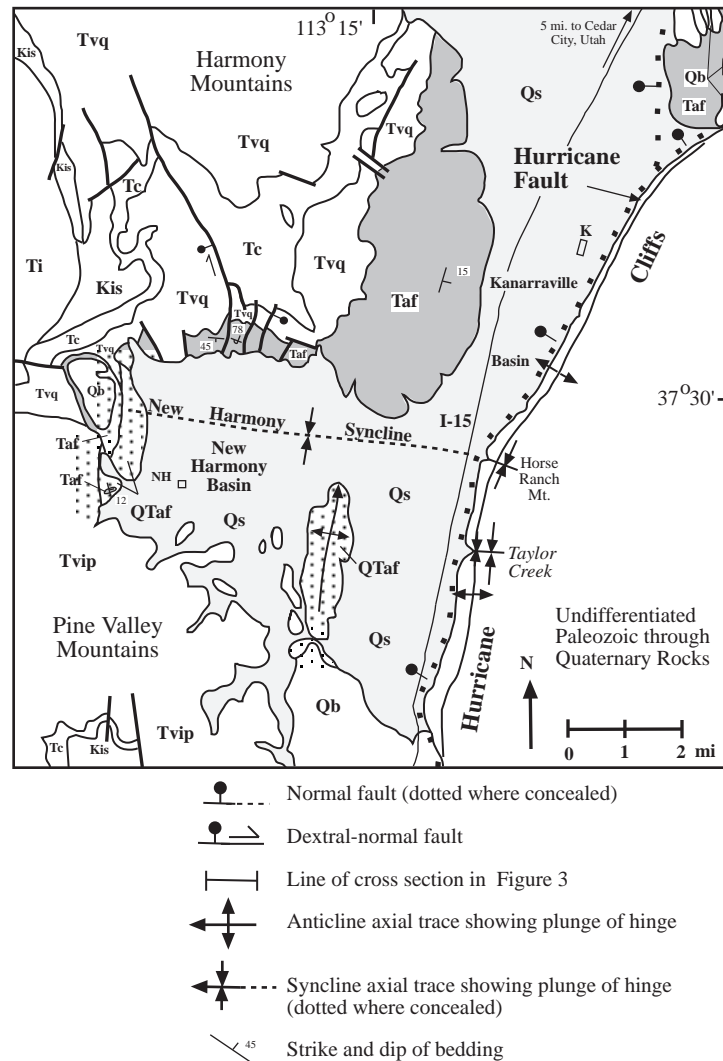
## APPENDIX C

### *Late Tertiary - Quaternary Tectonic Evolution of the New Harmony and Kanarraville Basins, Southwestern Utah*

#### Introduction

Parts of this appendix appear in a separate publication (Stewart and others, 1997) related to the Geological Society of America 1997 national meeting, so there is some overlap in content with parts of the main text of this report. The material is included to provide a broader geologic perspective of the evolution of the New Harmony and Kanarraville basins, and because recognition of the New Harmony syncline is a new contribution that has important implications for the late Tertiary to Quaternary tectonic evolution of the region.

The structural evolution of the New Harmony and Kanarraville basins, two relatively small Tertiary-Quaternary depositional centers in southwestern Utah (figures C.1, 7a, and 7b), illustrates aspects of late Tertiary to Quaternary deformation in the Colorado Plateau-Basin and Range transition zone. The New Harmony basin is underlain by a late Tertiary syncline, herein named the New Harmony syncline, formed by north-south horizontal shortening that was coeval with regional east-west crustal extension (Anderson and Barnhard, 1993a, 1993b; Hurlow, 1996). The Kanarraville basin formed due to Quaternary normal slip on the Hurricane fault.



**Figure C.1.** Generalized geologic map of New Harmony and Kanarraville basins and vicinity.








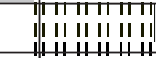

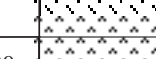


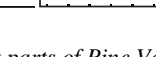
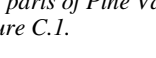
## Geologic Setting

The New Harmony and Kanarrville basins lie between Miocene volcanic fields to the west and the Hurricane Cliffs, which comprise the footwall of the Hurricane fault to the east (figure C.1). The New Harmony basin trends west-northwest, perpendicular to the regional structural grain defined by the Hurricane fault and Kanarrville basin. The Kanarrville basin is east of the New Harmony basin and has approximately the same surface area, but has a long, narrow form that trends north-northeast.

The New Harmony basin is filled with Quaternary sediments deposited on unit Taf, a folded and faulted sequence of Miocene to Pliocene(?) volcaniclastic alluvial-fan deposits (figure C.2; cross sections A-A' through D-D', plate 2). Unit Taf was derived from volcanic terrain to the west and deposited over a much wider area than the New Harmony basin (Anderson and Mehnert, 1979).

Unit Taf consists of three informal members, based on reconnaissance field work and local detailed mapping. The upper member is unconsolidated boulder gravel that is about 700 feet (213 m) thick (figure 6b). Clasts include Miocene volcanic and plutonic rocks and Tertiary through late Paleozoic sedimentary rocks exposed to the northwest and west. This unit is the "clastic debris" that Anderson and Mehnert (1979) described in both the hanging wall of the Hurricane fault, where it is overlain by 1 million-year-old basalt, and in its footwall. These relations indicate that the Hurricane Cliffs and the presently observable slip on the Hurricane fault developed after about 1 million years ago in the Cedar City-Kanarrville area (Anderson and Mehnert, 1979).

The middle member of unit Taf is about 450 feet (137 m) of poorly to laminar-bedded, orange-tan, tuffaceous siltstone with local conglomerate beds containing clasts of white biotite-feldspar crystal tuff. This member strongly resembles units north and northwest of the Pine Valley Mountains that were mapped as Muddy Creek Formation by Cook (1960) and Hintze and others (1994).

Age			Symbol	Thickness (ft)	Lithology
Quaternary	Quaternary sediments		Qs	0-1500	
	Quaternary basalt		Qb		
	Alluvial-fan deposits		QTaf		
Pliocene	Alluvial-fan deposits	Upper member	Taf	0-700	
		Middle member	Taf	0-450	
		Lower member	Taf	350	
Miocene	Racer Canyon Tuff		not shown		 19 Ma
	Pine Valley monzonite & latite		Tvip		 21 Ma
	Stoddard Mt. intrusion		Tis		 22 Ma
	Quichapa Group		Tvq	1000	 23 Ma
Eocene-Oligocene	Claron Formation			700-1000	 24 Ma
Cretaceous	Iron Springs Formation		Kis	3800	

**Figure C.2.** Lithologic column for New Harmony and Kanarrville basins and adjacent parts of Pine Valley and Harmony Mountains. Shading and patterns correspond to those in figure C.1.

The lower member of unit Taf is tan to gray, planar-bedded, cemented diamictite, breccia, and tuffaceous sandstone and siltstone. Clasts are derived chiefly from the Miocene Quichapa Group and Stoddard Mountain and Pine Valley intrusions. This member is about 350 feet (107 m) thick and is interbedded at its base with a white crystal tuff that Peter Rowley of the U.S. Geological Survey (personal communication, 1996) correlated with the Racer Canyon Tuff, which yielded a K-Ar date of 19 Ma (Rowley and others, 1979).

Unit QTaf is a sequence of alluvial-fan deposits, derived almost entirely from the Pine Valley monzonite, that overlie and locally incise unit Taf. Units Taf and QTaf were not distinguished by previous workers (Cook, 1960; Grant, 1995), but their differentiation is critical to deciphering the structural evolution of the New Harmony and Kanarrville basins. The pediment surface over which unit QTaf debris flows were transported and deposited slopes southeast from the Pine Valley Mountains and is visible from Interstate 15 between Pintura and Ash Creek Reservoir. The pediment surface is incised by modern drainages in the foothills of the Pine Valley Mountains, suggesting a Pleistocene age for unit QTaf deposits.

Quaternary sediments in the New Harmony and Kanarraville basins are fluvial and alluvial-fan deposits related to modern drainage systems. Quaternary basalt is interbedded with units QTaf and Qs, is cut by the Hurricane fault, and provides important constraints on timing and rates of faulting and erosional downcutting (Hamblin, 1984; Stewart and Taylor, 1996). A local eruptive field, devoid of cinder cones, is present along the southern margin of the New Harmony and Kanarraville basins. Flows that emanated from this field were cut by the Hurricane fault, and are exposed along the top of the Hurricane Cliffs (footwall of the Hurricane fault) and in roadcuts along Interstate 15 (hanging wall) between Pintura and Ash Creek Reservoir.

### Structural Geometry and Evolution

The New Harmony syncline is defined by opposing dips of unit Taf on the north and southwestern margins of the New Harmony basin (figure C.1). In the southern Harmony Mountains, unit Taf dips moderately to steeply south and is overturned adjacent to a north-striking dextral-normal fault. In the same area the stratigraphically lower Quichapa Group and Claron Formation are also steeply dipping to overturned, but a tight anticlinal hinge north of the syncline returns these units to moderate southward dips (cross section D-D', plate 2). The Quichapa Group and Claron Formation are cut by numerous north- and east-striking normal, dextral-normal, and reverse faults, the majority of which are not shown on figures C.1 and cross section D-D', plate 2. The New Harmony syncline is interpreted to reflect north-northeast to south-southwest horizontal crustal shortening. Units QTaf and Qs are not deformed by the New Harmony syncline, nor are they cut by faults that cut the fold.

Unit Taf dips about 10 degrees to 12 degrees east at the west end of the New Harmony basin, reflecting an eastward plunge of the New Harmony syncline and/or regional uplift of the Pine Valley Mountains. Unit Taf dips 15 degrees eastward along the east flank of the Harmony Mountains, due to a combination of rotation in the hanging wall of the Hurricane fault, uplift of the Harmony Mountains, and original depositional slope.

The New Harmony syncline is exposed in the lower Hurricane Cliffs in the footwall of the Hurricane fault where it is expressed in cliff-forming exposures of Permian Kaibab Limestone below Horse Ranch Mountain (figure C.1). To the south, another east-trending syncline is exposed along Taylor Creek at the entrance to the Kolob Canyons section of Zion National Park (figure C.1). To the southwest, the dome-and-basin structure along the hinge of the Virgin anticline (plate 1) may also reflect late Tertiary refolding of a Cretaceous-age fold. This interpretation contradicts previous workers who viewed the Virgin anticline as entirely Cretaceous in age (Cook, 1960; Grant and others, 1994), but cannot be rigorously tested due to lack of Tertiary rocks in the St. George basin.

Unit QTaf is exposed along a north-trending ridge that divides the New Harmony and Kanarraville basins (figure C.1; figure 7a). This ridge is interpreted as an anticline related to reverse drag in the hanging wall of the Hurricane fault (cross section B-B', plate 2). The Kanarraville basin is adjacent and parallel to the Hurricane fault and is interpreted as a synextensional basin. Quaternary sediments are interpreted to have a wedge-shaped geometry reflecting infilling of the structural depression that formed in response to reverse drag in the hanging wall of the Hurricane fault (cross section B-B', plate 2).

### Discussion

Deformation of late Tertiary and Quaternary units in the New Harmony and Kanarraville basins suggests the following structural chronology:

- 1) North-south horizontal crustal shortening during Neogene time, manifested by the New Harmony syncline and east-west folds in the Hurricane Cliffs. The age of folding is not tightly constrained because the age of the upper member of unit Taf and its age relative to the folding (deposition during or entirely before folding) are unclear. The probable time of folding is Late Miocene to Pliocene. North-south crustal shortening may have been widespread in the Colorado Plateau-Basin and Range transition zone in southwestern Utah (Anderson and Barnhard, 1993b), if the interpretation is correct that the structure of the Virgin anticline reflects Neogene shortening superposed on a Cretaceous-age fold.

The New Harmony syncline did not likely form as a transverse fold in response to an along-strike displacement gradient (Schlishe, 1995) on the Hurricane fault because: (a) the Hurricane fault lacks apparent geometric segment boundaries at either end of the New Harmony basin; (b) the displacement-gradient model does not explain the extreme tightness and overturning of the synclinal and adjacent anticlinal hinges (cross section D-D', plate 2); and (c) the footwall lacks a corresponding anticline as required by Schlishe's (1995) model. In fact, the footwall contains the uplifted eastward continuation of the New Harmony syncline, as described above.

- 2) Faulting on a complex system of north- and east-striking normal and reverse faults deformed the New Harmony syncline but may also have been partly coeval with it. The structural style in the southern Harmony Mountains resembles the model of "diapiric upwelling" of the upper crust resulting from horizontal shortening plus vertical constrictional strain illustrated by Anderson and Barnhard (1993b, p. 11) for parts of southeastern Nevada and southwestern Utah. If their interpretation also applies to the New Harmony basin area, then genesis of the New Harmony syncline, normal and reverse faulting, and uplift of the Harmony Mountains were all coeval and reflect a component of shortening perpendicular to the regional extension direction during Neogene time.

- 3) The Kanarraville basin formed beginning in Late Pliocene to Quaternary time due to normal displacement on the Hurricane fault.

Although most displacement on the Hurricane fault in the New Harmony-Kanarraville area is clearly younger than the New Harmony syncline, the timing of first movement on the Hurricane fault is unclear. In contrast to Anderson and Mehnert (1979), Stewart and Taylor (1996) presented evidence that the Hurricane fault accommodated normal slip prior to deposition of Quaternary basalt near Toquerville. Either the Hurricane fault had a diachronous slip history along strike, or evidence of late Tertiary displacement along the eastern margin of the New Harmony basin was eradicated by erosion and deposition of younger units.

## APPENDIX D

## Control Points for Structure-Contour Maps

<i>Table D.1. Well data constraining elevation of base of Navajo Sandstone (see plate 5A).</i>		
Contour Map Designation	Local Well ID Number	Comments
A.	(C-41-17) 8cda	Jn to 2,980 ft elevation
B.	(C-41-17) 17bdd-1	Jn to 2,730 ft
C.	(C-40-16) 17daa	Top of Jn at 4,220 ft
D.	(C-40-16) 35bcd	Top of Jn at 4,285 ft
E.	(C-41-16) 9cba	Jn to 2,400 ft
F.	(C-41-16) 16bbd	Jn to 2,610 ft
G.	(C-41-16) 16cbd-1	Base of Jn at 2,750 ft
H.	(C-41-16) 21abb	Jn to 2,800 ft
I.	(C-41-16) 3dbc	Jn to 2,500 ft
J.	(C-41-16) 23bba-2	Jn to 2,790 ft
K.	(C-41-16) 26bbb	Jn to 2,955 ft
L.	(C-41-16) 24cba	Jn to 2,780 ft
M.	(C-42-15) 10bc	Jn to 2,650 ft
N.	(C-42-15) 3cdd	Jn to 2,650 ft
O.	(C-41-15) 36ada	Base of Jn at 2,555 ft
P.	(C-40-13) 28dcb	Jn to 3,310 ft
Q.	(C-41-13) 34bcc	Jn to 3,000 ft
R.	(C-42-10) 10ada	Carmel Fm. at 3,000 ft
S.	(C-42-13) 7bcc-1	Jn to 1,040 ft
T.	(C-42-13) 15baa	Jn to 2,950 ft
U.	(C-42-13) 20abc-1	Jn to 2,175 ft
V.	(C-42-13) 21aab-1	Jn to 2,935 ft
W.	(C-42-13) 15ccc	Jn to 2,800 ft
X.	(C-42-14) 15daa	Base of Jn at 2,720 ft
Y.	(C-42-13) 30caa	Jn to 2,450 ft
Z.	(C-42-13) 33bbb	Jn to 2,600 ft
AA.	(C-42-13) 28dad	Jn to 2,870 ft
BB.	(C-42-14) 34cad	Jn to 2,830 ft
CC.	(C-42-13) 5bdd-1	Jn to 2,900 ft

<i>Table D.2. Well data constraining elevation of top of Navajo Sandstone (see plate 5B).</i>		
Contour Map Designation	Local Well ID Number	Comments
A.	(C-40-16) 17daa	Top of Jn at 4,220 ft elevation
B.	(C-40-16) 35bcd	Top of Jn at 4,285 ft
C.	(C-42-13) 3aba	Top of Jn at 2,850 ft
D.	(C-42-13) 10ada	Carmel Fm. at 3,000 ft
E.	(C-42-13) 15baa	Top is below 2,950 ft
F.	(C-42-13) 15ccc	Top is below 2,800 ft

## APPENDIX E

### *Methods of Fracture Data Acquisition*

The orientations and density of fractures in the Navajo Sandstone were quantified at outcrop scale and with 1:20,000-scale aerial photographs. Outcrop data is more detailed and pertains to ground-water conditions at approximately the scale of a well and its related draw-down cone. Aerial-photograph data provide the orientations and density of major fracture zones and are relevant at a scale of several square kilometers.

Data acquisition on the outcrop utilized the scanline technique (LaPointe and Hudson, 1985), in which the position, orientation, aperture, infilling minerals or coatings (if any), and length of fractures intersecting two perpendicular sampling traverses are recorded. Nineteen sites were selected for scanline analysis, most of which were near water wells for which specific capacity data were available. In most surveys 25 fractures were recorded along each tape length, resulting in survey areas of approximately 75 to  $1 \times 10^5$  square feet ( $7\text{--}1,000\text{ m}^2$ ) depending on fracture density. The distribution of fracture density was heterogeneous at many sites, so either (1) two or three scanline surveys were performed or (2) fifty measurements were made per sampling traverse to better characterize the heterogeneity and average properties of the fracture population.

Fracture-trace maps were generated from the aerial photographs for the entire outcrop area of the Navajo Sandstone in the study area. Circular sampling areas representing either  $8.73 \times 10^6$  square feet ( $8.11 \times 10^5\text{ m}^2$ ) or  $2.18 \times 10^6$  square feet ( $2.03 \times 10^5\text{ m}^2$ ) were selected from the fracture-trace maps where bedrock exposure was nearly 100 percent. Finally, the sampling areas were scanned and analyzed for orientation and length of fracture traces using standard graphics software.

Rose-diagram plots in plate 6 depict different information for scanline and aerial-photograph data. The length of each rose petal for scanline data is proportional to the relative frequency of joints of the corresponding orientation range. To construct rose-diagram plots for aerial photograph data, each fracture was assigned a weight proportional to its length, with an upper truncation value equal to the diameter of the sample circle.

The reproducibility of the aerial photograph fracture-trace analysis for a single worker is indicated by comparison of samples sm-1a and sm-1b (plate 6 and table G.1), which are based on fracture-trace maps drawn from different aerial photographs of the same area. The reproducibility of the computer graphics method is indicated by comparison of samples c-2a and c-2b (plate 6 and table G.1), which were derived from analysis of the same fracture-trace map.

Field observations indicated that the most conspicuous lineaments on the aerial photographs are joint zones and joints that have weathered sufficiently to support vegetation along their traces and/or have enough relief to cast a shadow. Thus, there may be a sampling bias favoring observation of joint zones over individual joints, and perhaps favoring joints and joint zones oriented at high angles to the direction of the sun at the time the photograph was taken.



## APPENDIX F

### *Fracture Heterogeneity*

This section describes the heterogeneous distribution of fractures in the Navajo Sandstone in greater detail than in the main text and discusses the problems this heterogeneity poses for sampling methods. Data from Snow Canyon (sample f-7-scw, plate 6 and table G.2) and Sandstone Mountain (sample f-6-ssm, plate 6 and table G.2) are used as examples.

Figure F.1 is a simplified geologic map of the upper Snow Canyon area, including fracture traces derived from 1:20,000-scale, black and white aerial photographs. North- to northwest-striking faults and northeast-striking joints and joint zones are clearly the dominant structural features, although discrete areas of north- and west-northwest-striking joints are present. The Snow Canyon fault zone bifurcates northward, occupying West and East Canyons of Snow Canyon State Park (figure 8b). The faults shown on figure F.1 are interpreted as reactivated joint zones.

Four water wells that supply the cities of St. George and Santa Clara occupy upper Snow Canyon (figure F.1). All of the wells are located in or adjacent to the Snow Canyon fault zone, probably in the high-permeability area associated with its damage zone. Snow Canyon well #6 (figure F.1) has a specific capacity of 8 gallons per minute per foot (table G.3) (V. Heilweil, U.S. Geological Survey, verbal communication).

Joint distribution in Snow Canyon is markedly heterogeneous (figure 9a) and is representative of patterns observed throughout the Navajo Sandstone. Joint zones are common and are spaced about 30 to 1,000 feet (10-305 m) apart. This heterogeneity raises the question of the scale to which the results of a single scanline survey that covers approximately  $75 \times 10^5$  square feet ( $7 \times 1,000 \text{ m}^2$ ) can be extrapolated, and highlights the importance of sample-site selection. Study of outcrops in Snow Canyon, Sandstone Mountain, and other locations indicate that joint distribution is characterized by three distinct relative degrees of joint density (figure 9a). The highest joint density is in the cores of joint zones, medium joint density is present adjacent to joint zones or in weakly developed joint zones, and low joint density characterizes the remainder of the bedrock. In Snow Canyon, joint populations in areas of high, medium, and low density have similar orientations, but vary in density (figure F.2 and table G.2). Scanline surveys at Sandstone Mountain display even greater variation in joint density and orientation (figure F.2 and table G.2).

Fracture densities calculated from scanline surveys in heterogeneously fractured areas depend strongly on selection of sample sites. To produce data that can be extrapolated over a relatively large outcrop area, either several scanlines covering the range of observed fracture densities were averaged or traverses crossed areas of variable joint density, for example beginning within a joint zone and ending in a zone of low joint density. These procedures were followed in collecting the fracture data presented in plate 6 and in performing the calculations relating fracture characteristics to specific capacity.

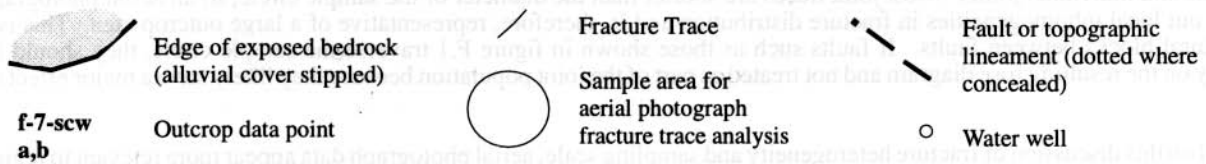
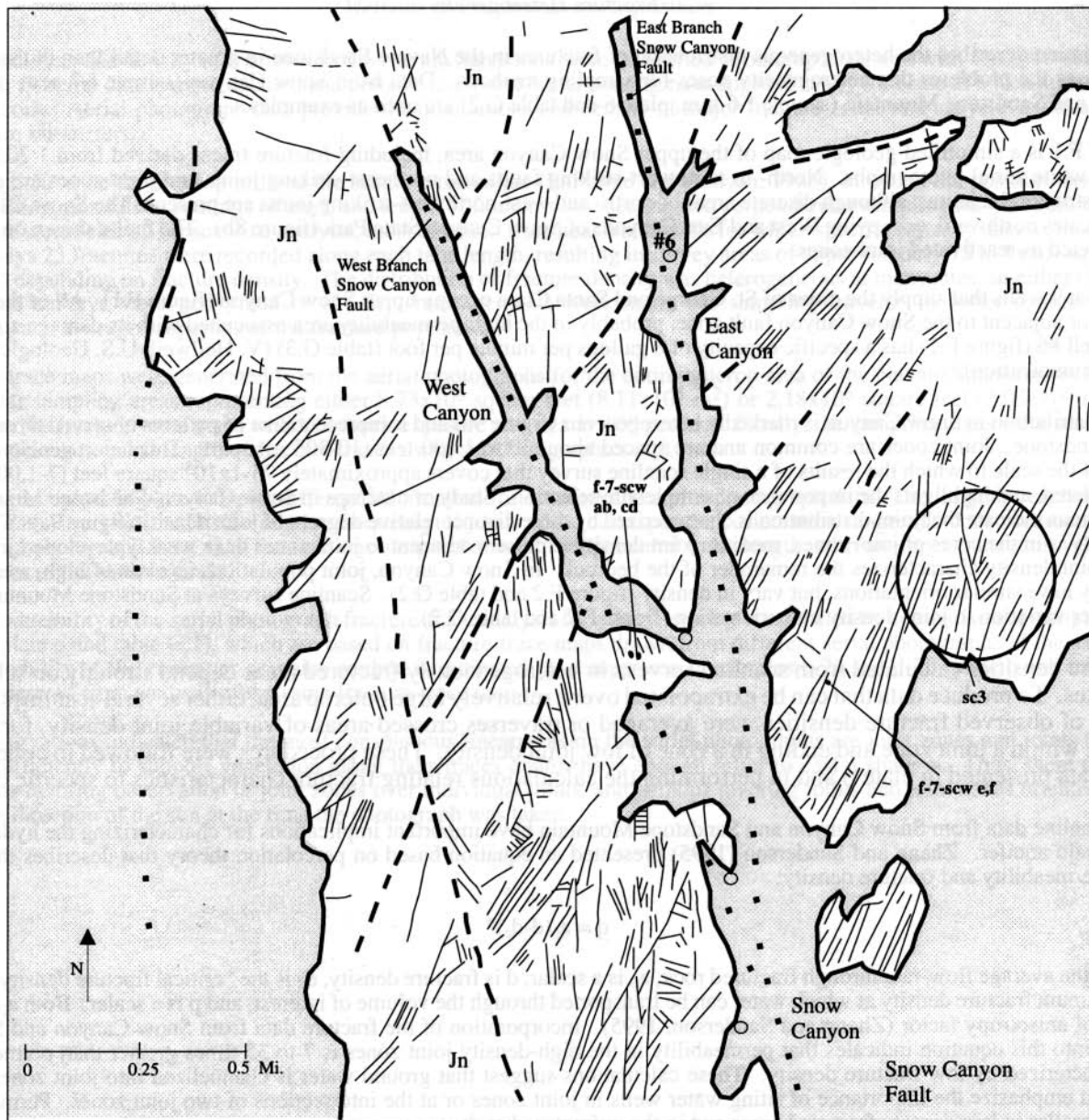
The scanline data from Snow Canyon and Sandstone Mountain have important implications for characterizing the hydrogeology of the Navajo aquifer. Zhang and Sanderson (1995) presented an equation based on percolation theory that describes the relation between permeability and fracture density:

$$q = a_p(d-d_c)^p$$

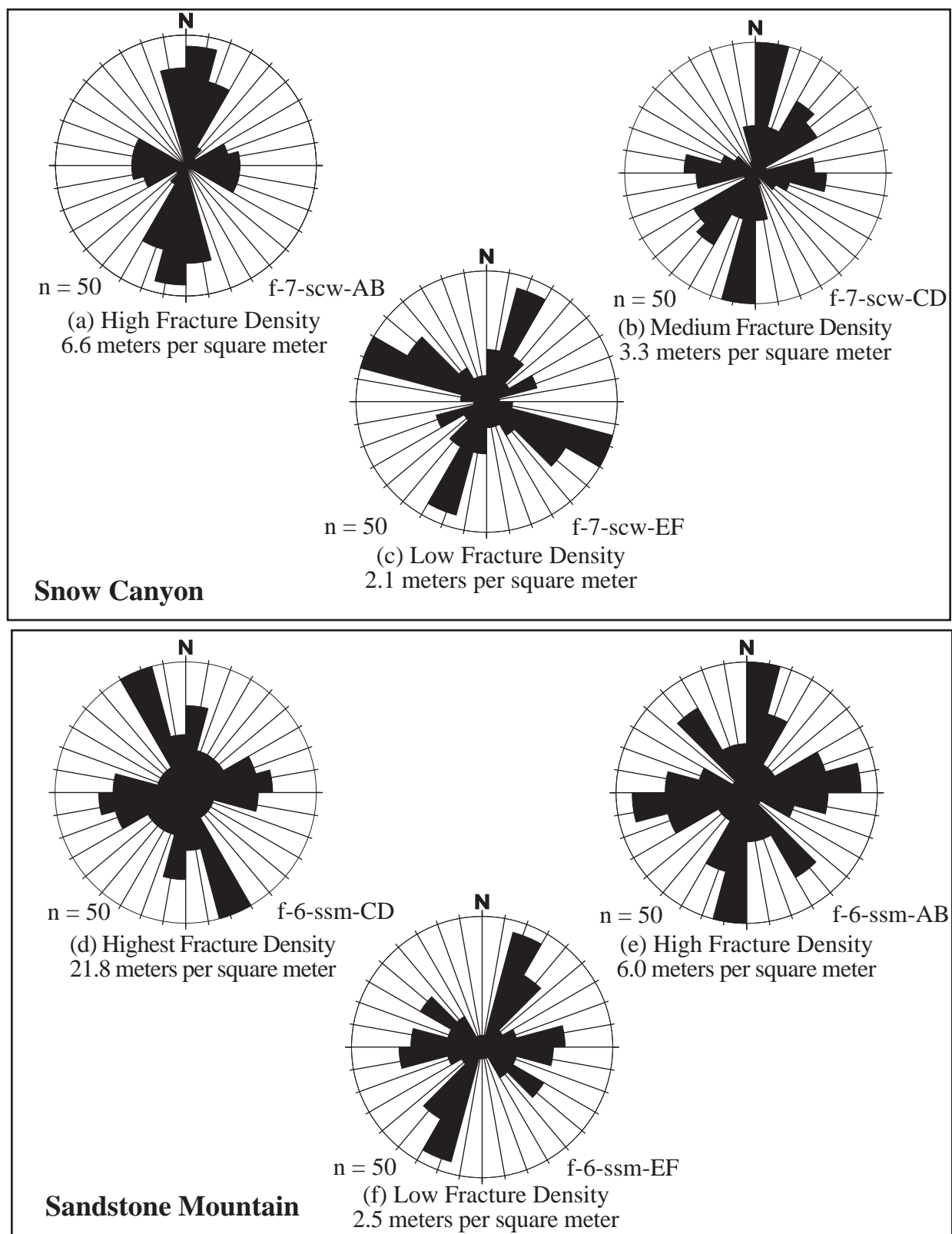
where  $q$  is the average flow-rate through fractured rock,  $a_p$  is a scalar,  $d$  is fracture density,  $d_c$  is the "critical fracture density," defined as the minimum fracture density at which water can be transported through the volume of interest, and  $p$  is a scalar. Both  $a_p$  and  $p$  are functions of anisotropy factor (Zhang and Sanderson, 1995). Incorporation of the fracture data from Snow Canyon and Sandstone Mountain into this equation indicates that permeability in the high-density joint zones is 7 to 35 times greater than permeability in areas characterized by low fracture density. These calculations suggest that ground water is channelized into joint zones to some degree, and emphasize the importance of siting water wells in joint zones or at the intersections of two joint zones. Permeability is probably smaller in less densely fractured areas and in the unfractured rock mass.

The area covered by aerial photograph sample sc3 is shown in figure F.1. The fracture traces within the sample circle represent joint zones and individual joints. Most joint traces are shorter than the diameter of the sample circle, so an aerial photograph sample averages out local inhomogeneities in fracture distribution and is, therefore, representative of a large outcrop area. This is true only for structural blocks between faults. If faults such as those shown in figure F.1 traverse the sample circle, they should be plotted separately on the resulting rose diagram and not treated as part of the joint population because they likely have a major effect on ground water.

Based on this discussion of fracture heterogeneity and sampling scale, aerial photograph data appear more relevant to regional-scale ground-water flow than scanline data. Unfortunately, the aerial photograph data are only weakly correlated with specific capacity data from individual wells ( $R^2 = 0.33$ ) and with fracture density measured by the scanline technique ( $R^2 = 0.1$ ), making it difficult to estimate transmissivity values from fracture densities measured from aerial photographs. The best approach is to estimate hydraulic conductivity from carefully located scanlines using equation (2), and to estimate saturated thickness from local water levels and either plate 5A or more detailed cross sections.



**Figure F.1.** Simplified geologic map of the upper Snow Canyon area, showing fracture traces derived from 1:20,000-scale aerial photographs and sample locations for scanline and aerial-photograph fracture analyses. Water well #6 is discussed in text. Jn is Navajo Sandstone.



**Figure F.2.** Rose diagrams for high, medium, and low joint density zones at Snow Canyon (sample site f-7-scw) and Sandstone Mountain (sample site f-6-ssm)

## APPENDIX G

### Fracture Data Tables

<i>Table G.1. Aerial photograph fracture data.</i>		
Site (1)	Fracture Density (2)	Orientations and Axial Ratios of Maxima (3)
bh1	0.4 (1.4)	0(15), 82(7); 5.7:1
c1	0.5 (1.8)	45(15); >10:1
c2a	0.5 (1.5)	45(15), 300(15); 1.6:1
c2b	0.5 (1.5)	45(15), 300(15); 1.7:1
gpw1	0.6 (2)	37(22), 307(22); 1:1
gpw2	0.6 (2.1)	38(22), 292(7); 3.4:1
gw1	1.1 (3.7)	67(22), 352(7); 2.6:1
gw1	1.0 (3.4)	292(7)
gw3	1.1 (3.6)	300(15), 15(15); 1.3:1
jw1	0.9 (3.1)	15(15); >10:1
jw2	1.0 (3.4)	15(15), 60(15); 3.3:1
lc1	0.8 (2.6)	295(15), 75(15), 22(7); 1.8:1.6:1
qc1	0.6 (2)	30(15), 300(15); 4:1
qc2	0.8 (2.6)	45(15), 307(7); 4.9:1
rh1	0.7 (2.4)	30(15), 292(22); 4.1:1
rm1	0.7 (2.2)	7(22), 270(15); 2.1:1
rm2	0.7 (2.2)	75(15), 352(22), 37(7); 1.3:1.3:1
rm3	0.9 (3)	15(15); >10:1
sc1	0.7 (2.2)	15(30), 292(22); 3.3:1
sc2	0.9 (2.9)	75(30), 7(22); 1.7:1
sc3	0.7 (2.2)	22(22); >10:1
sc5	1.1 (3.6)	352(22), 60(15); 1.8:1
scv1	1.2 (3.8)	0(15); 97(7); 1.6:1
scv2	1.0 (3.2)	292(22), 37(22); 1.4:1
scv4	1.4 (4.6)	0(15), 67(7); 9.4:1
sgn1	0.5 (1.8)	7(7), 315(15); 2.6:1
sgn2	0.5 (1.8)	0(15), 277(7); 3.4:1
sm1a	0.6 (1.9)	60(15), 337(7); 3.6:1
sm1b	0.6 (1.9)	67(7), 22(7), 337(7); 2.7:1.7:1
sm2	1.0 (3.2)	60(15), 315(15); 2.4:1
sm4	0.9 (2.9)	330(15), 60(15); 1.8:1
ssm1	1.3 (4.2)	270(15), 7(22), 315(15); 1.7:1.4:1
ssm2	0.6 (2.1)	37(7), 297(7); 2.2:1
ssm3	1.6 (5.1)	330(15), 60(15); 1:1
wh1	0.5 (1.6)	52(22), 330(15); 1.6:1
wh2	0.5 (1.8)	60(15), 337(7); 3.2:1
ws1	0.7 (2.4)	37(7), 67(7), 292(7); 1.5:1.5:1
yk1	0.7 (2.2)	45(15), 0(15); 2.2:1

**Notes:**

(1) See plate 6 for locations.

(2) Fracture density is in units of feet of fracture length per square foot of outcrop area x 100 (meters per square meter x 100).

(3) See plate 6 for rose diagrams. Values listed are mean azimuth(s) of principal set(s) with uncertainties, in degrees, in parentheses, followed by ratios of petal lengths.

Table G.2. Scanline data

Site (1)	Tape Azimuth, Length Number of Fractures (2)	Fracture Density (3)	Average Aperture (4)	fd*aa (5)	Orientations & Axial Ratios of Principal Fracture Sets (6)	Anisotropy Factor (7)
f-1-bh Buckskin Hollow	(A) 80, 21.28, 51; (B) 350, 36.11, 50	0.2 (0.8)	(A) 0.79 (20), (B) 0.08 (2); 0.39 (10)	7.8 (8)	7(7), 82(7); 2.2:1	1.9
f-2-csm Sand Mt.	(A) 320, 30.72, 50; (B) 50, 61.12, 50	0.1 (0.2)	(A) 0.11 (3), (B) 0.08 (2); 0.1 (2.5)	0.6 (0.5)	45(15), 7(7); 4:1	5.2
f-3-gw Gunlock Wells	AB	0.3 (1.1)	(A) 0.12 (3), (B) 0.04 (1); 0.08 (2)	2.6 (2.2)	75(15), 345(15); 1.3:1	1.5
	CD	0.7 (2.2)	(C) 0.04 (1), (D) 0.04 (1); 0.04 (1)	2.7 (2.2)	300(30), 52(22); 1.2:1	2.1
Combined	(A) 40, 5.26, 25; (D) 310, 13.05, 25	0.5 (1.5)	0.06 (1.5)	2.8 (2.3)	77(22), 330(30); 1:1	1.7
f-4-mcw Middle Millcreek	A(40, 12.12, 25; (B) 300, 8.94, 25	0.4 (1.2)	(A) 0.39 (10), (B) 0.24 (6); 0.32 (8)	11.8 (9.8)	345(30), 52(7); 4.7:1	1.2
f-5-gpw Grapevine Pass	(A) 315, 20.7, 30; (B) 50, 54.24, 25	0.1 (0.2)	(A) 0.04 (1), (B) 0.04 (1); 0.04 (1)	0.2 (0.2)	322(7), 30(15); 1:1	2.4
f-6-ssm Sandstone Mt. Medium Fracture Density AB High Fracture Density CD Low Fracture Density EF Combined	(A) 70, 3.66, 25; (B) 335, 4.06, 25	1.8 (6)	(A) 0.11 (3), (B) 0.08 (2), 0.1 (2.5)	18 (15)	15(15), 75(15), 322(7); 2.2:1.7:1	1.1
	(C) 65, 1.57, 25; (D) 335, 1.46, 25	6.6 (21.8)	(C) 0.12 (3), (D) 0.08 (2), 0.1 (2.5)	66 (54.5)	352(22), 82(22); 1.1:1	2.7
	(E) 20, 8.61, 25; (F) 320, 8.08, 25	0.8 (2.5)	(E) 0.08 (2), (F) 0.08 (2); 0.08 (2)	6.1 (5)	30(15), 307(22); 1.6:1	1.1
		1.2 (3.8)		12 (9.5)	22(22), 75(15), 330(15); 1.7:1.1:1	1
f-7-scw Snow Canyon High Fracture Density AB Medium Fracture Density CD Low Fracture Density EF Combined	(A) 75, 2, 25; (B) 10, 6.2, 25	2.0 (6.6)	(A) 0.12 (3), (B) 0.08 (2); 0.1 (2.5)	20 (16.5)	15(30), 292(7); 5.1:1	3.7
	(B) 80, 5.47, (D) 25; 5, 7.5, 25	10. (3.3)	(C) 0.08 (2), (D) 0.04 (1); 0.06 (1.5)	6 (5)	7(22), 90(30); 1.7:1	1.4
	(E) 290, 10.53, 25; (F) 20, 8.42, 25	0.6 (2.1)	(E) 0.04 (1), (F) 0.04 (1); 0.04 (1)	2.4 (2.1)	45(15), 0(15), 82(7); 3.2:3.2:1	1.3
		0.9 (2.9)	0.07 (1.7)	6.3 (4.9)	15(30), 292(7); 5.1:1	1.3
f-8-wh Winchester Hills	(A) 295, 8.06, 25; (B) 30, 9.5, 25	1.0 (3.2)	(A) 0.2 (5), (B) 0.08 (2); 0.14 (3.5)	14 (11.2)	30(15), 307(7); 3.2:1	3.7
f-9-aj Anderson Junction	(A) 270, 4.55, 25; (B) 25, 7.38, 25, 25	1.7 (5.7)	(A) 0.16 (4), (B) 0.16 (4); 0.16 (4)	27 (22.8)	7(7), 307(7); 1.8:1	2.4
f-10-qc Quail Creek	(A) 300, 12.19, 50; (B) 20, 9.6, 49	1.1 (3.5)	(A) 0.24 (6), (B) 0.12 (3); 0.18 (4.5)	20 (15.8)	30(15), 292(7); 6.7:1	2.8
f-11-ds1 Lower Dry Sandy	(A) 340, 4.55, 26; (B) 70, 10.5, 25	1.1 (3.7)	(A) 0.32 (8), (B) 0.28 (7); 0.3 (7.5)	33 (27.8)	75(15), 345(15); 2.2:1	3
f-12-ds2 Middle Dry Sandy	(A) 320, 10.63, 25; (B) 50, 10.46, 25	0.9 (2.8)	(A) 0.16 (4), (B) 0.12 (3); 0.14 (3.5)	13 (9.8)	52(7), 307(7); 2.4:1	1.7
f-13-le1 Leeds Creek	(A) 320, 6.6, 25; (B) 20, 12.82, 25	0.7 (2.3)	(A) 0.12 (3), (B) 0.24 (6); 0.18 (4.5)	13 (10.4)	22(7), 52(7); 2.6:1	3.9
f-14-cc1 City Creek #1	(A) 15, 3.61, 25; (B) 125, 10.65, 25	1.3 (4.4)	(A) 0.2 (5), (B) 0.16 (4); 0.18 (4.5)	23 (20.7)	315(15), 15(15); 1.2:1	3.7
f-15-lmc Lower Mill Creek	(A) 90, 9.48, 25; (B) 15, 11.71, 25	0.4 (1.3)	(A) 0.47 (12), (B) 0.2 (5); 0.32 (8)	13 (10.9)	15(15), 75(15); 1.2:1	1.5
f-16-umc Upper Mill Creek	(A) 135, 6.33, 25; (B) 40, 9.69, 30	0.5 (1.5)	(A) 0.16 (4), (B) 0.04 (1); 0.1 (2.5)	5 (4.1)	30(15), 337(7); 3.6:1	3.2
f-17-sh1 Sand Hollow	(A) 90, 13.91, 25; (B) 0, 7.86, 25	0.4 (1.4)	(A) 0.06 (1.4), (B) 0.04 (1); 0.05 (1.2)	2 (1.7)	22(22), 67(7); 5.7:1	2
f-18-hcw Hurricane City Well	areal survey of small outcrop	0.2 (0.5)	0.04 (1)	0.8 (0.5)	0(30), 277(22); 3.5:1	n/a
f-19-sh2 Sand Hollow	(A) 175, 16.55, 25; (B) 345, 9.72, 25	0.2 (0.6)	(A) 0.04 (1), (B) 0.04 (1); 0.04 (1)	0.8 (0.7)	15(30); >10:1	3.1

## Notes:

- (1) See plate 6 for locations.
- (2) Individual traverses are assigned capital letters, followed by their azimuth, length in meters, and number of fractures intersected.
- (3) Feet of fracture length per square foot of outcrop area (meters per square meter).
- (4) Average apertures in inches (mm) for each traverse, followed by average for both traverses. Tight fractures were recorded as having apertures of less than one, which translated into a value of 0.04 inches (1 mm) for calculation of averages. Thus, all average aperture values in this table are overestimates and should be used for comparison of sample sites only.
- (5) Product of fracture density and average aperture.
- (6) See plate 6 for rose diagrams. Values listed are mean azimuth(s) of principal fracture sets with uncertainties in parentheses, followed by ratios of principal set exists.
- (7) See page 23 of text for definition and discussion.

**Table G.3.** Fracture parameters and hydraulic conductivity.

Well	Sample (1)	Fracture Density (2)	Average Aperture (3)	fdxaa x 1000	Thickness (4)	Specific Capacity (5)	Hydraulic Conductivity (6)
Gunlock #7 (C-41-17)8acc-1	f-3-gw	0.46 (1.5)	0.06 (1.5)	2.3	1150 (350)	3.5	1.02 (0.31)
Winchester Hills #1 (C-41-16)23bba-2	f-8-wh	1.0 (3.2)	0.14 (3.5)	11.2	1365 (416)	4.6	4.6 (1.40)
Snow Canyon #6 (C-41-16)4cbc-1	f-7-scwcd	1.0 (3.3)	0.06 (1.5)	5	1030 (314)	8.3	2.2 (0.67)
City Creek #1 (C-42-15)6dcc-1	f-14-cc1	1.3 (4.4)	0.18 (4.5)	20.7	850 (259)	21	7.34 (2.24)
St. George Millcreek #1 (C-41-15)34aab	f-16-umc	0.5 (1.5)	0.1 (2.5)	4.1	1000 (305)	6.8	1.9 (0.58)
Wash. City Millcreek #5 (C-42-15)3acd-1	f-4-mcw	0.4 (1.2)	0.32 (8)	9.8	630 (192)	9.4	6.0 (1.83)
Wash. City-Sullivan (C-42-15)10bcd-1	f-15-lmc	0.4 (1.3)	0.32 (8)	10.9	542 (165)	9	4.26 (1.30)
Grapevine Pass (C-41-15)36ada	f-5-gpw	0.1 (0.2)	0.04 (1)	0.2	1000 (305)	0.4	0.2 (0.06)
Anderson Junction (C-40-13)28dcb	f-9-aj	1.7 (5.7)	0.16 (4)	22.8	625 (190)	5.2	22.7 (6.92)
Winding Rivers (C-42-14)12dbb-2	f-19-sh2	0.2 (0.6)	0.04 (1.1)	0.7	1450 (442)	2	0.77 (0.23)
Hurricane City Well (C-42-13)6cad-1	f-17-sh1	0.4 (1.4)	0.05 (1.2)	1.7	1570 (479)	7.6	3.34 (1.02)

**Notes:**

1. See plate 6 and table G.2 for sample location, rose diagram, and fracture data.
2. Units are fracture length in feet per square foot of outcrop (meters per square meter).
3. Units are inches (mm).
4. Vertical thickness of Navajo Sandstone at well, in feet (m).
5. Units of gallons per minute per foot of drawdown, for the initial 24 hours of a pump test. Specific capacity and hydraulic conductivity value for Anderson Junction and Winding Rivers wells were provided by Victor Heilweil of the U.S. Geological Survey, Water Resources Division.
6. Units of feet per day (meters per day).

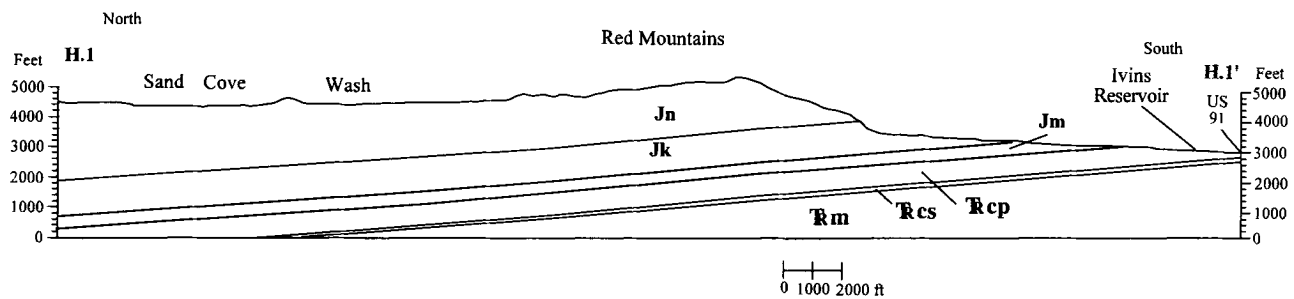


## APPENDIX H

### *Structure of the Red Mountains and Implications for Artificial-Recharge Projects*

Artificial recharge of the Navajo aquifer is currently being evaluated to increase the water supply for the central Virgin River basin. The Utah Division of Water Rights has expressed interest in an artificial recharge site north of the Red Mountains, southwest of the town of Veyo (figure 1a). The proposed site utilizes a pipeline from the Santa Clara River and two small reservoirs associated with an inactive power plant. This appendix briefly discusses the geologic setting of this area.

The proposed site is underlain by the upper part of the Navajo Sandstone (plate 1), which dips approximately 5 degrees north to northeast. Figure H.1 and plate 5A show that over 2,000 feet (610 m) of Navajo Sandstone lie below the site, providing a large volume of porous media (presently unsaturated) for infiltration from an artificial recharge source. The potentiometric surface in the study area is presently unknown and needs to be characterized if the project proceeds. Fractures in the area dominantly strike north-south (plate 6). The north to northeast dip of the Navajo Sandstone below the Red Mountains (figure H.1) may affect ground-water flow, because the elevation of the less permeable Kayenta Formation progressively increases to the south, perhaps favoring raising of the water table below the central Red Mountains over north-to-south flow. A particularly interesting potential site for the artificial-recharge project is Upper Sand Cove Reservoir (plate 1), which is near the northern trace of the Snow Canyon fault zone. The Snow Canyon fault zone may provide a high-permeability pathway for north-to-south migration of ground water, providing additional recharge to the existing Snow Canyon well field (figure 1a). More detailed geologic and hydrologic investigations are needed to substantiate these suggested flow paths and to evaluate the suitability of this site.



**Figure H.1.** Cross section through central Red Mountains. See plate 1 for location.



INTERIM GEOLOGIC MAP OF THE ST. GEORGE,  
AND PARTS OF THE CEDAR CITY, CALIENTE,  
AND CLOVER MTNS. QUADRANGLES,  
WASHINGTON AND IRON COUNTIES, UTAH

Compiled by Hugh A. Hurlow  
Water Resources Bulletin 26

Plate 1  
1998

SCALE 1:100,000

0 1 2 3 4 5 6 7 8 9 10 KM  
0 1 2 3 4 5 6 7 8 9 10 MI





# Cross Sections and Correlation of Map Units by Hugh A. Hurlow

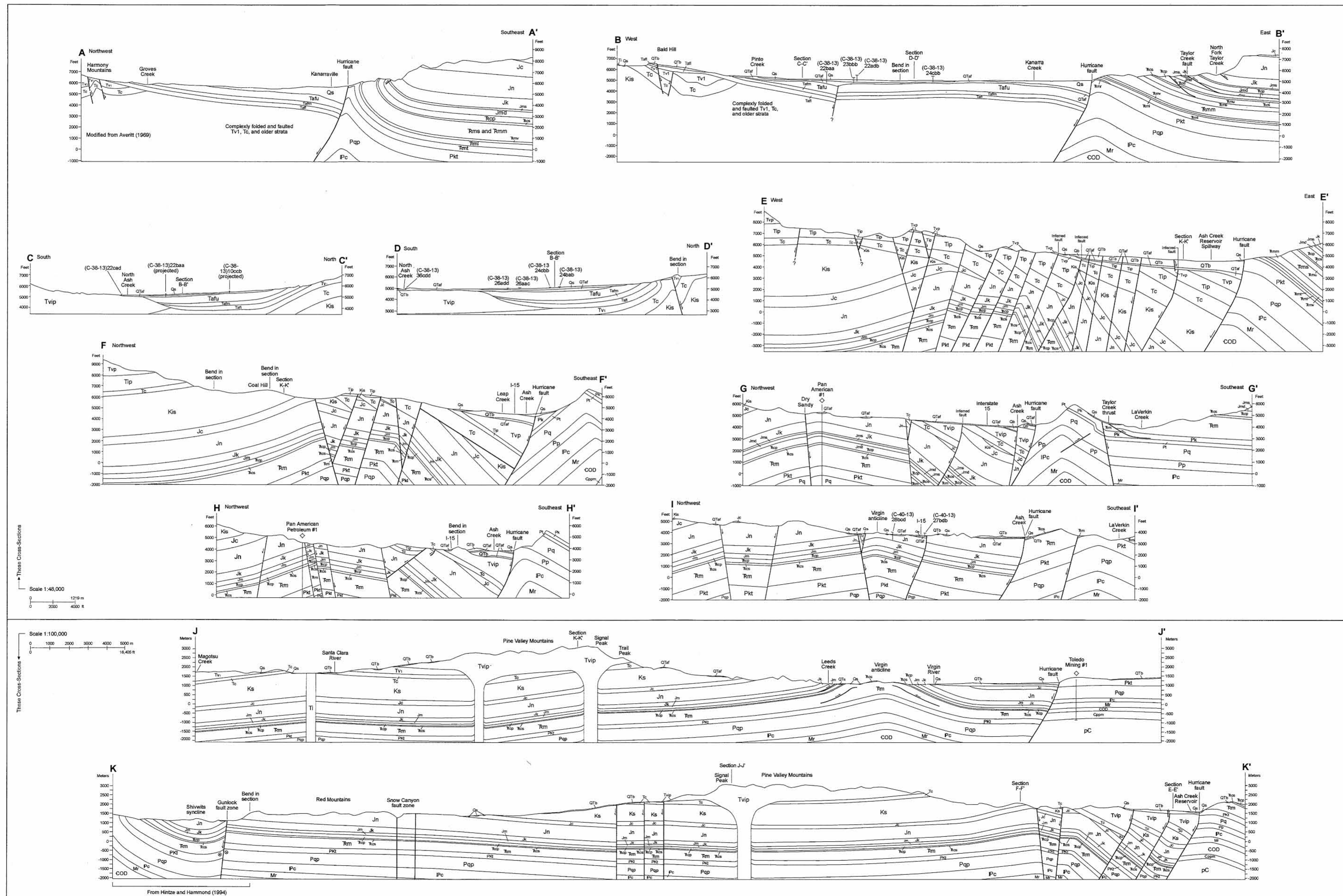
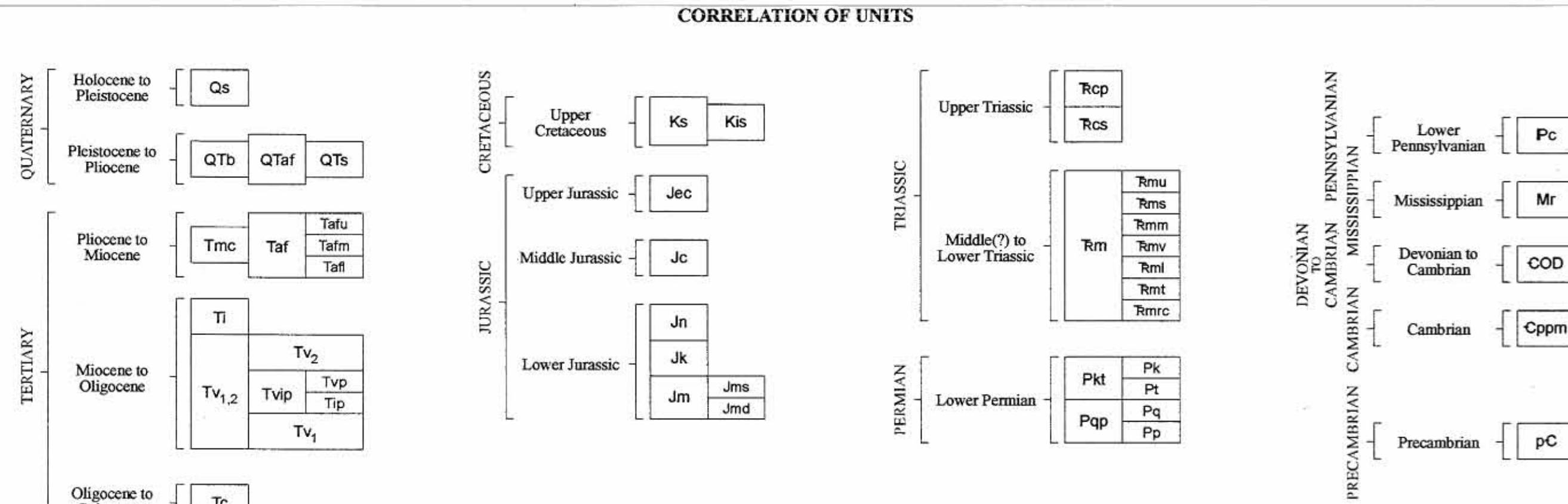
UTAH GEOLOGICAL SURVEY  
a division of  
UTAH DEPARTMENT OF NATURAL RESOURCES  
*A description of map units is in Appendix A of text.*

Cross sections A-A' through I-I' were constructed at 1:24,000 scale from published maps, which were locally modified by the author, (see appendix B for sources), and are printed at 1:48,000 scale on plate 2. The level of structural detail and the precise locations of some contacts in the cross sections, therefore, may not exactly match the geology shown on plate 1. Some geologic units that are undivided on plate 1 are divided into members on plate 2 to provide greater detail (see stratigraphic correlation charts). Cross sections J-J' and K-K' were constructed at 1:100,000 scale from plate 1.

## MAP SYMBOLS FOR PLATE 1

- Depositional or intrusive contact (dashed where inferred or approximately located, dotted where concealed)
- High-angle normal fault, ball and bar on downthrown side (dashed where inferred or approximately located, dotted where concealed)
- High-angle normal fault with oblique slip; ball and bar on downthrown side (dashed where inferred or approximately located, dotted where concealed); arrow shows horizontal component of movement
- Low-angle normal fault, sawtooth on upper plate (dashed where inferred or approximately located, dotted where concealed)
- Thrust fault, sawtooth on upper plate (dashed where inferred or approximately located, dotted where concealed)
- Anticline axial trace, showing plunge of hinge (dashed where approximately located, dotted where concealed)
- Syncline axial trace, showing plunge of hinge (dashed where approximately located, dotted where concealed)

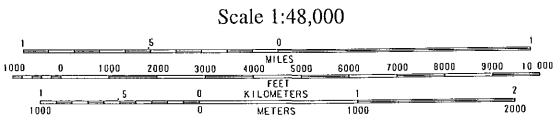
A A'





Water Resources Bulletin 26  
Plate 3  
1998

**Schematic Isopach Map of Depth  
to Base of Unconsolidated Deposits,  
New Harmony-Kanarrville Area,  
Washington and Iron Counties, Utah**  
by  
**Hugh A. Hurlow**



— Contact —  
— 1,000(305) —  
Contour lines, showing thickness of unconsolidated deposits in feet (m); dashed in areas lacking well control. Datum is mean sea level.

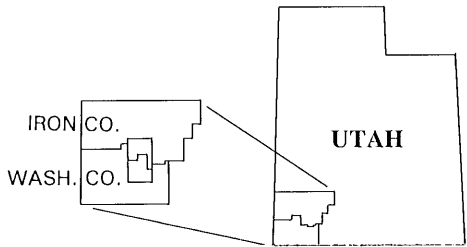
— B —  
Margin of unconsolidated deposits

(C-38-13)  
16cad  
O  
Water well

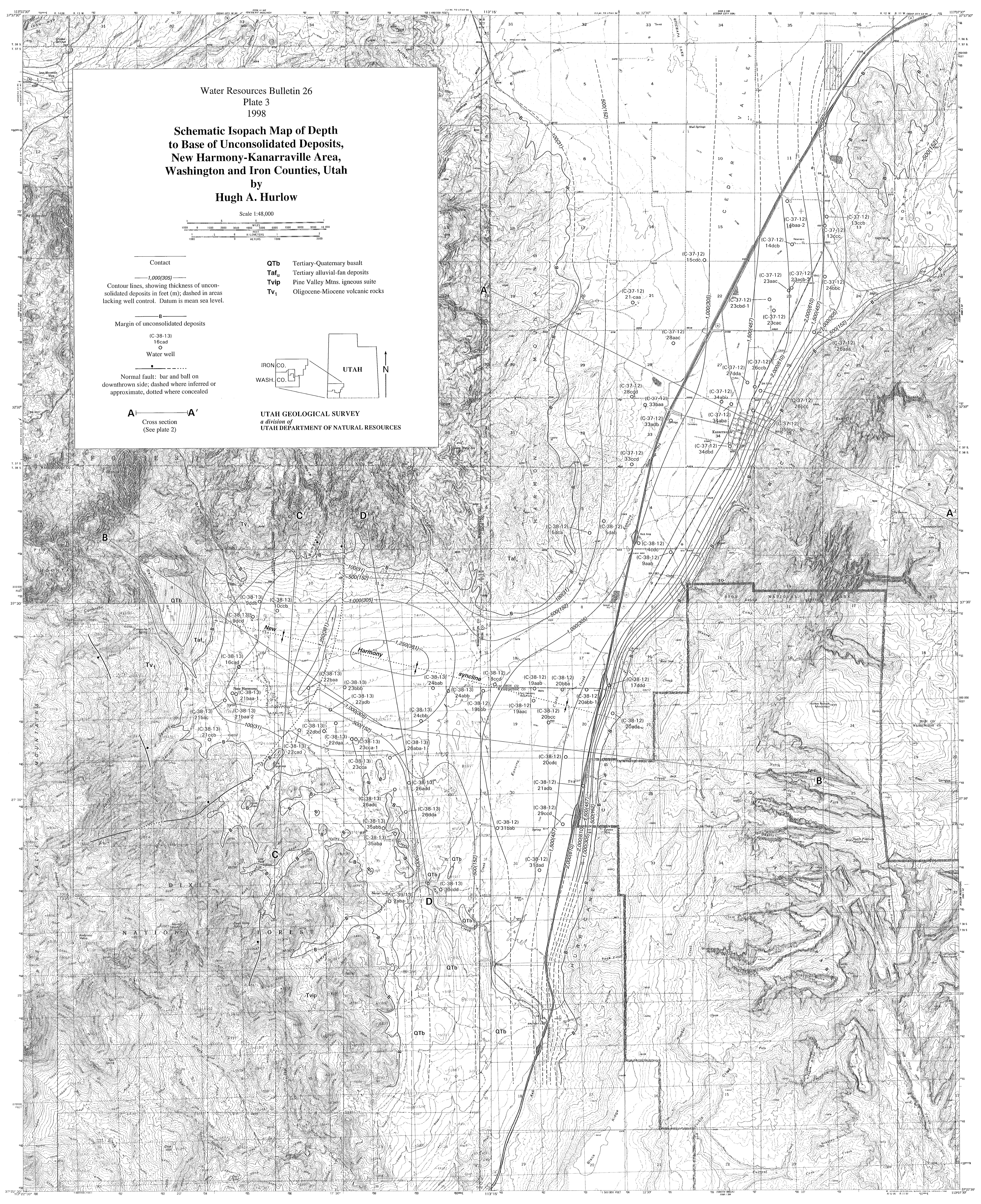
Normal fault: bar and ball on downthrown side; dashed where inferred or approximate, dotted where concealed

A — A'  
Cross section  
(See plate 2)

**QTb** Tertiary-Quaternary basalt  
**Taf<sub>u</sub>** Tertiary alluvial-fan deposits  
**Tvip** Pine Valley Mtns. igneous suite  
**Tv<sub>1</sub>** Oligocene-Miocene volcanic rocks



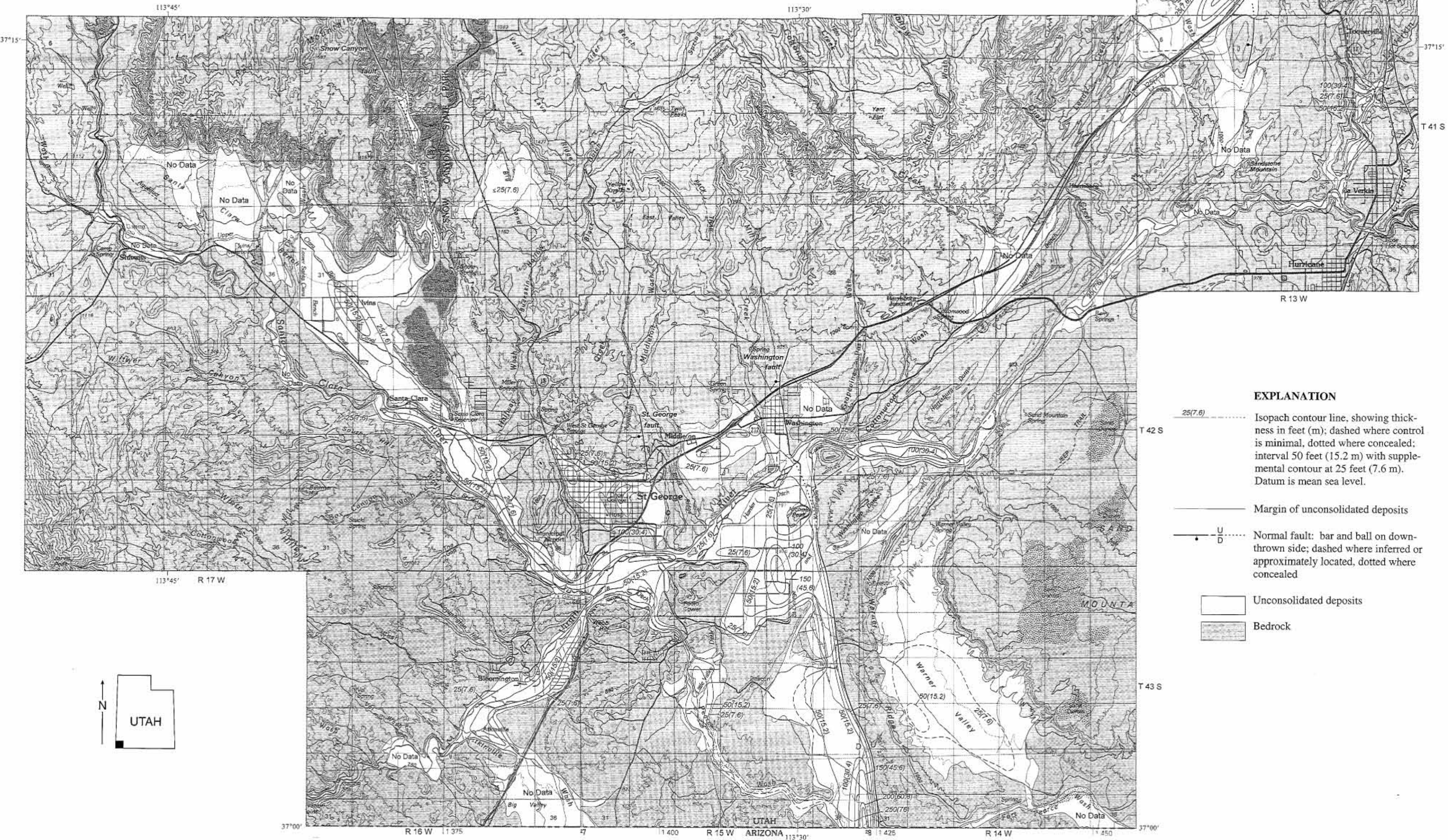
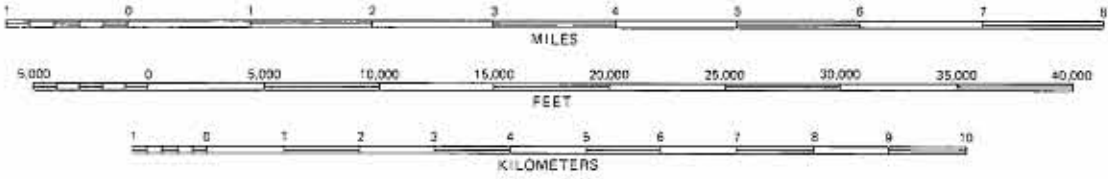
UTAH GEOLOGICAL SURVEY  
a division of  
UTAH DEPARTMENT OF NATURAL RESOURCES





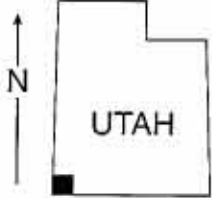
Schematic Isopach Map of Unconsolidated Deposits,  
St. George Basin, Washington County, Utah  
by  
Hugh A. Hurlow

SCALE 1:100,000



EXPLANATION

- Isopach contour line, showing thickness in feet (m); dashed where control is minimal, dotted where concealed; interval 50 feet (15.2 m) with supplemental contour at 25 feet (7.6 m). Datum is mean sea level.
- Margin of unconsolidated deposits
- Normal fault: bar and ball on down-thrown side; dashed where inferred or approximately located, dotted where concealed
- Unconsolidated deposits
- Bedrock





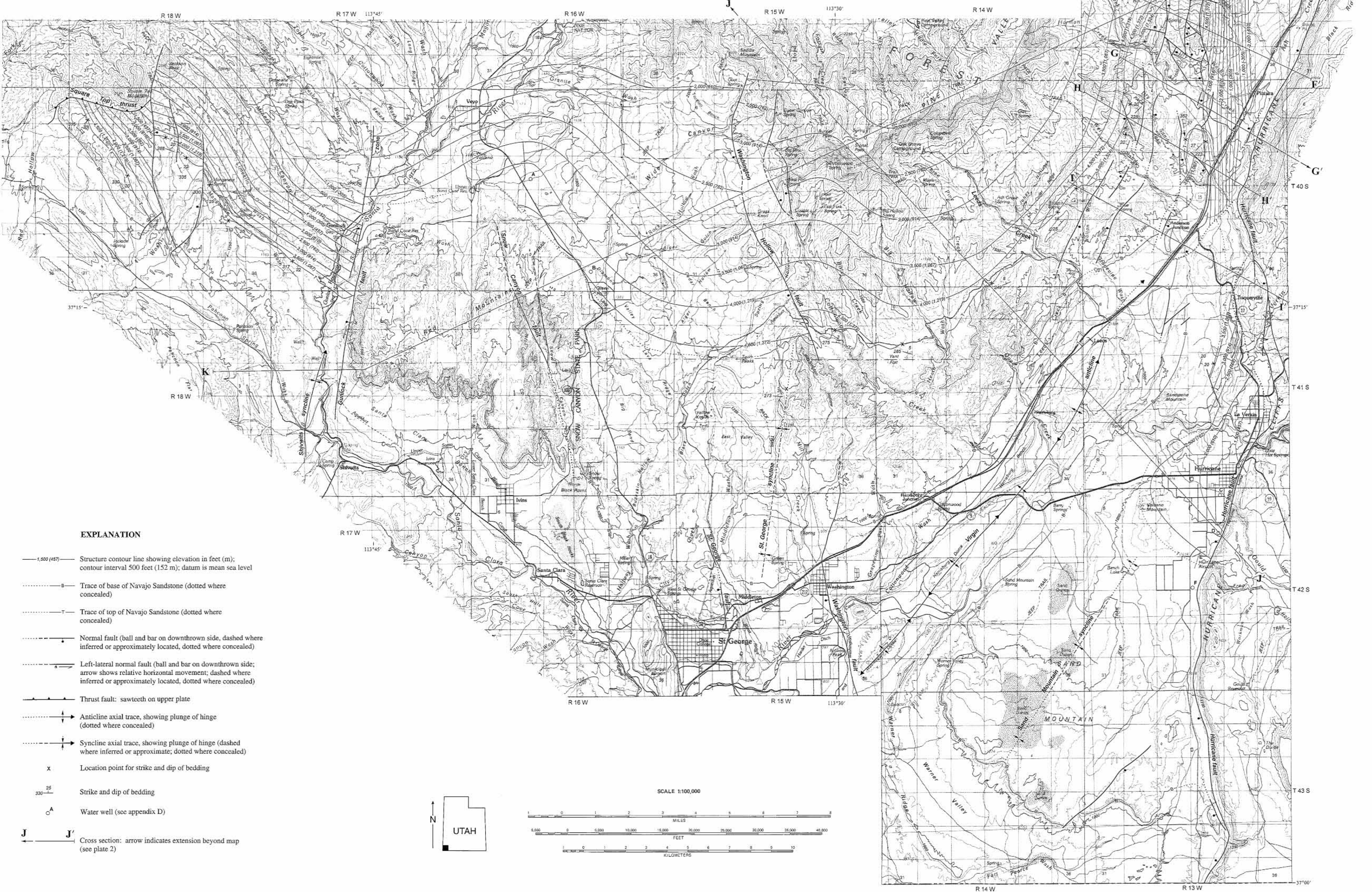
STRUCTURE-CONTOUR MAP  
OF THE BASE OF THE NAVAJO SANDSTONE  
IN SOUTHWESTERN UTAH  
by  
Hugh A. Hurlow





UTAH GEOLOGICAL SURVEY  
a division of  
UTAH DEPARTMENT OF NATURAL RESOURCES

STRUCTURE-CONTOUR MAP  
OF THE TOP OF THE NAVAJO SANDSTONE  
IN SOUTHWESTERN UTAH  
by  
Hugh A. Hurlow





UTAH GEOLOGICAL SURVEY  
a division of  
UTAH DEPARTMENT OF NATURAL RESOURCES

Structural Compartments and Fracture Domains  
in the Navajo Sandstone Outcrop Area  
West of the Hurricane Fault, Southwestern Utah  
by  
Hugh A. Hurlow

